REPORT DOCUMENTATION PAGE	Form Approved OMB No. 0704-0188

1. AGENCY USE ONLY *(Leave blank)*	2. REPORT DATE 11 JUL 97	3. REPORT TYPE AND DATES COVERED

4. TITLE AND SUBTITLE
OZONE AND OTHER AIR QUALITY RELATED VARIABLES AFFECTING VISIBILITY IN THE SOUTHEAST UNITED STATES

5. FUNDING NUMBERS

6. AUTHOR(S)
JEFFREY SCOTT BRITTING

7. PERFORMING ORGANIZATION NAME(S) AND ADDRESS(ES)
NORTH CAROLINA STATE UNIVERSITY

8. PERFORMING ORGANIZATION REPORT NUMBER

97-079

9. SPONSORING/MONITORING AGENCY NAME(S) AND ADDRESS(ES)
DEPARTMENT OF THE AIR FORCE
AFIT/CI
2950 P STREET
WRIGHT-PATTERSON AFB OH 45433-7765

10. SPONSORING/MONITORING AGENCY REPORT NUMBER

11. SUPPLEMENTARY NOTES

12a. DISTRIBUTION AVAILABILITY STATEMENT

DISTRIBUTION STATEMENT A
Approved for public release;
Distribution Unlimited

12b. DISTRIBUTION CODE

13. ABSTRACT *(Maximum 200 words)*

14. SUBJECT TERMS

15. NUMBER OF PAGES
92

16. PRICE CODE

17. SECURITY CLASSIFICATION OF REPORT	18. SECURITY CLASSIFICATION OF THIS PAGE	19. SECURITY CLASSIFICATION OF ABSTRACT	20. LIMITATION OF ABSTRACT

DTIC QUALITY INSPECTED 3

ABSTRACT

BRITTIG, JEFFREY SCOTT. Ozone and Other Air Quality Related Variables affecting Visibility in the Southeast United States.

An analysis of ozone (O_3) concentrations and several other air quality related variables was performed to assess their relationship with visibility at five urban and semi-urban locations in the Southeast United States during the summer seasons of 1980 to 1996. The role and impact of ozone on aerosols was investigated to ascertain a relationship with visibility. Regional trend analysis of the 1980s reveals an increase in maximum ozone concentration coupled with a decrease in visibility. However, the 1990s shows a leveling-off of both ozone and visibility; in both cases the results were not statistically significant at the 5% level. Site specific trends at Nashville Tennessee followed similar trends. To better ascertain the relationships and forcing mechanisms, the analysis was changed from yearly to daily and hourly averaged values. This increased resolution showed a statistically significant inverse relationship between visibility and ozone. Additionally, by performing back trajectory analysis, it was observed that the visibility degraded both by airmass migration over polluted areas and chemical kinetics.

Ozone and Other Air Quality Related Variables

Affecting Visibility in the Southeast United States

by

JEFFREY SCOTT BRITTIG

A thesis submitted to the Graduate Faculty of
North Carolina State University
in partial fulfillment of the
requirements for the Degree of
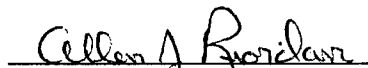Master of Science

Department of Marine, Earth, and Atmospheric Sciences

Raleigh

1997

APPROVED BY:

_____   _____
Gerald F. Watson   Alan J. Riordan

_____
Viney P. Aneja
Chair of Advisory Committee

BIOGRAPHY

Jeffrey S. Brittig ▬▬▬▬▬▬▬▬▬▬▬▬▬▬▬▬ He graduated from Glenbard East High School, Lombard, Illinois in 1980. He immediately enlisted in the Air Force and, after completing technical training at Keesler AFB, Mississippi, was assigned to Mather AFB, California as a B-52 and KC-135 Aircraft Communication Technician.

From November of 1982 until January of 1988, Jeff was assigned as an Airborne Communication Technician with the 552nd AWAC Wing, Tinker AFB, Oklahoma. He served in various capacities and saw temporary duty throughout the world while accumulating over 1500 flying hours.

In January 1988, Jeff was selected for the Airman Scholarship and Commissioning Program and attended the University of Oklahoma where he earned a degree in meteorology and a commission in the Air Force.

After graduation Jeff was assigned to Fort Hood, Texas as a Staff Weather Officer and led a team responsible for supporting a Corp level aviation brigade. In 1991 he was re-assigned to a regional forecast center in the Republic of South Korea, where he served a one year tour. Upon his return to the States in 1992, Jeff was selected as a Weather Instructor instructing aviation weather at Randolph, AFB, Texas.

In 1995, Jeff was accepted into the AFIT/CI program to attend graduate school at North Carolina State University, studying toward a Master's degree in Atmospheric Sciences.

Jeff is currently a Captain in the U.S. Air Force. After graduation, Captain Brittig will be assigned to the Air Force's climatological support unit located within the National Climatological Data Center (NCDC) in Asheville, North Carolina.

ACKNOWLEDGMENTS

TABLE OF CONTENTS

LIST OF TABLES

LIST OF FIGURES

vii

.

CHAPTER 1. INTRODUCTION

1.1 INTRODUCTION

Visual Air Quality (VAQ) has become a major concern not only in pristine areas such as

national forests, but in urban environments as well (Middleton et al., 1984). Good visual air

quality improves peoples' daily lives as well as improves many recreational opportunities such

as the enjoyment of national parks and monuments. When visibility is reduced by airborne

pollution, the human eye perceives a loss in color, contrast and detail; objects no longer appear

crisp and clear (Environmental Protection Agency (EPA), 1997a).

In 1952 Haagen-Smit first used the term "photochemical smog" to describe the mix of air

pollutants that arise in the Los Angeles area as a result of the oxidation of volatile organic

compounds (VOCs) or non-methane hydrocarbons (NMHC) and nitrogen oxides in the presence

of sunlight and water vapor. Tropospheric ozone is a product of this photochemical process.

Ozone, an oxidant itself, generates hydroxyl radicals (OH), which in turn influence the

concentration of trace gases and the production of fine particles (aerosols) which reduce

visibility.

Visibility reduction is caused largely by the presence of secondary fine particle aerosols,

produced by gas-to-particle conversion, whose production depends on the oxidizing capacity of

the atmosphere. The rate of this oxidation is dependent on the availability of free radicals and

other oxidants such as ozone, hydrogen peroxide, and nitric acid. Ozone is important because of

its abundance, oxidizing capacity and its ability to produce free radicals.

Reductions in visibility occur when particles, and to a lesser extent gases, scatter and absorb

light; this process is known as light extinction. Aerosol fine particles between 0.1 and 1.0 μm in

diameter are most effective on a per mass basis in reducing visibility (Friedlander, 1977).

Visibility can be associated indirectly to atmospheric loading (the amount of airborne

1

constituents) through the use of Koschmeider's equation which relates visual Range to light extinction. It is therefore hypothesized that the *ozone* produced in a polluted environment reacts to produce free radicals - in addition to its own oxidizing capacity - which increases the oxidizing capacity of the atmosphere and helps to convert primary precursor pollutants (i.e., SO_2) into visibility reducing fine aerosol particles (i.e., SO_4^{2-}). This reduction of horizontal visibility due to atmospheric aerosols has been suggested as a possible indicator and method for monitoring pollution. Middleton (1997) has recommended further analysis on the relationship between ozone and air quality variables (such as visibility) for summertime pollution episodes.

1.2 BACKGROUND

Ambient ozone concentrations found in the lower atmosphere (i.e., troposphere) continue to be a major air pollution problem in the United States (National Resource Council (NRC), 1991). Despite significant efforts over the past two decades to control tropospheric ozone, ambient ozone concentrations continue to exceed the ozone standard established by the EPA in many parts of the country. This is particularly true in the eastern United States where 40 percent of the nation's nonattainment areas are found (Rao et al., 1996; Aneja et al., 1991).

Ozone, a secondary gas pollutant, has been designated a criterion pollutant by EPA's Clean Air Act. Ozone is highly membrane reactive and is harmful to both plants and animals. Health effects to humans range from eye irritation to asthmatic episodes, while the effects to vegetation have resulted in crop loss estimated in the billions of dollars (Southern Oxidant Study (SOS), 1994).

Of primary interest in this investigation, is the role ozone plays in affecting visual air quality or visibility. Visual air Quality (VAQ) is often refered to in terms of visual range, the farthest

distance a person can visually separate an object from its background; or in terms of light extinction, the ability to scatter and absorb light energy.

The EPA has designated National Ambient Air Quality Standards (NAAQS) under the Clean Air Act of 1970 as a measure of the overall air quality. The standards were designed to protect human health and environmental welfare with respect to six "criteria pollutants": Lead (Pb), Sulfur Dioxide (SO_2), Carbon Monoxide (CO), PM10 (Particulate Matter of less than 10 microns diameter), NO_X (Nitric Oxide (NO) and Nitrogen Dioxide (NO_2)), and Ozone (O_3). For ozone, the NAAQS is based on a one hour average concentration; for which the standard is 0.12 parts per million by volume (ppmv). In addition to naming these criterion pollutants and establishing threshholds, Congress in its 1977 Clean Air Act Amendments declared a national visibility goal by calling for "the prevention of any future, and the remedying of any exsisting, impairment of visibility in mandatory class I Federal areas which impairment results from manmade air pollution."

In 1980, the first phase of the EPA's overall visibility protection program was set in motion to address reductions in visibility attributable to small group sources. These smaller local-scale impairments are generally defined as a plume or layered haze from a single source or group of small sources (Gray and Kleinhesselink, 1996). On the other hand, regional haze impairs visibility over large areas and in all directions. It is difficult to determine a source from this type of regional visibility reduction.

The EPA avoided action addressing the regional haze problem until further research had been conducted, including the relationship between visibility impairment and emitted pollutants (EPA, 1997a). The EPA is currently deliberating over new proposals to change the NAAQS for ozone and particulate matter. Although the motivation behind this move is primarily health related, the consequences to visibility should be noticable.

3

The mix of air pollutants that arise as a result of the oxidation of volatile organic compounds (VOCs) or of non-methane hydrocarbons (NMHC) and nitrogen oxides in the presence of sunlight and water vapor, is known as "photochemical smog." Photochemical smog is now recognized to be responsible for the high *ozone* levels typically found in areas with large VOC and nitrogen oxides (NO_x) emissions and adequate sunlight (where $NO_X = NO + NO_2$) (Lindsay et al.,1989).

VOCs and NO_x are often found together in the urban environment as pollutant products from automobiles. They are also produced from biogenic emissions: hydrocarbons are emitted from plants; NO_X from soils, particularly from fertilized soils (Penkett, 1991; Aneja and Robarge, 1996). Up to 25% of NO_x is estimated to be emitted from agricultural fields (Sullivan et al., 1996), while as much as 50% of hydrocarbons are thought to be emitted from plants and trees in rural areas of the southeastern United States (Chaimeides, et al., 1988).

Tropospheric ozone is of interest in this study due to its oxidizing capacity and ability to produce free radicals. Ozone plays a large role in generating hydroxyl radicals (OH), which in turn influence the concentration of many other trace gases and fine particles which reduce visibility (Moy et al., 1994; Mathur et al., 1994).

1.3 OZONE FORMATION

Ozone is produced when the sun's ultraviolet radiation dissociates the NO_2 molecule found in the atmosphere into an NO molecule and an oxygen atom, $O(^3P)$. This oxygen atom combines with a free oxygen molecule, O_2, to produce ozone. In an idealized photostationary state, one free of significant ambient hydrocarbons, the dissociated NO will react with the newly formed O_3 to reform NO_2 and an oxygen molecule. In this process all reactants are recycled and there is no net accumulation of ozone (figure 1.1).

Unfortunately, the idealized photostationary state is disrupted with the introduction of hydrocarbon emissions (pollutants) into the atmosphere. Hydrocarbons will react with the abundant free hydroxyl radicals, OH, to produce hydrocarbon radicals which in turn react with O_2, producing a peroxy radical. This highly reactive peroxy radical quickly and preferentially reacts with the previously disassociated NO, removing the pathway for ozone to be recycled. Here, the net result is an accumulation of tropospheric ozone (figure 1.2).

Ozone generates a substantial amount of free OH radicals which in turn influences reaction rates and concentrations of other pollutants. These reactions are not only a function of chemical reaction rates and and chemical pollutant precursor abundance, but also of environmental conditions which affect the mix within an airmass (King and Vukovich, 1982).

The species and concentration of ozone precursors transported with or emitted into an airmass often change during a pollution episode and affect ozone levels. Episodes of high ozone concentrations are often associated with slow moving or *stagnant high pressure systems* which allow large residence times for the oxidation of pollutants. These systems are often associated with high concentrations of other non-ozone producing chemical pollutants such as sulfur dioxide (SO_2), which when oxidized produce fine particle matter which reduces visibility (NRC, 1991; Vukovich et al.,1977). These high pressure systems are also characterized by widespread subsidence which compresses and warms the air, increases stability and decreases the potential for convective mixing of precursor pollutants. Subsidence impedes the formation of clouds which in turn increases the solar radiation component needed for ozone production. The low speed winds associated with high pressure systems also help preserve the polluted air mass, allowing the sun to "cook" the mixture more effectively. As the slow-moving or stagnant air in these high pressure systems passes over metropolitan and/or industrial areas, pollutant concentrations rise, and as the air slowly flows around the high-pressure system, the

photochemical production of ozone occurs at peak rates (NRC, 1991); as does the production of visibility reducing secondary pollutants. King and Vukovich (1982) have shown in their work that the concentration of ozone within these high pressure systems is a function of residence time as well as air mass origin (polluted vs. pristine). The back trajectory analysis as part of this investigation also substantiates these results.

Cleansing of tropospheric ozone on the other hand, generally occurs during *low-pressure* episodes when the weather associated with low pressure and rising motion assist in the removal of chemical pollutants and fine particles alike. Cold fronts, clouds and precipitation (wet deposition), higher speed winds (capable of mixing the airmass), cooler temperatures and higher relative humidity all act to decrease ozone concentrations (O'Conner, 1996; Logan, 1989).

Additionally, the dry deposition of O_3 through molecular diffusion, eddy diffusion and turbulence occurs and reduces concentration levels. Photolysis of ozone as it reacts with NO, NO_2, and hydrocarbons also serve as an ozone sink.

1.4 AEROSOLS

An aerosol particle is formally defined as a solid or liquid particle mostly consisting of some substance other than water, and without the stable bulk liquid or solid phases of water on it (Vali, 1985). Aerosols are formed either by the conversion of gases to particles or by the disintegration of liquids or solids. Formation through gas-to-particle conversion tends to produce finer particles than by the disinegration process, usually less than one micron (1μm); a size range critical to visibility reduction (Friedlander, 1977). In the atmosphere, precurser pollutant gases which convert to fine particle aerosols include: SO_2, NO_2, olefins and ammonia (NH_3). Gas-to-particle conversion takes place either by homogeneous nucleation - the formation of many tiny *new* particles (<100 angstroms in diameter), or by heterogeneous nucleation - condensation on

6

existing nuclei (Friedlander, 1977). All fine particle aerosols, except soot, have their origins primarily as pollutant gases. Fine particle aerosols which affect visibility include: sulfates, organics, nitrates, and soot (elemental carbon particles). These ambient sulfates, nitrates and organics are secondary particulate matter; produced in the atmosphere through oxidation mechanisms from primary pollutants and reactive organic species. Additionally, the contribution of natural non-methane hydrocarbons (NMHC) to the aerosol mass is likely to be very significant, especially in the Southeast where emissions of terpines and other hydrocarbons are large (Jonas, 1996). Global emissions of natural NMHCs has been estimated to be 700Tg/yr (1 $Tg = 10^{12}g$), of which about 10% may be converted to aerosols (Andreae, 1995).

In addition, there can be a substantial amount of particle-bound water depending on the relative humidity which can increase the size and scattering efficiency of the particle (Malm, 1994).

Cleansing of *aerosols* from the atmosphere occurs in much the same way as ozone cleansing, either by precipitation (wet deposition) or uptake at a surface (dry deposition). However, the efficiency of these processes depends largely on aerosol particle size, especially in the diameter range 0.1 - 10μm (Friedlander, 1977). Particles in this size range are removed mostly by wet deposition. While larger aerosol particles are removed mostly by settling (dry deposition). The time an aerosol particle spends in the atmosphere is a complex function of of its physical and chemical composition and of the time and location of release.

1.5 OXIDATION OF PRECURSER GASES

As mentioned earlier, the sulfate aerosol (SO_4^{2-}) is the result of the gas-to-particle conversion and oxidation of SO_2. Likewise, the nitrate aerosol (NO_3^-) results from the oxidation of the

primary pollutant NO_2 emitted by automobiles and fossil fuel combustion (Friedlander, 1977).

The source for the primary pollutant SO_2 includes the combustion of gasoline, refining of crude oil and the combustion of heavy fuels such as coal.

The reduction in visibility is caused largely by the presence of secondary fine particle aerosols and other gases which depend on the oxidizing capacity of the atmosphere for their production. The rate of this oxidation is largely dependent on the availability of free radicals and other oxidants such as ozone, hydrogen peroxide, and nitric acid. Ozone is the most important because of its great abundance in the atmosphere compared to the other oxidants. Low visibility pollution episodes (regional haze, photochemical smog) contain high concentrations of these oxidants, mainly ozone and peroxidic compounds which were produced by photochemical reactions (Warneck, 1988). They also contain large numbers of free radicals. The most important free radical responsible for the oxidation of many trace gases, and subsequent production of visibility reducing aerosols is the hydroxyl radical (OH). The hydroxyl radical is produced by a photochemical process. An important source of the hydroxyl radical is the photolysis of ozone:

$$O_3 + h\nu \rightarrow O^1D + O_2$$
$$O^1D + H_2O \rightarrow OH + OH$$
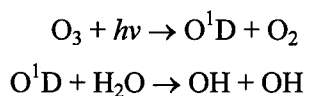
It is therefore hypothesized that the production of ozone in a polluted environment reacts to produce free radicals which increases the oxidizing capacity of the atmosphere and readily converts selected primary precurser pollutants (ie. SO_2) into visibility reducing aerosol particles. Additionally, ozone itself, like the OH radical, is an oxidant strengthening this conversion process. Ehhalts' 1991 investigation has shown a correlation between ozone photolysis and the

concentration of OH radicals. Given these known relationships between: ozone, free radicals, aerosols, and visibility; a similar relationship should be observed in actual data.

1.6 VISIBILITY

Reductions in visibility occur when particles and gases in the atmosphere scatter and absorb light. An abundance of suspended particles and gases creates a hazy appearance, a decrease in contrast, and a change in the perceived color of distant objects (PAB). Rayleigh scattering is scattering from molecular sized particles and is the reason the sky in a clean atmosphere appears blue. The constituent *molecules* in the air scatter out the blue wavelengths of light. Rayleigh scattering by molecules in clean air accounts for about 10 percent of the scattering and absorption estimated by the Southern Appalacian Mountain Initiative (SAMI) a test area located within our southeastern study region (Gray and Kleinhesselink, 1996).

Scattering by aerosol particulate matter of the same diameter as the wavelength of light (about 0.52 μm) is called Mie scattering and is responsible for most visibility degregration. Aerosol fine particles, including sulfates and nitrates, between 0.1 and 1.0 μm in diameter are most effective on a per mass basis in reducing visibility (Jonas, 1996; Waggoner et al.,1981). This size range of particles is known as the *accumulation mode*; a size range in which the smaller nucleation mode particles (< 0.02μm) produced by gas-to-particle conversion accumulate their mass by Brownian diffusion. The effects of Brownian diffusion decrease as the particle grows. As such, particles approaching diameters 1 μm in diameter are unable to grow further through diffusion; the result is an accumulation of particles less than 1 μm and larger than 0.1 μm. As already mentioned, this accumulation mode is the size range most effective on a per mass basis for visibiliity degregation.

The human ability to see through the atmosphere (visibility) depends on the concentration of suspended particles and gases, which scatter and absorb light. Visibility can be associated indirectly with this atmospheric loading (b_{ext}, the amount of airborne constituents affecting visibility) through the use of Koschmeider's equation which states:

$$X = 3.912 / b_{ext}$$

Where: X= visual range of maximum contrast discernability between a target and

its background.

b_{ext} = light extinction = sum of light scattering and absorption by airborne

constituent particles and gas.

In this study we will not excpicitly utilize Koschmeider's equation, but only infer relationships from the equation.

Recent data show that on median visibility days, the sulfate aerosol accounted for 60 percent of the extinction (Malm, 1994). On polluted days, sulfate contibutes between 70 and 80 percent to extinction (Gray and Kleinhesselink, 1994). Gray and Kleinhesselink (1996) report other minor contributers to low visibility pollution episodes as well; organics contribute between 11 to 20 percent to extinction, nitrates (a more common problem in other regions such as the western United States) contribute between 5 to 13 percent to extinction; and soot particles (elemental carbon) contribute between 4 to 11 percent to extinction. However, even though aerosols such as sulfate are major contributors to reduced visibility, their reduction does not necessarily produce an improvement in visibility as shown by Cass (1979) in his study of the Los-Angeles Basin. Clearly, other air contaminants must contribute to impaired visibility too. These include primary particulate emissions, such as *soot*, as well as primary precursor emissions of NO_x SO_x, and VOCs (Farber et al.,1994).

The scattering and absorbing charicteristics of carbon particles (*soot*) depend on the proportion of elemental and organic carbon. Man-made soot particles contain mainly elemental carbon and contribute more to the reduction in visibility than do natural soot particles (Hiddlemann et al., 1991). It is important to note that none of these primary pollutants, SO_2, NO, CO, and most organics (except aldehydes) are important *absorbers* of visible radiation. *Scattering* is the dominat process. NO_2 is the only significant absorber of visible radiation; and is only a factor in urban areas.

It is through the gas-to-particle conversion process and oxidation of these pollutants that significant visibility-reducing secondary species are produced. Diederen et al.'s (1985) results of a two year study in the Netherlands clearly show a relationship between visibility, particulate matter and ozone (figure 1.3). Modeling runs by King and Vukovich (1982) also suggest that lowest visibility correlates best with peaks in SO_4^{2-} (fine particulate matter), TSP (total particulate; includes fine particulate matter), and ozone.

The restriction of horizontal visibility due to haze and other atmospheric aerosols has been suggested as a possible indicator and method for monitoring pollution episodes (Diederen et al., 1982; King and Vukovich, 1982). Middleton (1997) recently recommended further analysis be conducted on the connection between ozone and air quality issues (visibility) for summertime pollution episodes in order to better understand the process.

The degregation of visibility is the most readily percieved indicator of air pollution. The advantage of using humanly observed visibility data as a measure of pollution is that this data source is in great abundance. The disadvantages associated with this method include the fact that visibility is not *directly* related to atmospheric loading by pollutants and aerosols, to nonuniform or nonideal range conditions , and to different human capabilities among observers.

Nonuniform skys and nonblack targets represent conditions which can drastically alter visibility observations under invariant pollution concentrations (Weintraub and Saxena, 1988). The threshhold of human visual perception is also a limitation. Even though there may be actual changes in visibility, the human eye is often unable to discern the difference. Studies have shown visual range changes as large as 40% have gone unnoticed by human observers in urban landscapes such as Los Angles (Farber, 1994). Significant reductions in fine mass particles will therefore result in only small observed changes in visibility (Farber, 1994).

Finally, the tendency of observers to discern more carefully visibility less than seven miles is greater because of the consequences to aviation safety. This phenomenon has been observed in our data and is displayed in figure (1.4). Notice the steady increments observed below seven miles compared with the erratic nature of the observations above seven miles. This does suggest that greater effort and care went into visibility observations equal to or less than seven miles. This is especially interesting given that actual non-polluted background visibility for the eastern United States is estimated to be between 59 and 93 ($\pm$ 30) miles (Gray and Kleinhesselink, 1996), far greater than what is observed in our data.

High relative humidity can also reduce visibility. Relative humidity itself does not degrade visibility; it is the affinity of water to some particles (like SO_2 and NO_x) which causes the particles to grow by condensation, therefore increasing the scattering cross section. The greatest variations of aerosol extinction due to meteorology are caused by varying relative humidity. Both the size distribution and the refractive index are modified by changes in the relative humidity (Friedlander, 1977). Chemical speciation of aerosol particles also helps determine the chemical-optical characteristics of a particle and its ability to grow by condensation (Malm, 1994). Therefore, some particles, especially sulfates, accumulate water and grow to a diameter near that of the wavelength of light and become more effective light scatterers. Because of their

12

chemical properties, and the efficiency with which sulfates and nitrates scatter light, these aerosols contribute more to the reduction of visibility than their mass concentration alone would indicate (Friedlander, 1977).

Deideren et al.'s study in the Netherlands concluded that the relative influence of relative humidity on visibility is independent of the mass concentration of the aerosol. The influence of mass concentration was found to be more pronounced than the influence of relative humidity alone by about a factor of two (Diederen et al., 1985). Additionally, in Derek's (1990) study of Southern England, the author concludes that annual trends in summer visibility show no significant differences between "all days" and "non-rain days", suggesting that meteorological influences are not paramount.
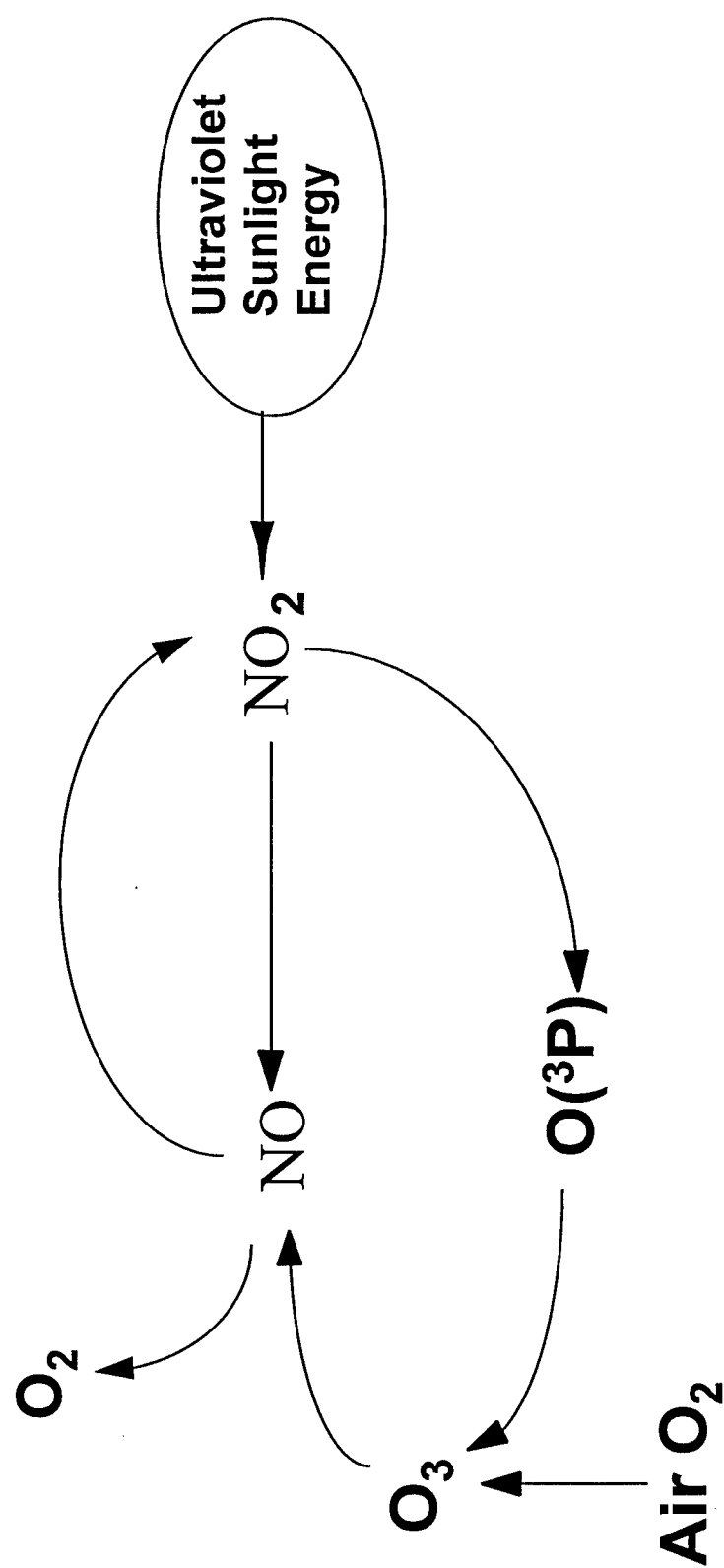
Figure 1.1. The idealized photostationary state's net result is no ozone accumulation.
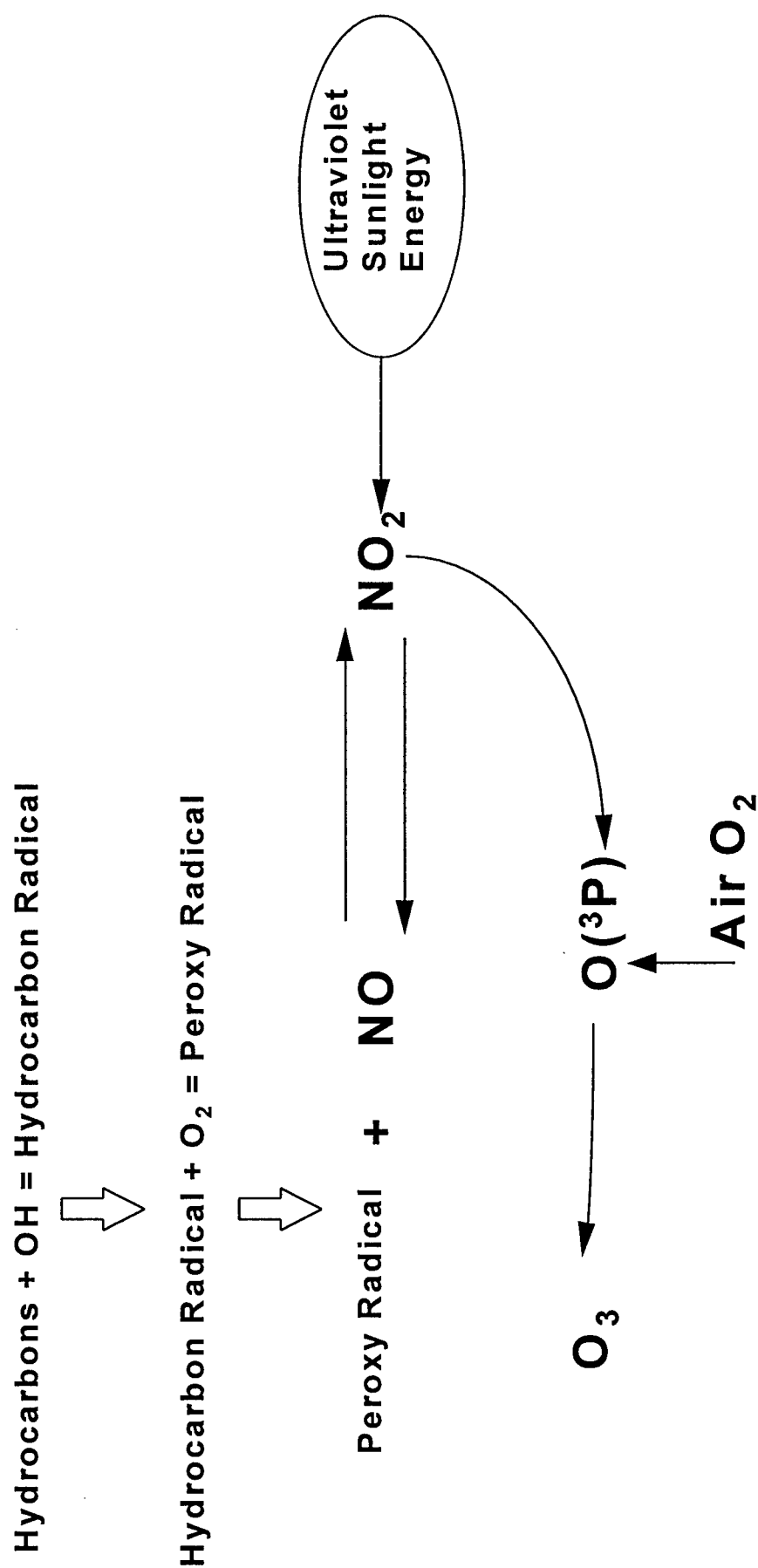
Figure 1.2. The idealized photostationary state is disrupted with the introduction of hydrocarbons into the atmosphere; net result is an accumulation of ozone.

15
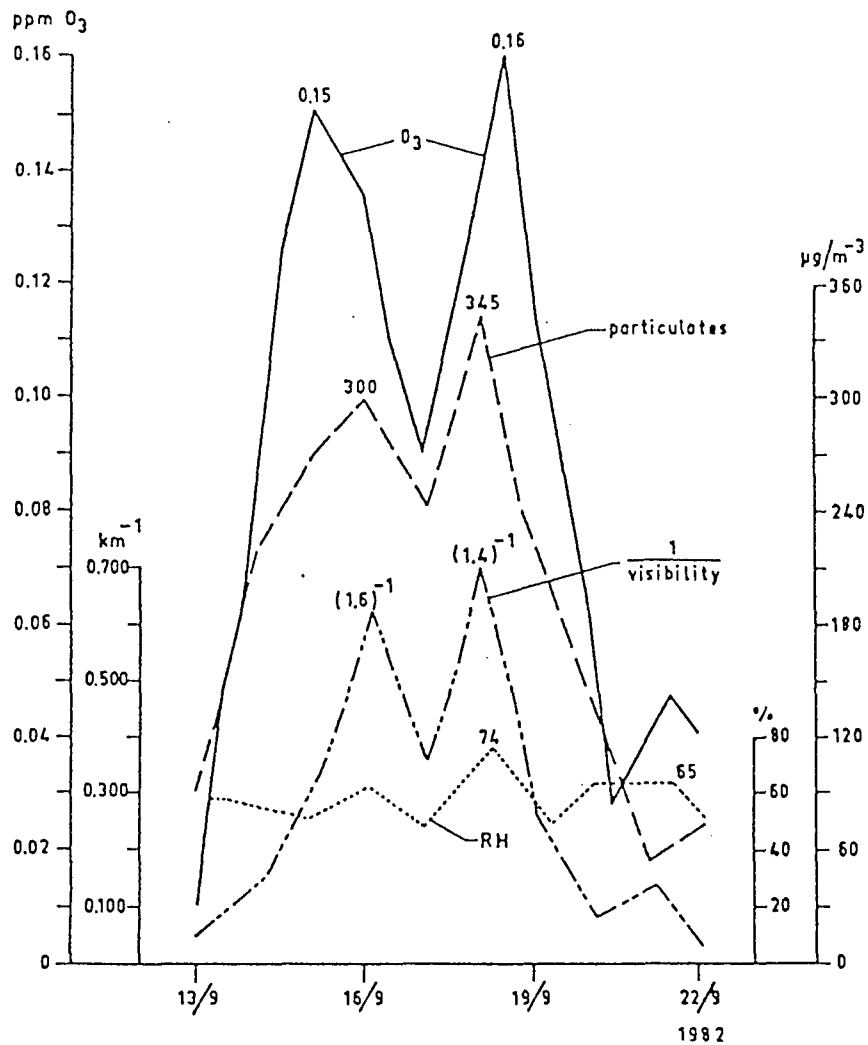
Photochemical oxidant episode of September 1982. Trend of daily
maximum O_3 concentrations, FPM loading, $\dfrac{1}{\text{visual range}}$ and r.h.

Figure 1.3. Diederen's (1985) results of a two year study in the Netherlands clearly show a relationship between visibility, particulate matter and ozone
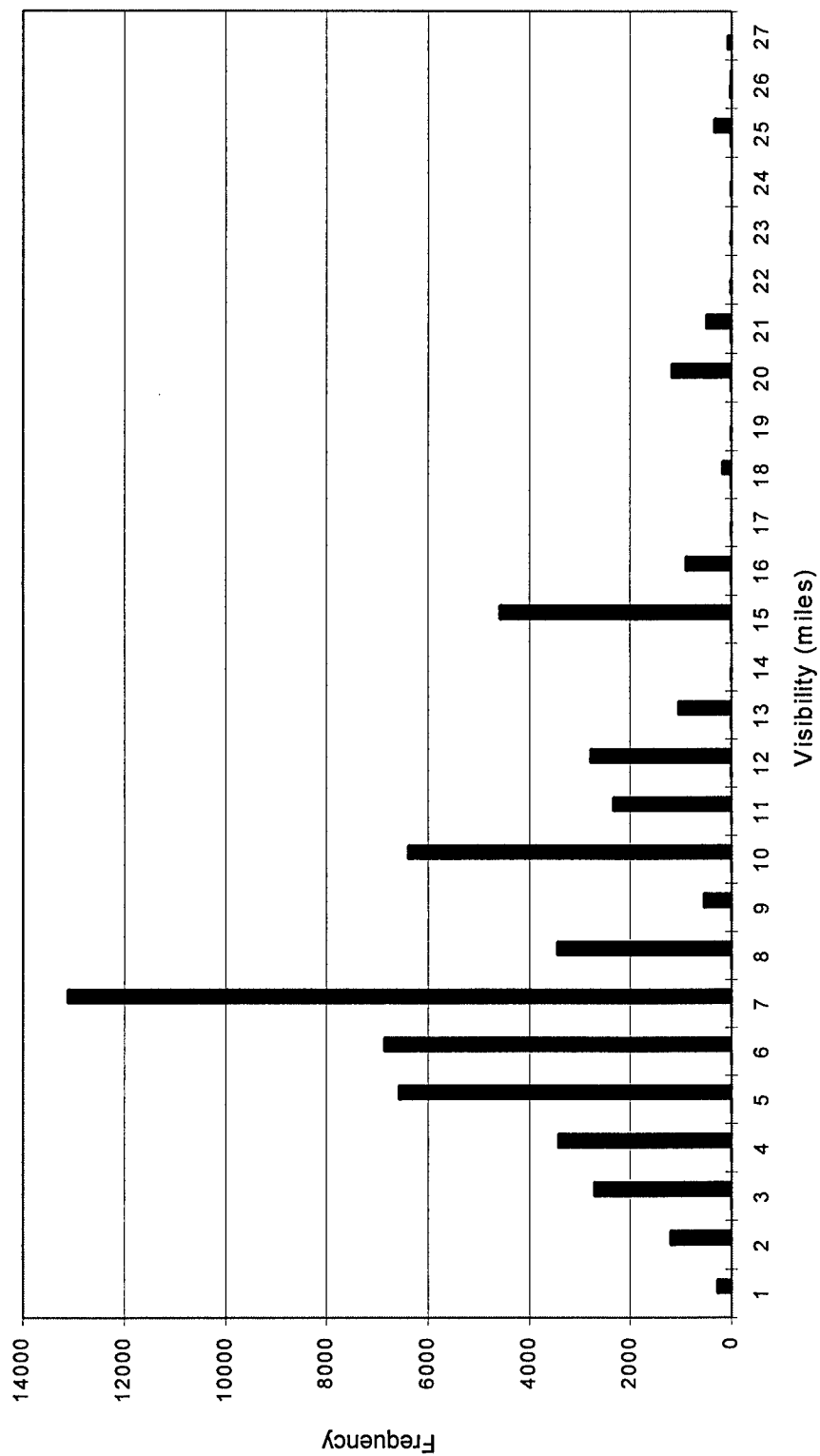
Figure 1.4. The tendency of observers to more carefully discern visibility less than seven miles is observed in the data. Notice the steady increments observed below seven miles compared with the erratic nature of the observations above seven miles indicating that greater effort and care went into visibility observations equal to or less than seven miles.

CHAPTER 2. DATA RETRIEVAL

2.1 STUDY PERIOD

In this work, nine sites in five different metropolitan statistical areas (MSAs) throughout the

Southeast United States were analyzed for ozone, meteorological trends, and visibility during a

seventeen year climatology (1980-1996).

Ozone formation in the lower troposphere is photochemically dependent; because of this,

elevated ozone levels are most likely to occur during the summer during periods of peak

incoming solar radiation. O'Conner (1996) concluded that the best time to investigate ozone's

relationship to meteorological parameters in the southeast was from June to August between the

hours of 1000 to 1600 local. This period showed the greatest correlation between ozone and

other air quality-related variables.

O'Conner (1996) concluded that, "As the potential ozone season was extended beyond the

three-month time-frame the strength of the correlations between O_3 concentration and the

meteorological variables diminished." His work demonstrated that a three-month ozone season

is adequate to capture the meteorological variation present on high ozone days, and to analyze

the relationship between ambient O_3 concentrations and meteorological parameters. An ozone

season is therefore defined as the months of June, July, and August, and includes observations

from 1000 to 1600 local; the peak solar heating hours.

This study shall adopt these same time constraints while extending the study period by two

years. The large data period (17 years) provides adequate chemical and physical climatology for

the region, and also provides a wide variety of meteorological conditions and the opportunity to

study several high ozone episodes.

18

2.2 SITE SELECTION

Nine sites in five different Metropolitan Statistical Areas throughout the Southeast United States were used to represent the urban and semi-urban areas in the region; see figure (2.1). Urban and semiurban areas were utilized since they are the areas that are most often in noncompliance with the NAAQS for ozone. More than 60 cities in the United States remained in violation of the NAAQS in 1988, and of those more than 40% were in the south (Chameides et al., 1988). The Southeast has the highest summertime ozone concentration by region in the United States (Chameides and Cowling, 1995). The southeast's climatology is ideal for ozone formation because of the stagnant and hot summer conditions that restrict the mixing of pollutants, thus resulting in low-level ozone accumulation (Vukovich et al., 1977; Vucovich, 1994; Korshover, 1976; Chameides and Cowling, 1995). The region's dense vegetation, when coupled with hot summer climatology, result in anomalously high emissions of isoprene, terpenes, and other natural hydrocarbons which aid in the formation of ozone (Chameides and Cowling, 1995; Lamb et al., 1987; Penkett, 1991; Trainer et al., 1987, 1991). These conditions also lead to ozone induced low visibility episodes and therefore make an excellent study area.

2.3 OZONE DATA

Hourly averaged ozone data from 1000 to 1600 local were downloaded from the EPA's Aerometric Information Retrieval System (EPA-AIRS) database. Missing data were recorded as such (interpolated values were not inserted); therefore some of the daily averages are based on fewer than six data points.

The EPA assigns a 9 digit identification code to each of its monitoring sites; the first two digits identify the state, the next three digits identify the county, and the last four identify the specific site. For simplicity when referring to sites, and to utilize the same notation as in

O'Conner's work, a reduced form of identification is presented. A six or seven character code is assigned to each site, for which the first three characters are letters corresponding to the airport identifier from which the meteorological data were used, followed by three digits corresponding to the county; which may be followed by another letter if there is more than one site used in this study in that particular county. The site location information and land use designations given for each site in the following paragraphs were obtained from the EPA-AIRS database in Research Triangle Park, NC. This information is summarized in table (2.1).

"Site ATL089 (EPA #130890002; see figure 2.2) is located at 33.691°N and 84.273°W; about 14.5 kilometers (km) southeast of the center of Atlanta, GA in DeKalb County, on the DeKalb County Community College Campus, on land designated for commercial use. Meteorological data used in the analysis for this site was taken from The Hartsfield Atlanta International Airport, about 16 km west-southwest from the ozone monitoring site.

Site ATL247 (EPA #132470001; see figure 2.2) is located at 33.586°N and 84.067°W; about 32 km southeast of the center of Atlanta, GA in Rockdale County at Conyers Monastery, on land designated for agricultural use. Meteorological data analyzed for this site was taken from The Hartsfield Atlanta International Airport, about 30.5 km west-northwest from the site.

Site BNA037 (EPA #470370011; see figure 2.3) is located at 36.205°N and 86.745°W; about 5.5 km north-northwest of downtown Nashville, TN along the Cumberland River in Davidson County, on residential land. Meteorological data used in the analysis was retrieved at the Nashville International Airport, about 15.2 km southeast of the site.

Site BNA165 (EPA #471650007; see figure 2.3) is located at 36.298°N and 86.653°W; in Sumner County about 19 km northeast of downtown Nashville, TN. Meteorological data used in the analysis for BNA165 was collected at the Nashville International Airport, about 21 km

south of the site. The site is located at the Old Hickory Dam in Rockland Recreation Area and is designated as industrial land.

Site CLT119H (EPA #371190034; see figure 2.4) is located at 35.247°N and 80.764°W; about 8 km east of the center of Charlotte, NC in Mecklenburg County. It is located at the corner of Plaza Road and Lakedell Drive, and land use is designated residential. Meteorological data was recorded at the Charlotte-Douglas International Airport, about 16 km west-southwest of the site.

Site CLT119I (EPA #371191005; see figure 2.4) is located at 35.113°N and 80.919°W; about 14.5 km southwest of downtown Charlotte, NC, also in Mecklenburg County on land that used industrially. Meteorological data was collected at the Charlotte-Douglas International Airport, about 10.5 km north of the site.

Site CLT119J (EPA #371191009; see figure 2.4) is located at 35.348°N and 80.693°W; on NC Highway 29 North at the border of Mecklenburg and Cabarrus Counties. Located in Mecklenburg County, this site is about 19 km northeast of the center of Charlotte, NC on land designated for agricultural use. Meteorological data used in the analysis for this site was collected at the Charlotte-Douglas International Airport, about 26.5 km southwest of the site.

Site GSO081 (EPA #370810011; see figure 2.5) is located at 36.113°N and 79.704°W; in Keely Park on Keely Road in Guilford County. The site is about 9.5 km northeast of Greensboro, NC. The land use designation is residential. Meteorological data used the analysis for this site was collected at the Piedmont Triad International Airport, located in Greensboro about 21.5 km west-southwest of the ozone monitoring site.

Site RDU183 (EPA #371832001; see figure 2.6) is located at 35.971°N and 78.491°W; about 24 km northeast of the center of Raleigh, NC in Wake County. The site is located at the Wake Forest water treatment plant on NC Highway 98 on land that is designated for agricultural

use. Meteorological data used in the analysis for this site was collected at the Raleigh-Durham International Airport, about 24 km southwest of the site."(O'Conner, 1996)

2.4 METEOROLOGICAL DATA

As in O'Conner (1996), meteorological data were extracted from databases at the Air Force Combat Climatology Center (AFCCC) at Scott Air Force Base, IL. Since meteorological data were not available for precisely the same locations as each ozone monitoring site, meteorological data were taken from the nearest available reporting station for each MSA. The World Meteorological Organization (WMO) identifiers used to retrieve data for Atlanta, Raleigh, Charlotte, Greensboro, and Nashville were 722190, 723060, 723140, 723170, and 723270, respectively.

Specific meteorological values retrieved include hourly observations for: temperature, dewpoint temperature, visibility and Airways weather codes for visibilities less than seven miles. The method of observing visibility changed at several of the sites from the human observation of prevailing visibility, to an automated sysytem. An automated, instrumentally-derived visibility observation is a sensor value converted to an appropriate visibility value using algorithms and is representative of the prevailing visibility (Federal Meteorological Handbook (FMH) No. 1, 1997). The commissioning of these automated systems occurred during the last two years of the study at all study areas except Charlotte, NC.

Missing data were recorded as such (interpolated values were not inserted); therefore some of the daily averages are based on fewer than six data points. Relative humidity was calculated using Teten's formula, an often used replacement for the Clausius-Clapeyron equation. The equation was provided along with the data sent from the AFCCC:

$$e = 6.11 * 10**((7.5*T_d)/(T_d + 237.3))$$

$$e_s = 6.11 * 10**((7.5*T)/(T + 237.3))$$

$$RH = \frac{e}{e_s}$$

Where e_s = saturation vapor pressure (mb)

e = vapor pressure at dewpoint temperature (mb)

T = ambient air temperature (°C)

T_d = dewpoint temperature (°C)

RH = relative humidity (fraction)

2.5 DATA PREPERATION

Once the data had been retreived, they were processed and reduced utilizing the statistical software package SAS ® (SAS Institute, 1990a; SAS Institute, 1990b; Delwiche and Slaughter, 1995). Individual analysis methods will be detailed in the following discussions. This particular section will address the generic procedures applied to the data set as a whole before the procedural breakdown.

Since certain transient weather is known to cleanse (via wet deposition and scavenging) both visibility reducing fine particles and ozone from the atmosphere, hourly observations containing any form of precipitation (from drizzle (L) to thunderstorms (T)) were removed. Fog was not included in this precipitation-removal process, since the occurrence of fog was not expected to be a factor after 1000L; actual occurrence of fog was less than two percent. This precipitation-removal process was performed on the hourly observations before any other data reduction or manipulation occurred. The most noticeable consequence of this removal was that higher relative humidities, generally associated with precipitation, were removed. For purposes of

observing visibility relationships, this did not present a problem. In fact , it may have actually contributed to the ease in which the visibility-ozone relationship was observed in our daily and hourly analysis. However, this data editing lowered the averaged value of relative humidity seen in our regional and Nashville yearly averaged data. Table (2.3) shows the amount of data removed together with the precipitation type.

The data were then prepared to allow for a yearly statistical analysis of the entire region. First daily maximum ozone values were determined (using a modified SAS $^{®}$ Proc Means procedure which determined a maximum value from the 1000-1600 hourly observations). These daily maximum values, along with the daily averages of other meteorological variables were averaged by the same method by year to produce a regional yearly averaged summary statistic for each of the seventeen years in our study. A maximum daily value for ozone was chosen to better highlight periods of maximum ozone concentration, believed to better indicate periods when the effects of ozone-induced low visibility would be the greatest. Averages were used for the other variables since averages would help negate transient extreme values. In addition to producing yearly averages, the SAS $^{®}$ output from the Proc Means procedure also provided standard deviations for each variable. Daily averaged and yearly averaged data were then exported to an Excel$^{®}$ Spreadsheet to determine yearly trends and anomalies.

Yearly, daily, and hourly regression analyses were then performed utilizing the SAS Proc Regress Procedure. The analysis of variance output provided correlation coefficients, P-values, and test statistics necessary to perform hypothesis tests.

Table (2.1). Site Characteristics from O'Conner, 1995.

| Site Code Monitor ID	MSA (Metropolitan Statistical Area)	Lat. (°N)	Long. (°W)	Elev. (m)	Land Use Designation
ATL089 130890002	Atlanta, GA	33.691	84.273	305	commercial
ATL247 132470001	Atlanta, GA	33.586	84.067	219	agricultural
BNA037 470370011	Nashville, TN	36.205	86.745	165	residential
BNA165 471650007	Nashville, TN	36.298	86.653	143	industrial
CLT119H 371190034	Charlotte, NC	35.247	80.764	239	residential
CLT119I 371191005	Charlotte, NC	35.113	80.919	195	industrial
CLT119J 371191009	Charlotte, NC	35.348	80.693	255	agricultural
GSO081 370810011	Greensboro, NC	36.113	79.704	229	residential
RDU183 371832001	Raleigh, NC	35.971	78.491	87	agricultural
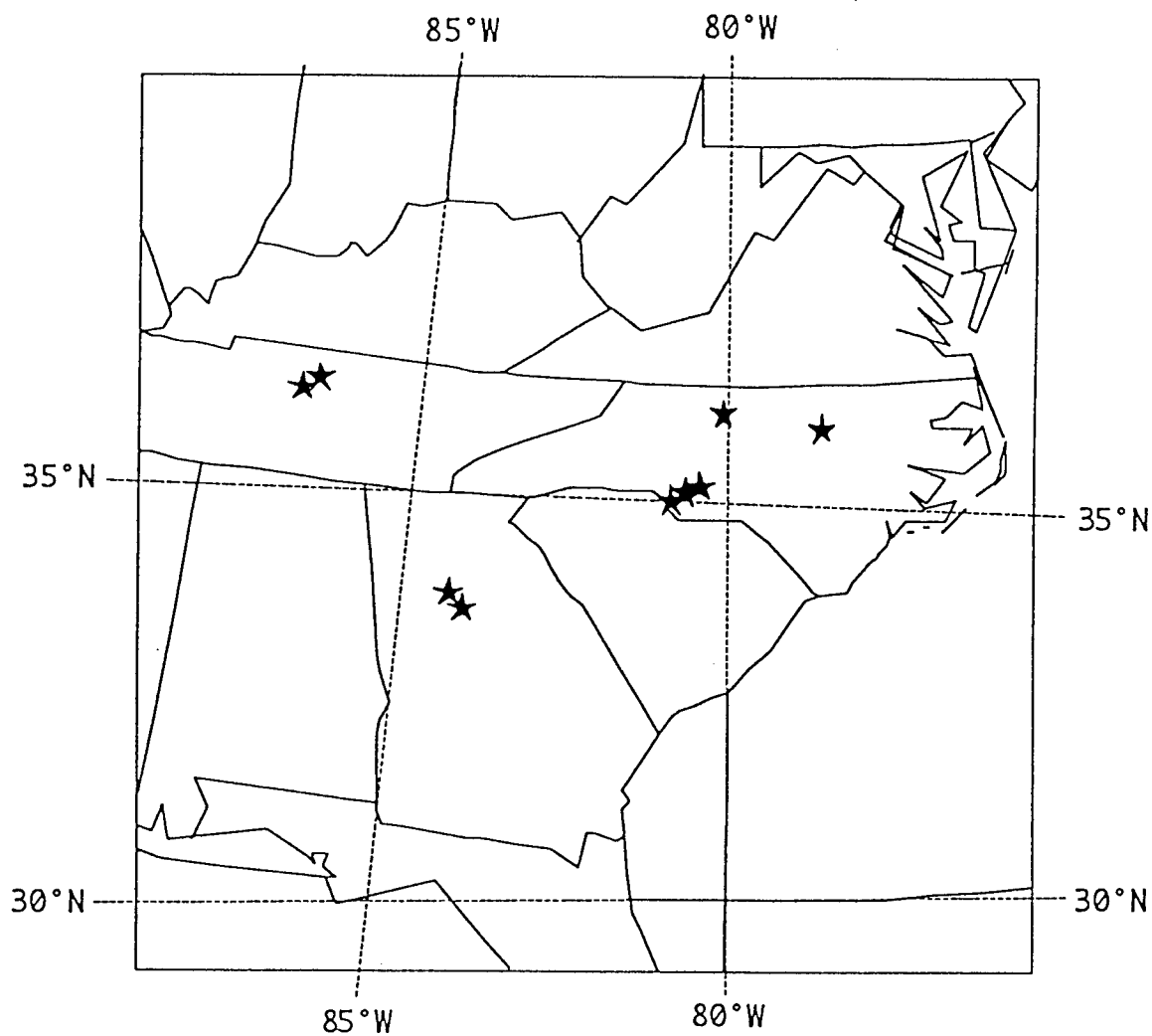
Figure (2.1) Regional map depicting sites used in the analysis. Nine sites were used in five different Metropolitan Statistical Areas (MSAs). Figures 2.2 through 2.6 show more detail on site location within each MSA (O'Conner, 1996).
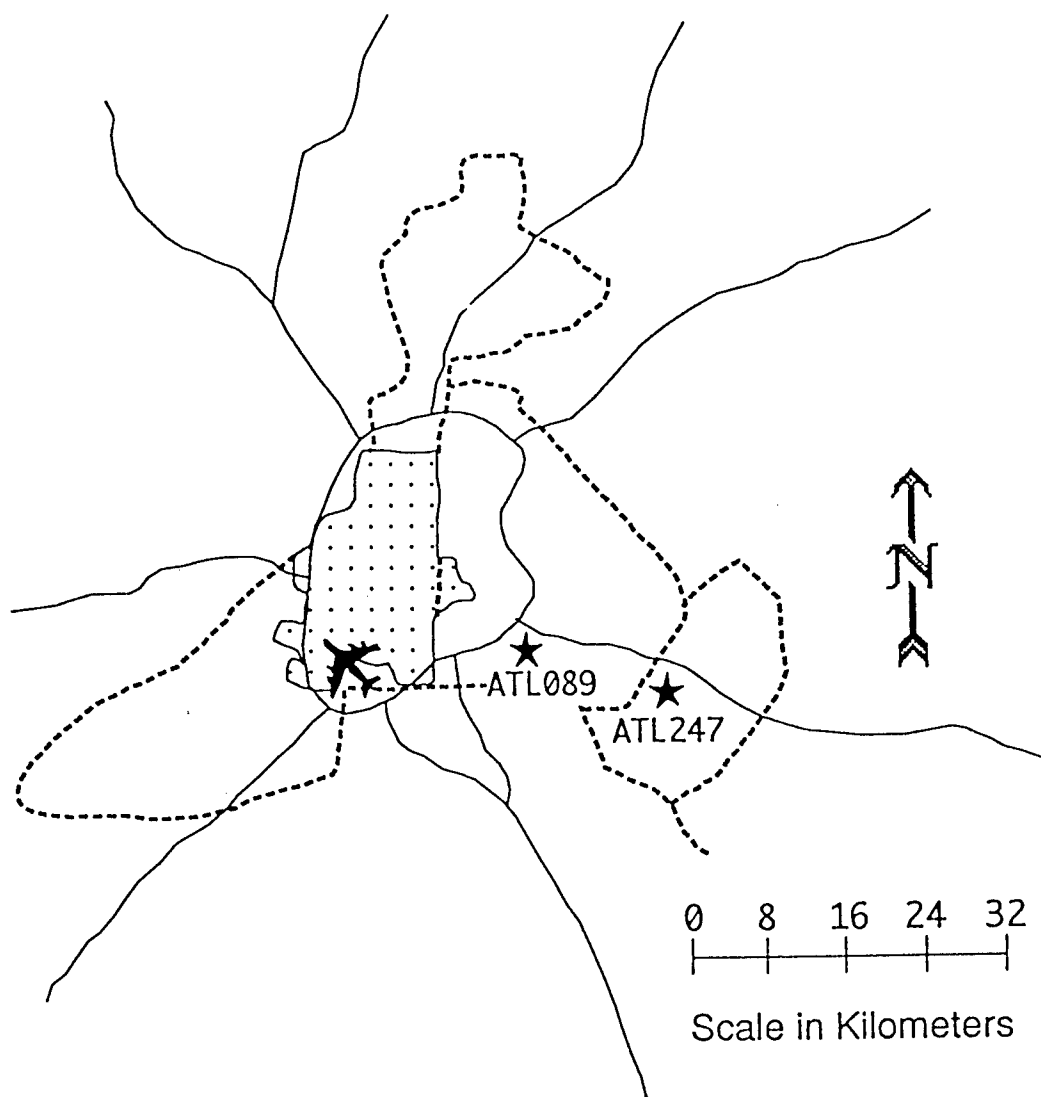
Figure (2.2) Map of Atlanta, GA Metropolitan Statistical Area (MSA) indicating location of US Environmental Protection Agency (USEPA) ozone monitoring sites used (stars) and World Meteorological Organization (WMO) weather station (airplane). The urban core is shaded with dots, dashed lines indicate county borders, thick solid lines represent major highways (O'Conner, 1996).

Figure (2.3) Map of Nashville, TN Metropolitan Statistical Area (MSA) indicating location of US Environmental Protection Agency (USEPA) ozone monitoring sites used (stars) and World Meteorological Organization (WMO) weather station (airplane). The urban core is shaded with dots, dashed lines indicate county borders, thick solid lines represent major highways. Dark shading represents major bodies of water (O'Conner, 1996).

28

CLT119J

CLT119I

CLT119H

0   8   16
Scale in Kilometers

Figure (2.4) Map of Charlotte,NC Metropolitan Statistical Area (MSA) indicating location of
US Environmental Protection Agency (USEPA) ozone monitoring the sites used (stars) and
World Meteorological Organization (WMO) weather station (airplane). The urban core is
shaded with dots, dashed lines indicate county borders, thick solid lines represent major
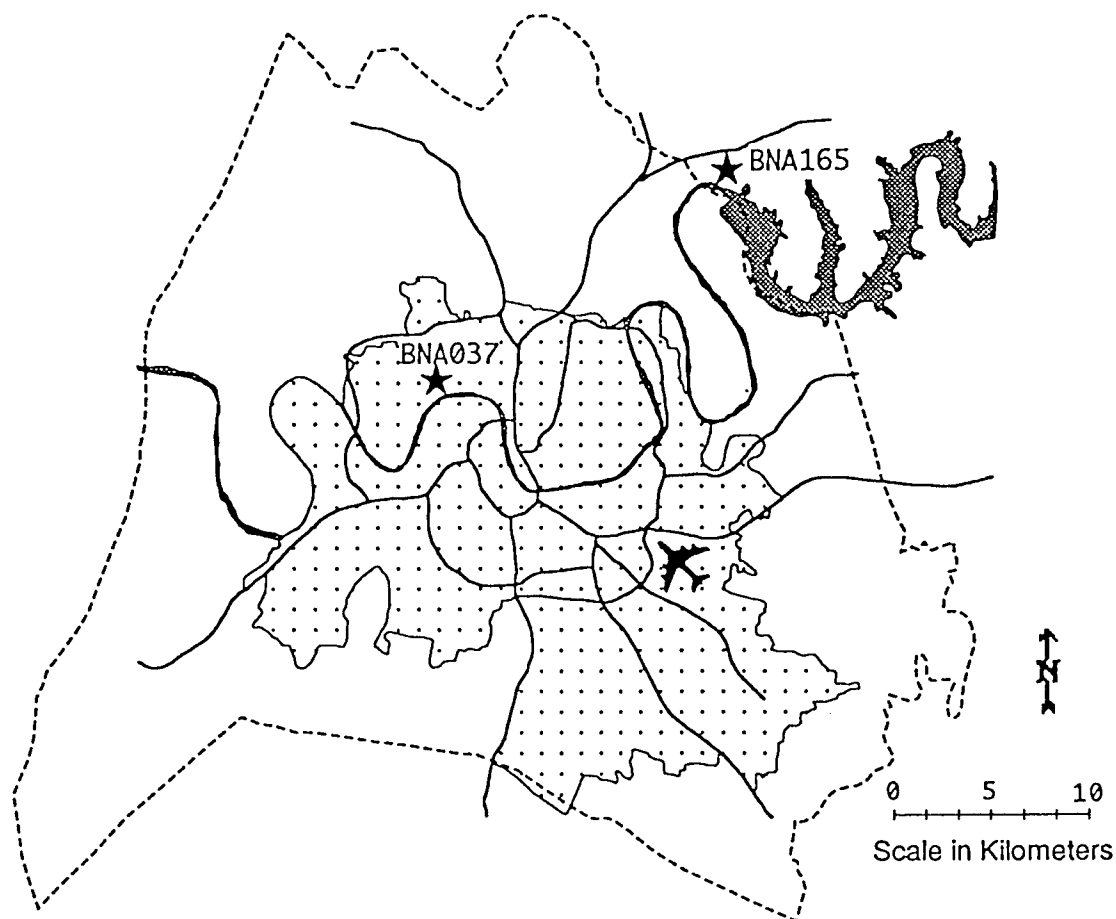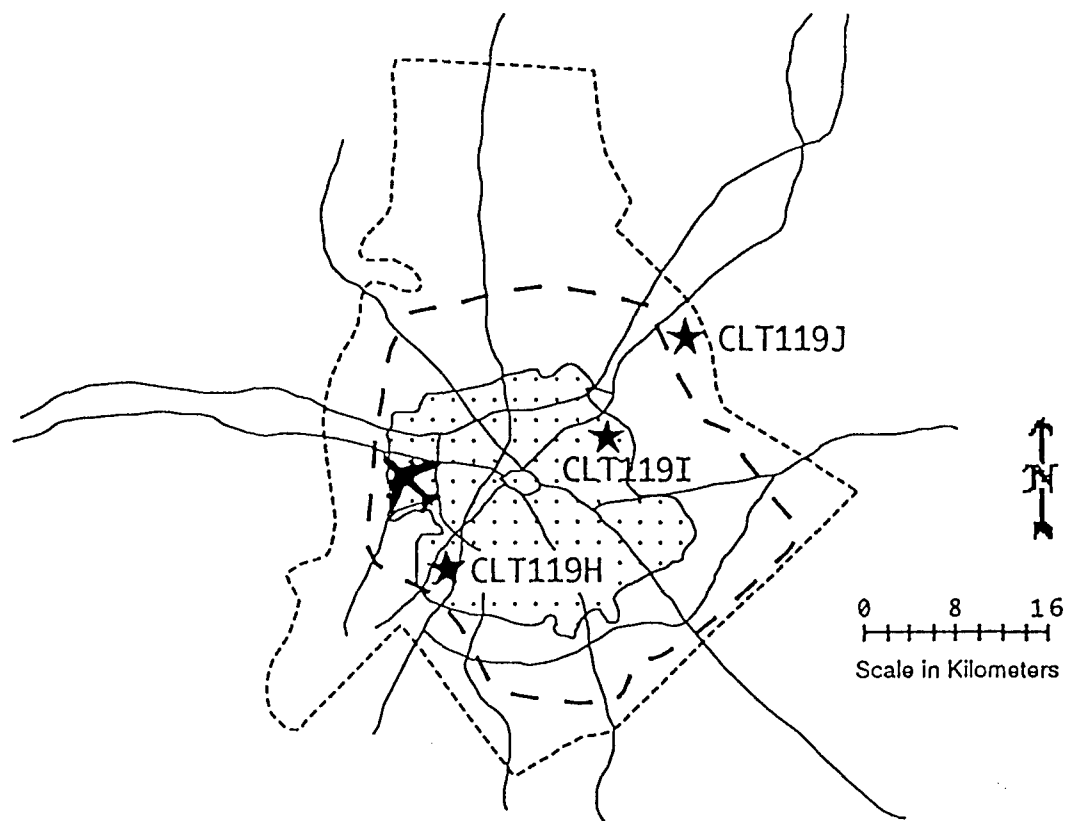highways (O'Conner, 1996).
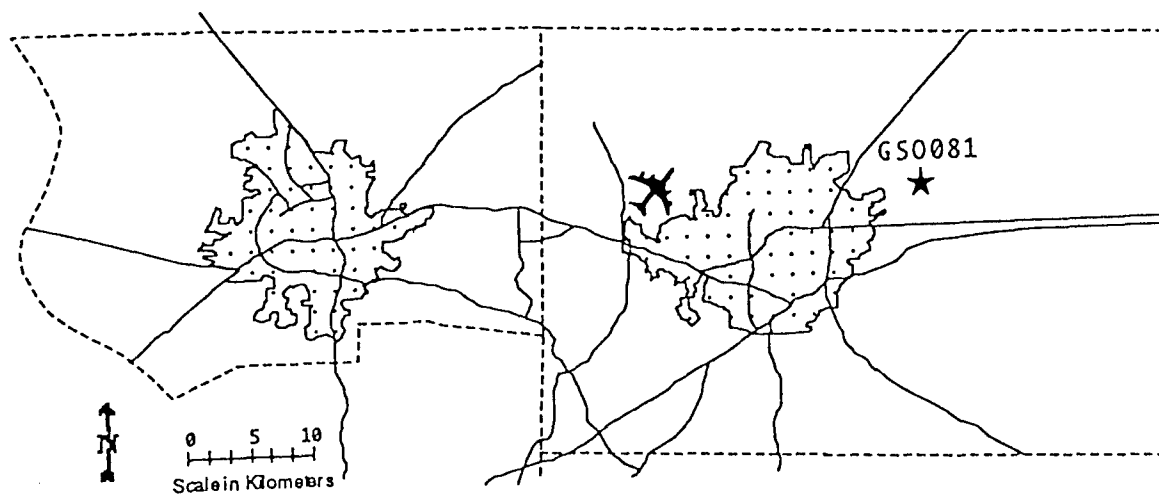
Figure (2.5) Map of the Greensboro - Winston Salem, NC Metropolitan Statistical Area (MSA) indicating location of US Environmental Protection Agency (USEPA) ozone monitoring site used (star) and World Meteorological Organization (WMO) weather station (airplane). The urban cores are shaded with dots (Greensboro is on the right, Winston-Salem is on the left). Dashed lines indicate county borders, thick solid lines represent major highways (O'Conner, 1996).

Figure (2.6) Map of Raleigh,NC Metropolitan Statistical Area (MSA) indicating location of US Environmental Protection Agency (USEPA) ozone monitoring the site used (star) and World Meteorological Organization (WMO) weather station (airplane). The urban core is shaded with dots, dashed lines indicate county borders, thick solid lines represent major highways. Dark shading represents major bodies of water (O'Conner, 1996).
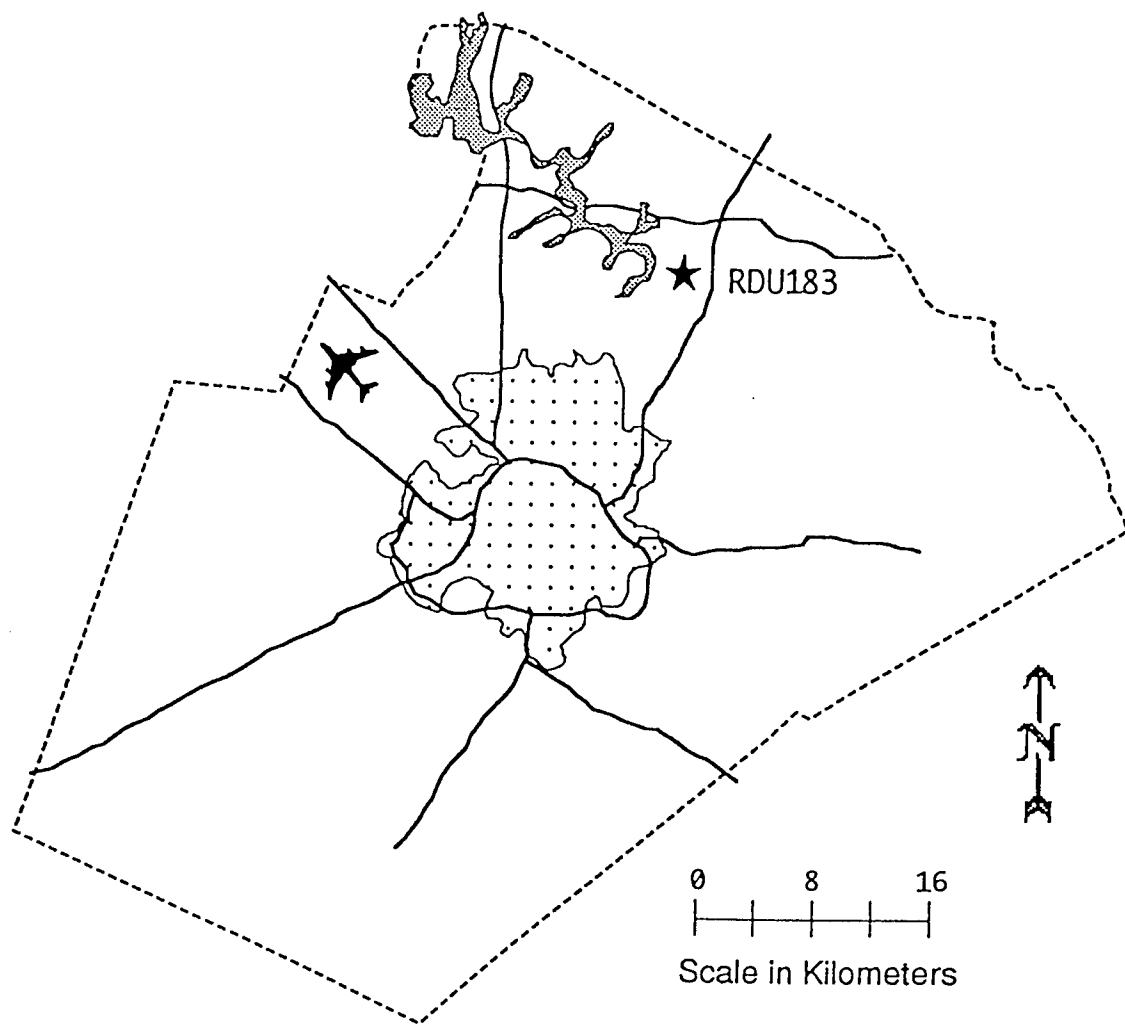
31

Table 2.2. Hourly observations containing any form of precipitation were removed. This reduction was performed on the hourly observations before any other data reduction or manipulation occurred. Five percent of the data were removed by this method.

Weather Type	Frequency	Description
L	23	L (drizzle)
LF	77	F (fog)
LFH	2	H (haze)
LH	2	
R	776	R (rain)
RF	730	
RFH	29	
RH	232	
RHF	1	
RHK	4	S (smoke)
T	425	T (thunderstorm)
TB	1	B (blowing dust, sand, etc...)
TBH	1	
TF	79	
TFH	7	
TH	197	
THF	3	
TLF	1	
TR	80	
TRF	32	
TRH	21	
Totals	2723	

CHAPTER 3.   ANALYSIS

3.1 REGIONAL YEARLY TRENDS

Long term trends for O_3 concentration have been analyzed by many other researchers. Oltmans and Komhyr (1986) noted that two remote northern hemispheric sites had positive trends in O_3 concentration from 1973 to 1984, while two remote southern hemispheric sites recorded negative trends during the same period. O'Conner's (1996) study of the Southeast showed an increasing regional trend during the 1980s and a decreasing regional trend during the 1990s (up to and including 1994).

O'Conner employed simple linear regression to the annually averaged seasonal maximum O_3 concentration for each decade to determine the trend in ozone concentration. The partitioning of the data into two decades, as is also done in this study, is meant to coincide with implementation of the EPA's Clean Air Amendment of 1990. Individual ozone trends for each site, collectively used to construct the regional trend, are presented in figure (3.1). The decreasing regional trend seen in O'Conners work for the 1990s levels off considerably in this study. The inclusion of data for 1995 and 1996, specifically at the Nashville sites, has changed the decreasing trend shown by O'Conner. For example, in O'Conner's work, all sites showed decreasing ozone trends in the 1990s up to and including 1994; data for 1995 and 1996 reverse this trend for at least two of the sites. The trend for the Raleigh site is misleading because data since 1993 is missing, which would result in an apparent upward trend during the 1990s, since a high O_3 year (1993) would be used as the last year in the regression analysis to determine the trend (O'Conner, 1996).

The overall regional ozone trend demonstrates that the average daily maximum ozone concentration appears to have increased during the 1980s (.0005ppmv/yr, r^2=.0497) and leveled off during the 1990s (-.00007ppmv/yr, r^2=.0007); however the trend, as was the case with all the *trend* analyses presented here, were not statistically significant (α=.05); see figure (3.2).

Statistical significance was determined by hypothesis testing (H_0: slope of trend = 0, H_1: slope of trend ≠ 0) utilizing a Student's-T distribution and test statistic via SAS[©] Proc Reg. Two-tailed significance probabilities (Prob > |T|) less than 0.05 (α =0.05) were considered statistically significant.

Regional visibility during the 1980s decreased (-0.0222miles/yr, r^2=0.0426) at a rate consistent with the increasing ozone. During the 1990s the trend increased (0.0802miles/yr, r^2= 0.3177); see figure (3.3). Regional temperature trends remained flat during both periods (1980s: 0.0285°F/yr, r^2=0.0032; 1990s: 0.0093°F/yr, r^2=0.0002); see figure (3.4).

Relative humidity trends decreased in the 1980s (-16.81%/yr, r^2=0.0203) and increase in the 1990s (27.86%/yr, r^2=.034); see figure (3.5). This is similar to visibility trends observed over the same period, but it does not fit the well-established and expected inverse relationship (visibility vs. relative humidity). However, other studies suggest the influence of relative humidity may not be the dominating factor affecting visibility (Diederen et al., 1985).

Ozone formation is a highly complex, non-linear reaction (NRC, 1988). Year-to-year fluctuation in the meteorology can easily mask and confuse its relationship to ozone. It has been recognized (Chameides et al., 1988; Lindsay et al., 1989; Logan 1989; O'Conner, 1996) that trends in ambient O_3 concentrations do not necessarily indicate that O_3 control strategies are attaining the desired result since interannual variation in meteorology may significantly affect the observed trend.

3.2 YEARLY REGIONAL ANOMALIES

Each variable's mean (ozone, visibility, relative humidity, and temperature) was calculated for the entire 17-year period and then subjectively compared against the respective yearly mean. The results were then plotted on a barograph to highlight anomalies by year. Ozone's inverse

relationship with relative humidity was evident in nearly all years; except for 1995 (94% of the time), see figures (3.6, 3.7). Likewise, the direct relationship between ozone and temperature was clearly evident, except for 1991; see figures (3.6, 3.8).

A consistent relationship between visibility and the other variables is not clearly evident in the anomaly analysis. Only seven of the 17 years show an inverse relationship between ozone and visibility (41%); see figures (3.6, 3.9). Eight of the years showed a positive relationship between visibility and relative humidity (47%) (figures 3.9, 3.7), while nine of the years revealed an inverse relationship between visibility and temperature (53%); see figures (3.9, 3.8). These ambiguous results suggest that the temporal and spatial resolution must be decreased to better understand and test our hypothesis.

3.3 NASHVILLE CASE STUDY

A site specific analysis of Nashville, TN was conducted utilizing both a yearly and daily summary. Nashville was chosen because it represented an area with more than one ozone measuring site. It also was an area experiencing increasing ozone concentrations as determined by the analysis and is currently in non-attainment according to EPA criteria.

The first step in the site specific analysis was to complete a regression analysis utilizing all Nashville hourly observations. A strong statistically significant inverse relationship between visibility and ozone was observed (P-value = 0.0001); however, the data were very noisy. See figure (3.10) for a scatter plot of the data. Further regression analysis is presented in section 3.3.3.

3.3.1 NASHVILLE YEARLY TRENDS

Nashville's ozone trend was positive in the 1980s (0.0013ppmv/yr, r^2=0.2244), and unlike the region as a whole, which leveled off during the 1990s, ozone continued to increase during the 1990s (0.0009ppmv/yr, r^2=0.0849); see figure (3.11). Nashville's visibility trend for the 1980s decreased (-0.902miles/yr, r^2=0.108) consistent with the rising ozone trend during the same period; clearly showing an inverse relationship. However, the inverse relationship is not as pronounced during the 1990s (0.0139miles/yr, r^2=0.0034); see figure (3.12). Temperature trends at Nashville were slightly positive during the 1980s (0.0387°F/yr, r^2=0.0035) and negative for the 1990s (-0.3616°F/yr, r^2=0.147); see figure (3.13). Relative humidity trends displayed a slightly negative slope for the 1980s (-13.79%/yr, r^2=0.009) and a relatively steep slope during the 1990s (109.8%/yr, r^2=0.3215); see figure (3.14). As previously mentioned, none of the trend analysis presented proved to be significant at or below the 5% level of significance, however the variances appeared to be constant over time, suggesting a consistent relationship.

3.3.2 NASHVILLE YEARLY ANOMALIES

Eleven of the seventeen years showed an inverse relationship between ozone and visibility (65% of the time); see figures (3.15, 3.16). Of those years not fitting this relationship, the relative humidity anomaly (figure 3.17) was noticeably different from the mean for that year; suggesting a strong influence of moisture on visibility.

Analysis of temperature versus ozone did not indicate a direct relationship for all years as it had in the regional analysis; see figures (3.15, 3.18). This suggests that warm days are more cloudy or that regional transport may play an important role in local ambient ozone concentrations and subsequent changes in visibility. Furthermore, there were large standard errors associated with the yearly averaged data. It is difficult to establish any noteworthy

relationships; especially with visibility, whose temporal variation is best evaluated on an hourly or daily -not yearly - basis.

3.3.3 NASHVILLE DAILY AVERAGED ANALYSIS

As was just stated, visibility's temporal variation is best measured in terms of days (or hours) not in years. Therefore, daily summary statistics were created for each day. These values were then normalized using the following method:

$C_i - C_{min} / C_{max} - C_{min}$

Where: C_i = the actual observed value

C_{min} = the minimum observed value for the period

C_{max} = the maximum observed value for the period

This method produced variables with values between 0 and 1, which could then be easily plotted and compared against one another. Normalized values of relative humidity were not included. They were not found to be a significant factor affecting visibility, since many of the high relative humidity days were purged along with precipitation events during the data reduction process.

Additionally, linear regression was used to analyze daily averaged and direct hourly observations for five arbitrarily selected above normal ozone years (based on yearly anomalies: 1980, 1983, 1988, 1990, 1995). The visibility and ozone relationship became evident in this *daily averaged* value analysis grouped by month; see table (3.1). Twenty-seven percent of these months displayed a statistically significant (α=0.05) inverse relationship. The three months exhibiting the best relationship were: July 1983, June 1988, and August 1990; see figures (3.19, 3.20, 3.21) respectively. Months exhibiting a poor relationship were July 1988 and August 1988; see figures (3.22, 3.24) respectively.

Regression analysis was also performed for Nashville utilizing *daily averaged* values grouped by year. The visibility and ozone relationship became more evident in this hourly

analysis. 71% of the years displayed a statistically significant (α=.05) inverse relationship between ozone and visibility; see table (3.1). Clearly the increased sample size (3 months per year vs. 1 month alone) is improving the statistical significance of the inverse relationship being investigated. Despite the statistical significance , the regression analysis was very noisy which led to R-squared values at or below 0.27.

3.4 AREA-SPECIFIC HOURLY REGRESSION ANALYSIS

3.4.1 OVERVIEW

Area-specific regression analysis was performed utilizing hourly observations falling within the ozone season for 1980, 1983, 1988, 1990 and 1995 and were grouped by month. Three months (the ozone season) for each year (except RDU for 1995) at four locations (excluding Nashville, since its analysis appears in section 3.3.3) yielded a sample size of 57 months (n = 57). Statistical significance was again determined through hypothesis (slope = or $\neq$ 0) testing utilizing a Student's T- distribution and T-test statistic (α =0.05). The visibility and ozone relationship again became clearly evident in these hourly observations as the next section shall demonstrate.

3.4.2 RESULTS

Seventy-two percent of the 57 months displayed a statistically significant *inverse* relationship between ozone and visibility. Four percent of the months showed a statistically significant *positive* relationship between ozone and visibility, while only 25% proved to be statistically insignificant. Table (3.2) displays a complete list of the months including their R-squared values. The regression analysis for these additional sites continued to be noisy which led to more low R-squared values.

Scatter plots of visibility vs. ozone were constructed for *August 1995* for Atlanta, Charlotte and Greensboro, and can be seen in figures 3.25, 3.26 and 3.27 respectively. These months were selected because of their relative high R-squared values. R-squared values for Nashville, TN were also high during this same time period. To gain additional insight and better understand the mechanisms affecting this analysis (especially August 1995), back trajectory analysis was conducted.

3.5 BACK TRAJECTORY ANALYSIS

3.5.1 OVERVIEW

O'Conner (1996) noted that, "Regional analysis suggests that not only the presence of high pressure stagnation, but also the *location* of concentrated areas of high pressure stagnation may play an important role in whether or not ambient O_3 levels are increased." Furthermore, Aneja et al. (1994) noted that the role of transport of high ozone concentration and/or its precursors to various sites may be more significant than that of mesoscale ozone production.

Likewise the spatial distribution of tropospheric aerosols is highly inhomogeneous and strongly correlated with their sources (Jonas, 1996). Aerosols have lifetimes of a few days to around one week due mainly to the frequency of recurrence of precipitation (Jonas, 1996). For example, fine mode sulfate particles released in the boundary layer at mid-latitudes had a typical lifetime of several days according to Chamberlain (1991). The gas-to-particle conversion processes which produce secondary fine particulate matter in the atmosphere are generally slow relative to transport times, hence visibility is considered a regional problem (Gray and kleinhesselink, 1996).

Back trajectories follow an air parcel backwards in time to describe the path followed by the air parcel; ideally locating the source region of the airmass. The process used in this analysis

utilizes the hybrid single-particle Lagrangian integrated trajectories (HY-SPLIT) model, administered by the National Ocean and Atmospheric Administration's (NOAA) Air Resources Laboratory (ARL). The model was accessed and run via their website (ARL, 1997) The model used archived nested grid model (NGM) data which was initialized every 12 hours (Moy et al., 1994). Model data prior to 1991 was not readily available therefore a single case study of August 1995 is presented. Figure (3.24) is the monthly plot of normalized values for August 1995. Note the strong inverse relationship which changes day to day. August 1995 data is statistically significant at the 5 percent confidence level.

Trajectories were then run from periods (days of the month) of relative high ozone concentrations during the case study month. Their sources and pathways were compared to regional data identifying areas producing the following pollutants: VOCs, SO_2, PM_{10}, CO, NO_2; see figures (3.28, 3.29, 3.30, 3.31, and 3.32) respectively. The emission sources (small black squares on figures) represent the available output data for sites with an emission output at or above 100 Tons Per Year (TPY). These figures do not represent quantitative emission flux values, only a 100 TPY threshold. Ideally, more accurate emission outputs would be preferred since by this method there is no way to differentiate a site with an emission of 100 TPY from a site with an output of 300 TPY.

In addition to emission source location, the trajectory analysis also yielded information concerning the air parcel's speed. Since all model runs were for 48 hours, longer pathlengths represent faster travel speeds and less stagnation time, thus influencing the kinetics of ozone formation.

3.5.2 RESULTS

The analysis began on the 2nd of the month. The air mass traveled (see figure 3.33), through a moderately high source region for VOCs, SO_2, and NO_2 , which increased its ozone content. A

consequence of this increased ozone was the observed reduction in visibility during this same period.

The model run for two days later, 4 August, shows that the air parcel had travelled a longer path length implying that it resided in a non-stagnating airmass. Additionally the airmass had traveled over cleaner non-polluted areas (see figure 3.34). As a consequence, visibility increased and ozone decreased.

In contrast to the long path length observed on 4 August, the run for 9 August is marked by a much shorter path length over a moderately polluted area (figure 3.35). The path is not direct and meanders over a moderate VOC area. The result is a stagnating airmass whose ozone levels have increased and visibility decreased. Further evidence of the effects of meandering comes from the 14 August's meandering run over a high VOC emission area; see figure (3.36).

August 20th was marked by a decrease in ozone and an accompanying increase in visibility; see figure (3.37). The path for this air mass originally traveled through the more polluted Virginia area and then into the cleaner region of Kentucky. The distance traveled was fairly long in a short period of time implying higher speed and lower stagnation. The run for another high ozone period, 25 August, is similar to our first run (on 2 August) except that the air mass travels over a more polluted corridor and its path length is greater; see figure (3.38).

August 26th's reduced ozone and increased visibility comes despite a polluted source region; see figure (3.39). In this case, the polluted airmass migrates out over the ocean where it is likely cleansed (via mixing or deposition) before continuing on to the Nashville site.

Finally, the model run for 30 August fits the classical example of short travel path (stagnation), meandering, and polluted source region. The results are as expected with high ozone levels and reduced visibility; see figure (3.40).

3.5 CONCLUSIONS

The results obtained support our original hypothesis that ozone displays an inverse relationship with visibility. The regional ozone trend appears to have increased during the 1980s (0.0005ppmv/yr, r^2=0.0497) and leveled off during the 1990s (-0.00007ppmv/yr, r^2=0.0007). Regional visibility trends during the 1980s decreased (-0.0222miles/yr, r^2=0.0426) at a rate consistent with the increasing ozone trend. During the 1990s this relationship weakened (0.0802miles/yr, r^2= 0.3177); see figures 3.2 and 3.3. Yearly trend analysis appears to support an inverse relationship; however, the trends were not statistically significant at the 5 percent level. Nashville's results were similar; however ozone levels did not level off, but instead continued to rise during the 1990s . This increase did not support an inverse ozone-visibility relationship during this period (figures 3.11 and 3.12).

The statistical significance of the analysis improved (became statistically significant at α =0.05) when temporal resolution was measured in days and hours and spatial resolution was reduced to specific areas (non-regional). A statistically significant inverse relationship was observed 27% of the time (n =15 months) when linear regression was performed on Nashville only data utilizing *daily averaged observations* grouped by month. In comparison, a statistically significant relationship between relative humidity and visibility occurred only 20% of the time. Nashville R-squared values ranged from 0.02 to 0.30 for ozone vs. visibility.

The best results were obtained when the four areas in the region (other than Nashville) were evaluated individually utilizing *hourly observations* grouped by month. Statistical significance was observed 72% of the time (n =57 months). R-squared values ranged from 0.03 to 0.43 collectively for these locations (RDU, CTL, GSO and ATL).

These findings are also similar to the results of other researchers. Diederen et al's (1985) results of a two year study in the Netherlands showed a relationship between visibility,

particulate matter and ozone. Modeling runs by King and Vukovich (1982) also suggest that lowest visibility correlates best with peaks in ozone and SO_4^{2-} (fine particulate matter).

Subjective yearly regional anomaly comparison showed a good correlation between ozone and temperature, and an inverse relationship between ozone and relative humidity. However, a consistent relationship was not observed between visibility and ozone. Site-specific yearly anomaly analysis showed an even less distinctive pattern of correlation. The impact of relative humidity did however appear to impact visibility correlation at Nashville more than the region as a whole. Site specific anomaly analysis was performed only for the Nashville MSA.

Back trajectory analysis showed that slow moving meandering air masses produced higher levels of ozone and lower visibility. In fact, the study month (August 1995) had persistent high pressure systems throughout the region which elevated ozone and reduced visibility at nearly all of the locations. Air mass source regions also influenced this relationship, with air masses passing over more polluted areas having an impact on both ozone levels and visibility.
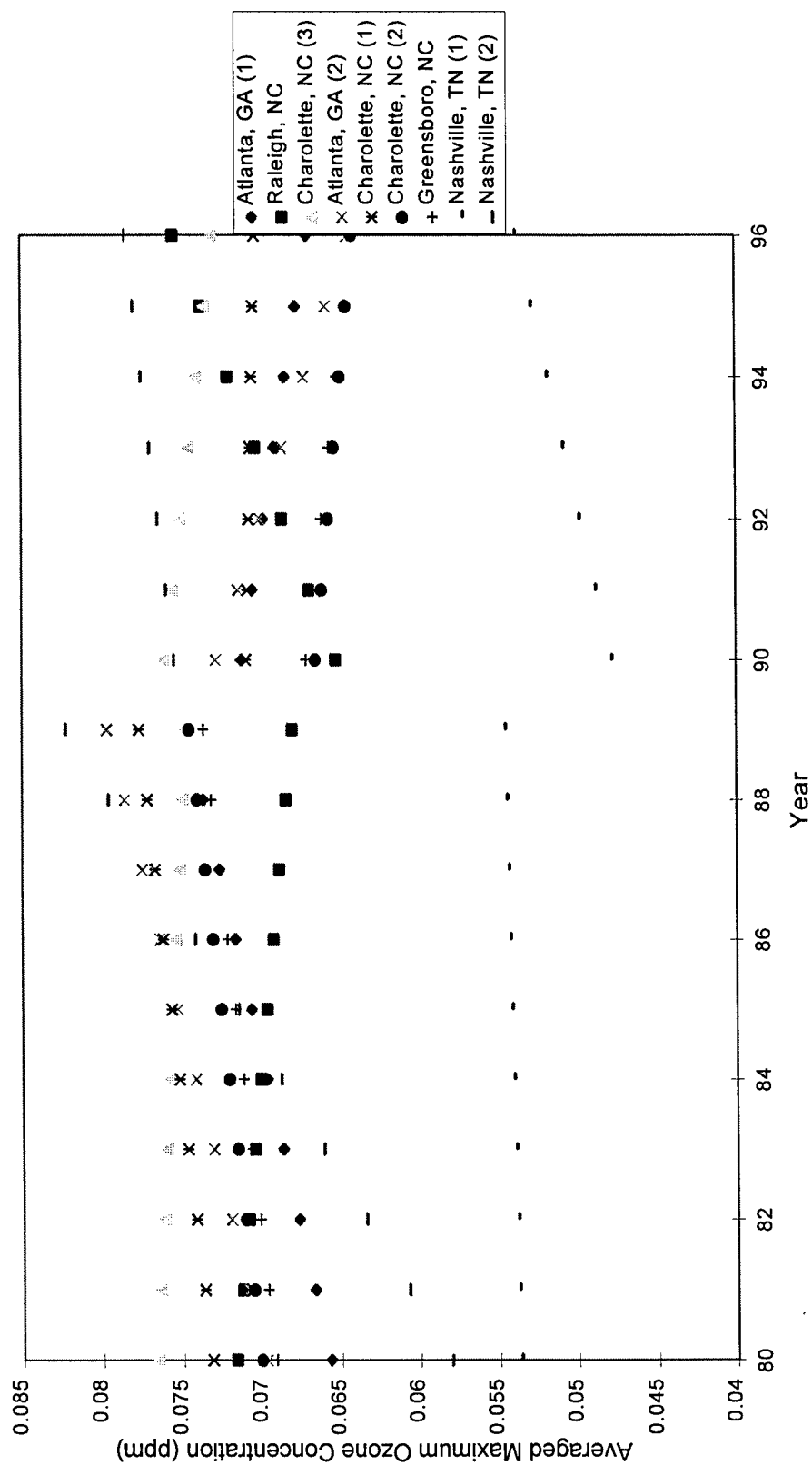
Figure 3.1. Individual ozone trends for each site, collectively used to construct the regional trend

44
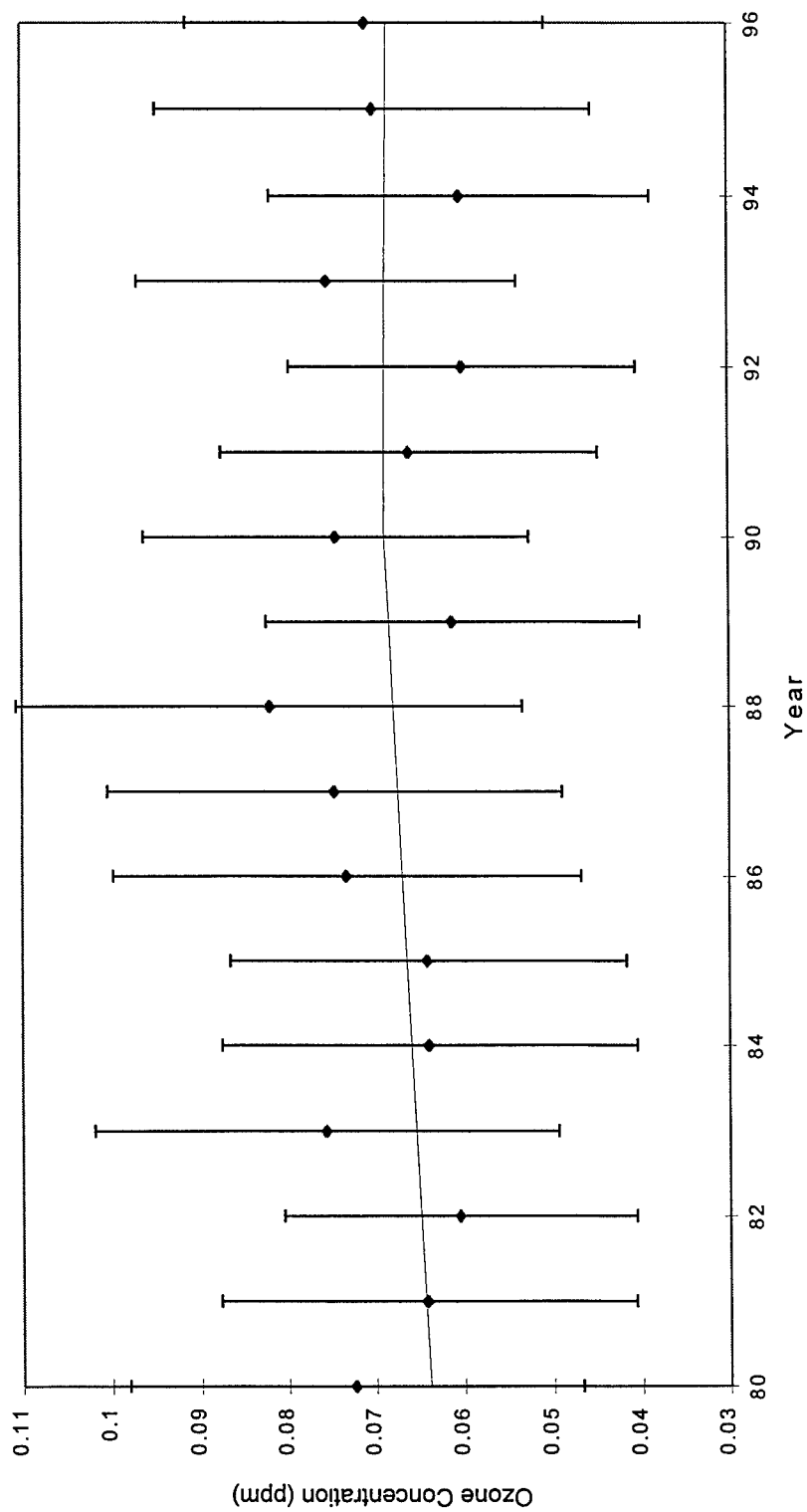
Figure 3.2. The overall regional ozone trend demonstrates that the average daily maximum ozone concentration appears to have increased during the 1980s and leveled off during the 1990s.
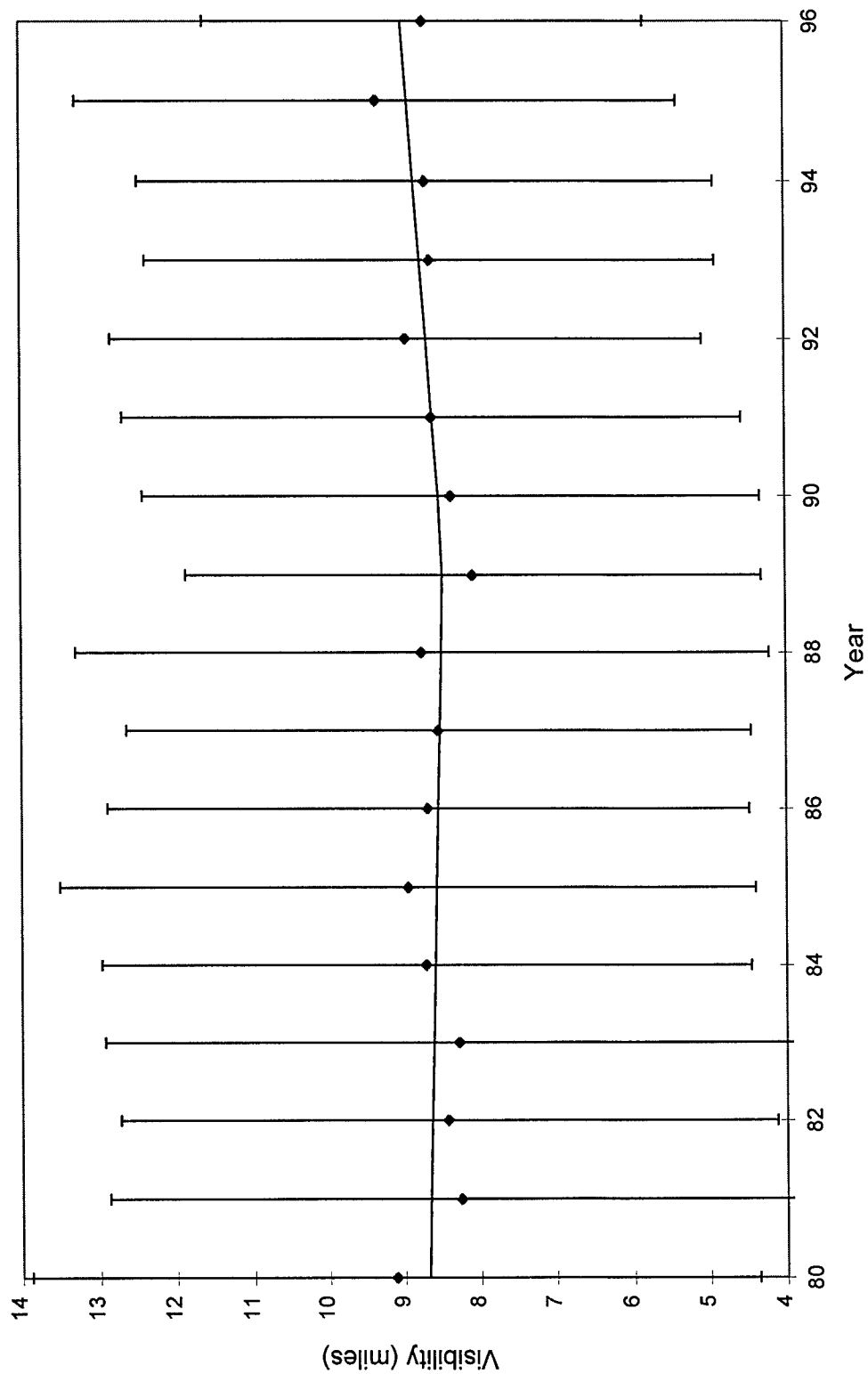
Figure 3.3. Regional visibility trends during the 1980s decreased at a rate consistent with the increasing ozone trend. During the 1990s the visibility trend appeared to increase.
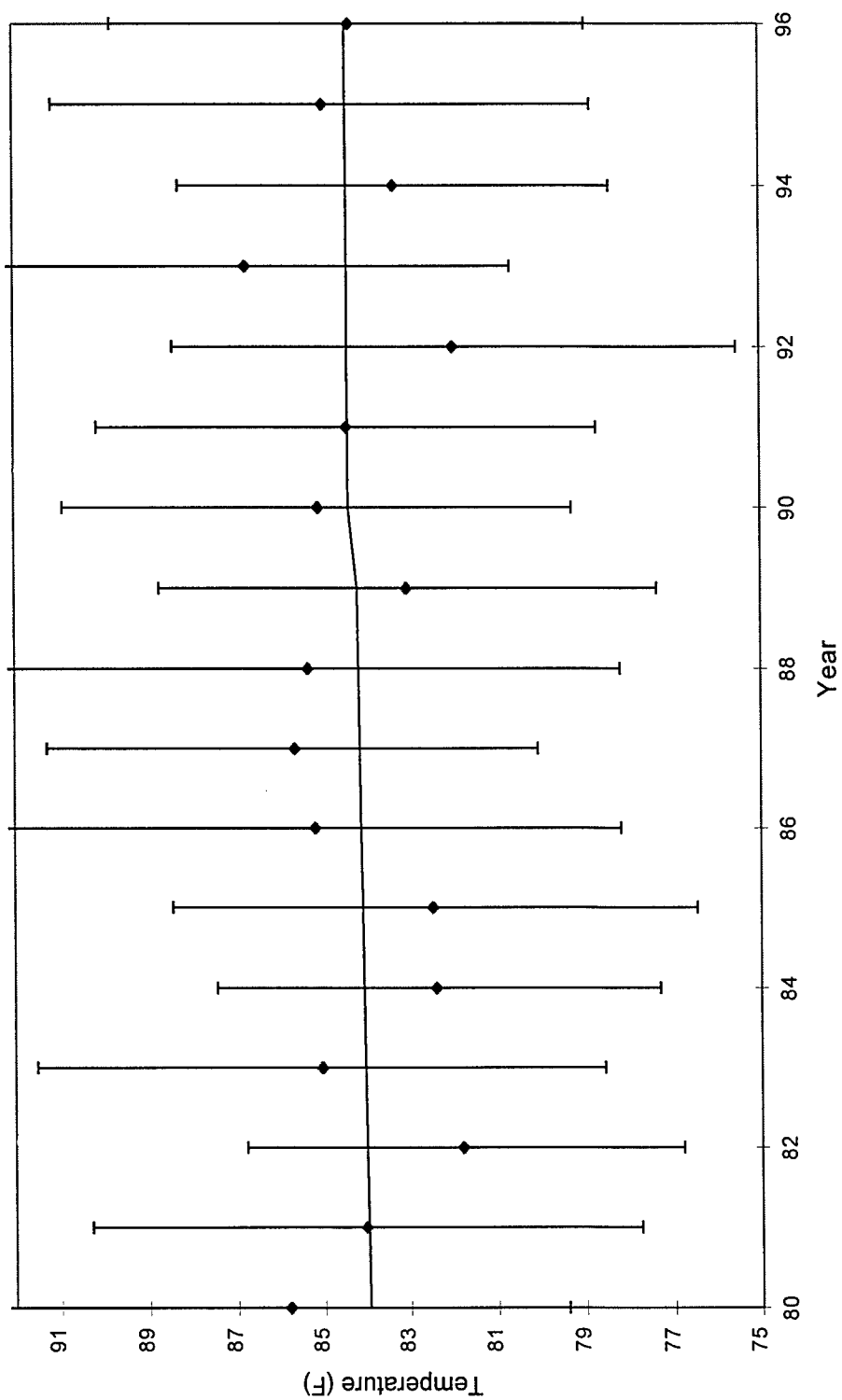
46

Figure 3.4. Regional temperature trends remained flat during both periods.
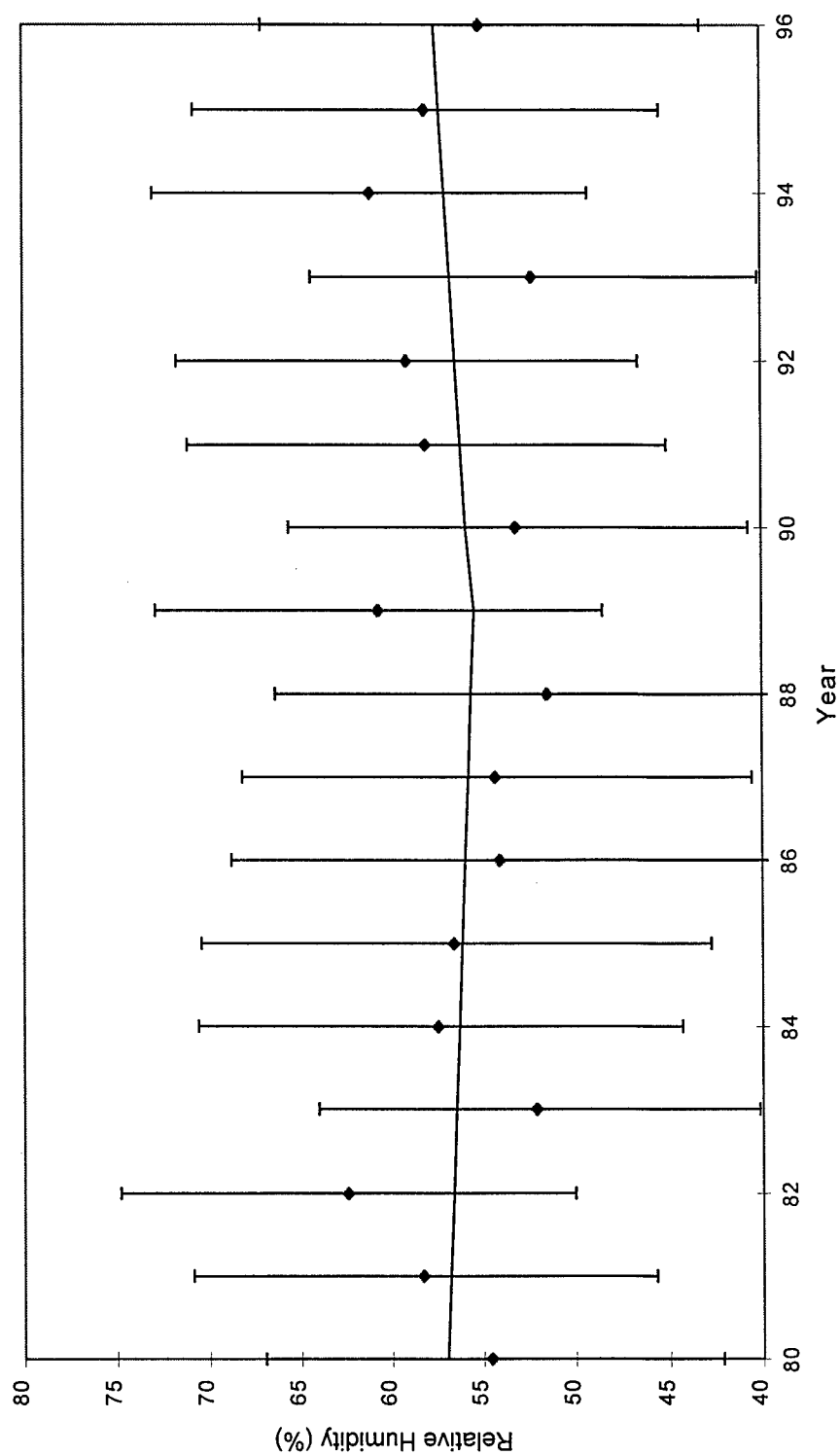
Figure 3.5. Relative humidity trends decreased in the 1980s and increase in the 1990s. This is similar to visibility trends observed over the same period, but it does not fit the well established and expected inverse relationship between visibility and relative humidity.
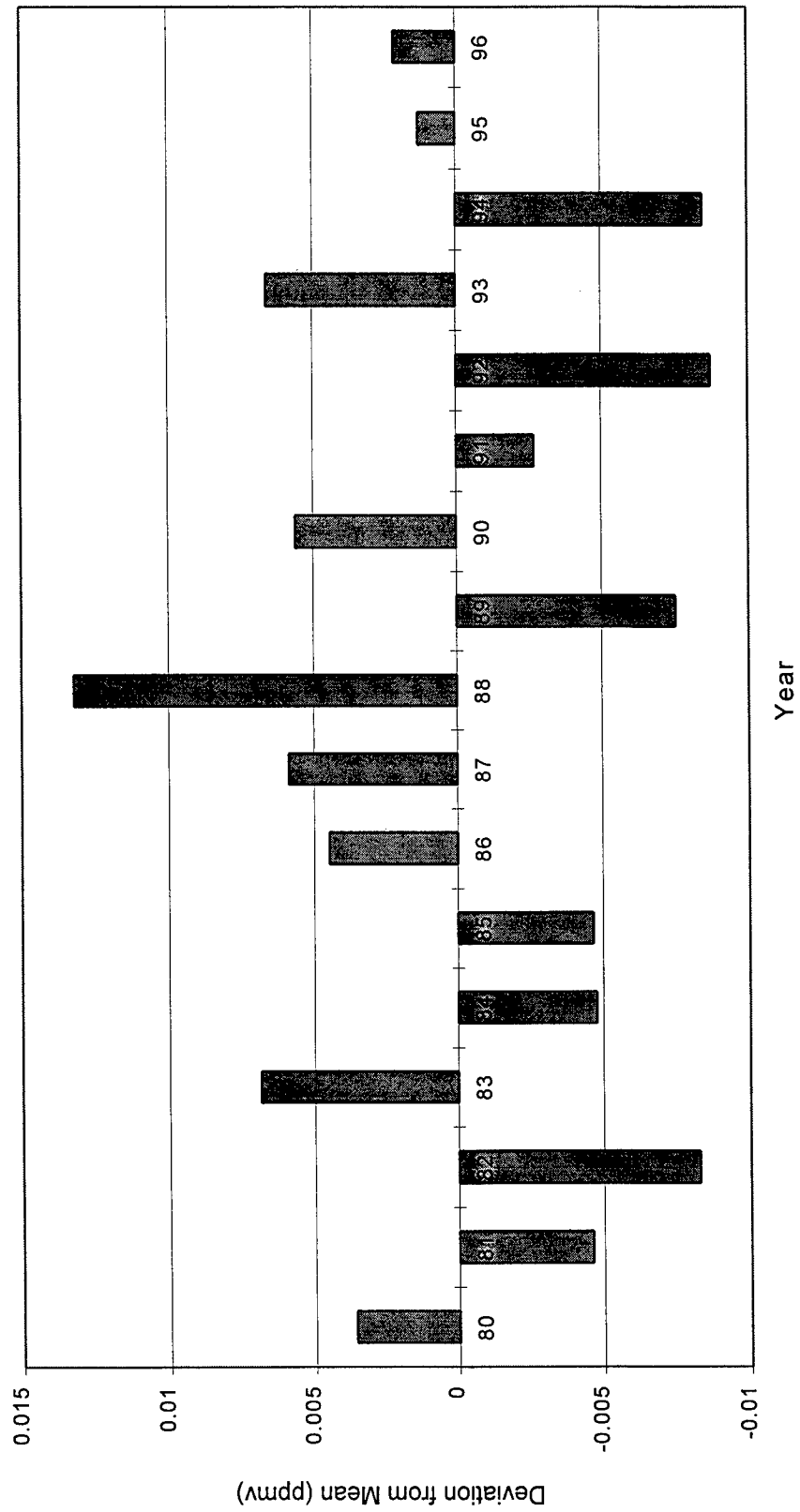
Figure 3.6. Ozone anomalies by year.
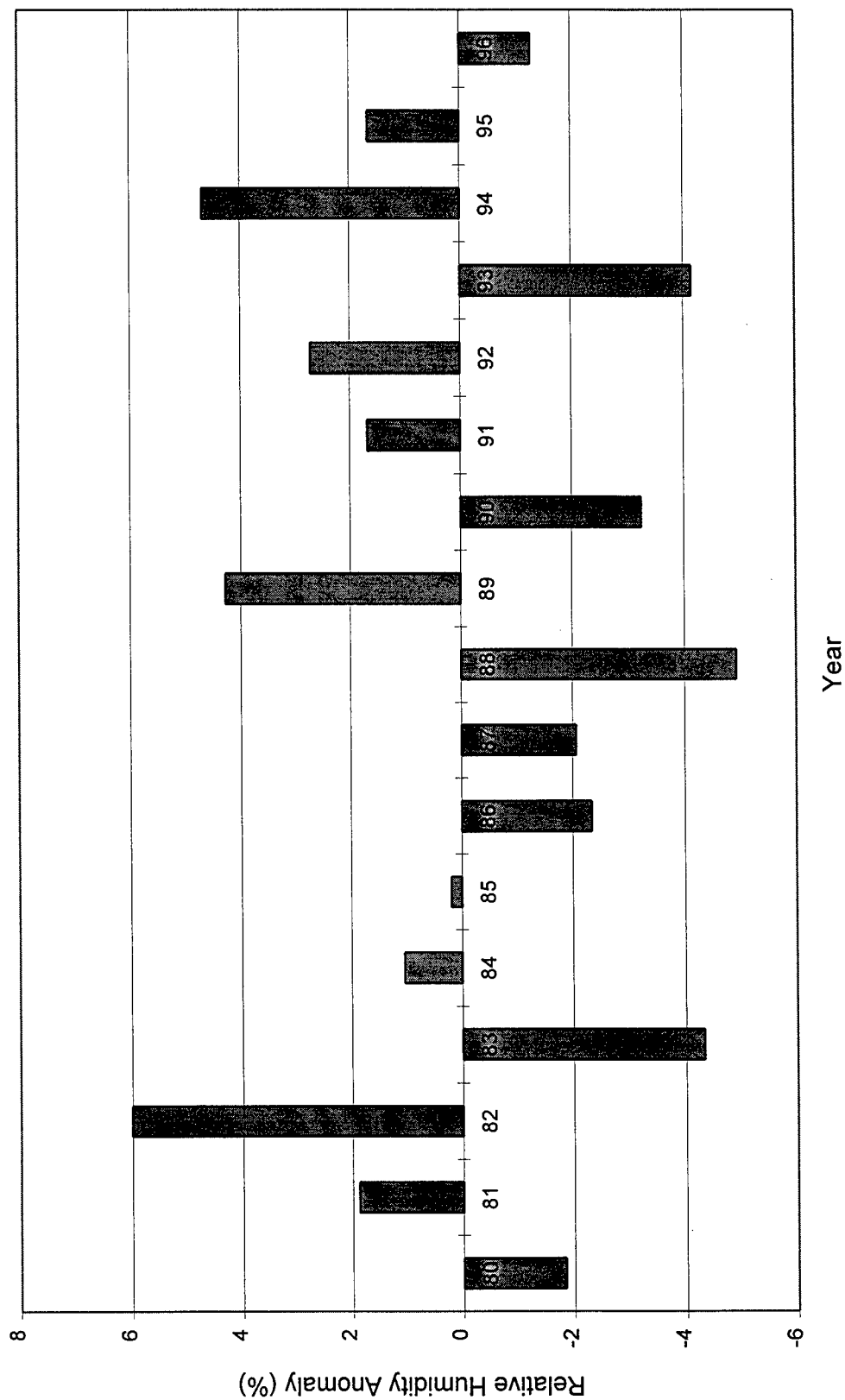
Figure 3.7. Regional relative humidity anamoly. Eight of the years showed a positive relationship between visibility and relative humidity.

50
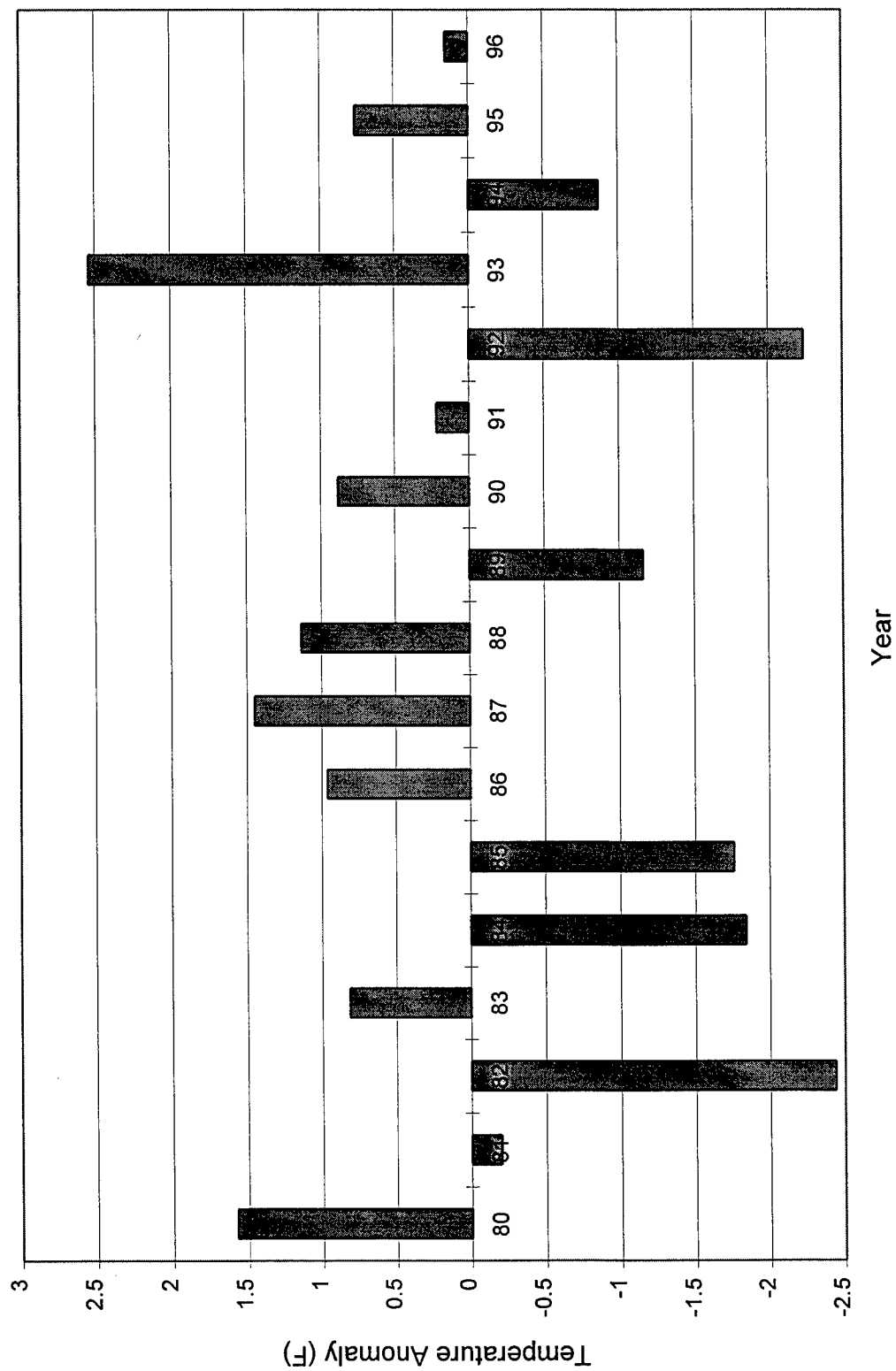
Figure 3.8. Regional temperature anamolies. Nine of the years revealed an inverse relationship between visibility and temperature.
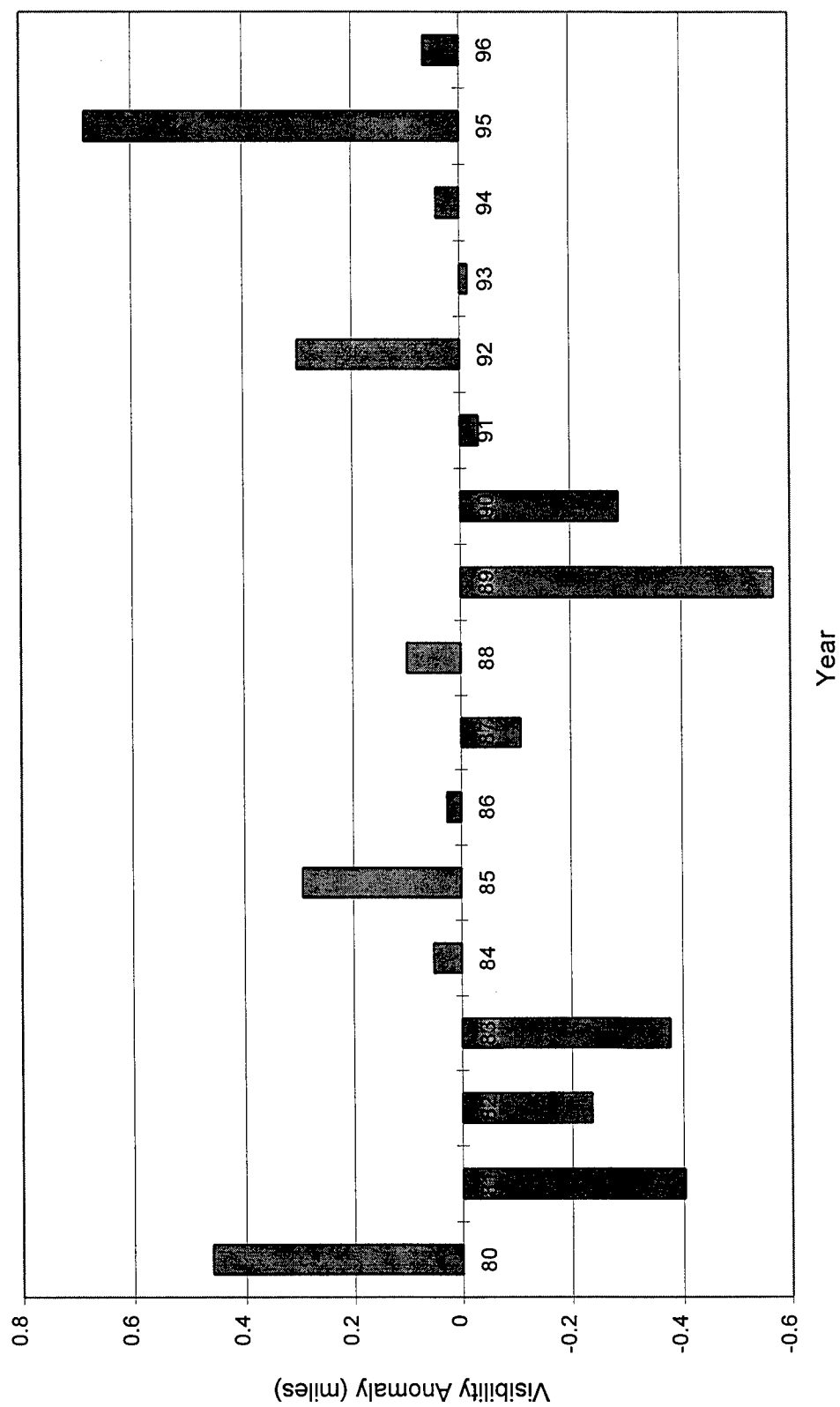
Figure 3.9. Regional visibility anamoly. A consistent relationship between visibility and the other variables is not clearly evident in the anomaly analysis. Only seven of the seventeen years show an inverse relationship between ozone and visibility.
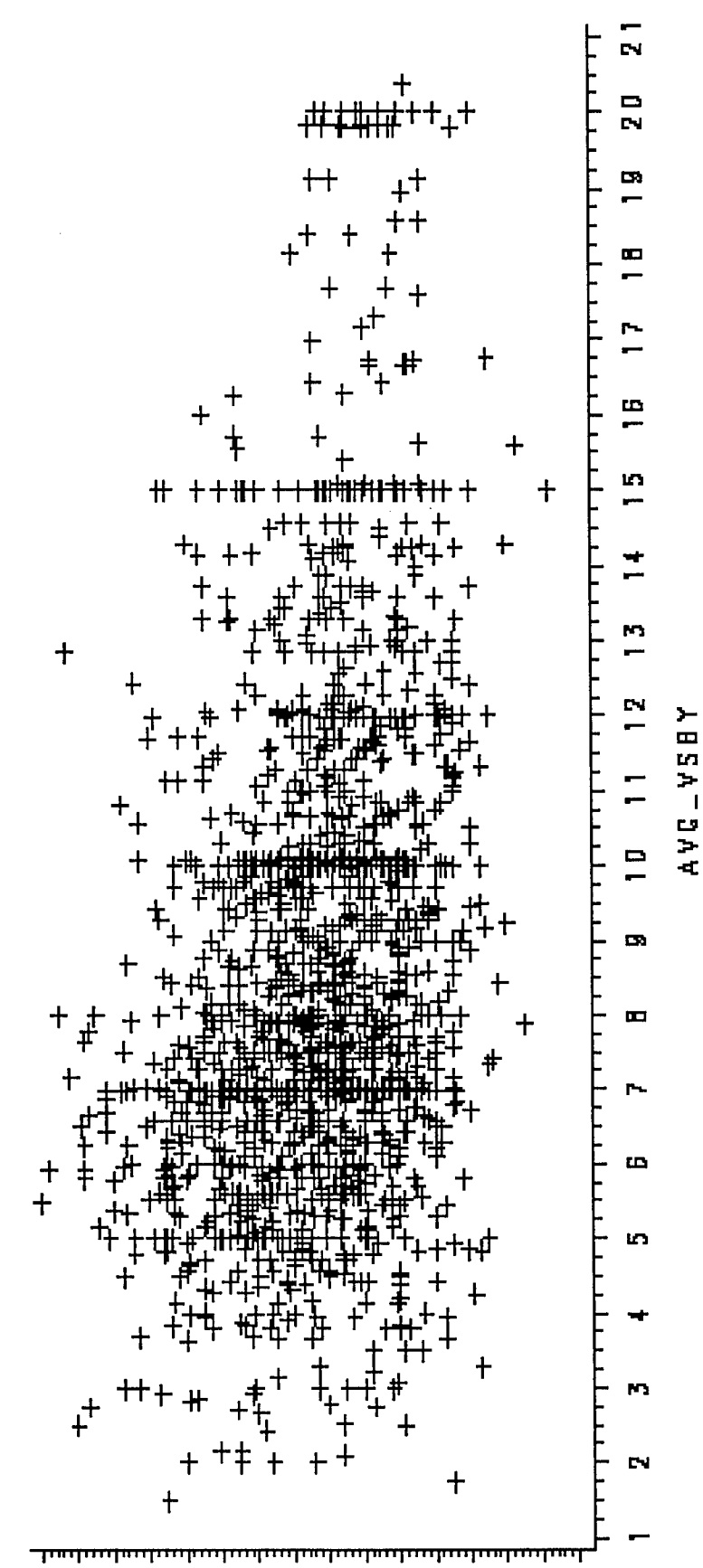
Figure 3.10. Scatter plot of visibility vs. ozone for all Nashville data.
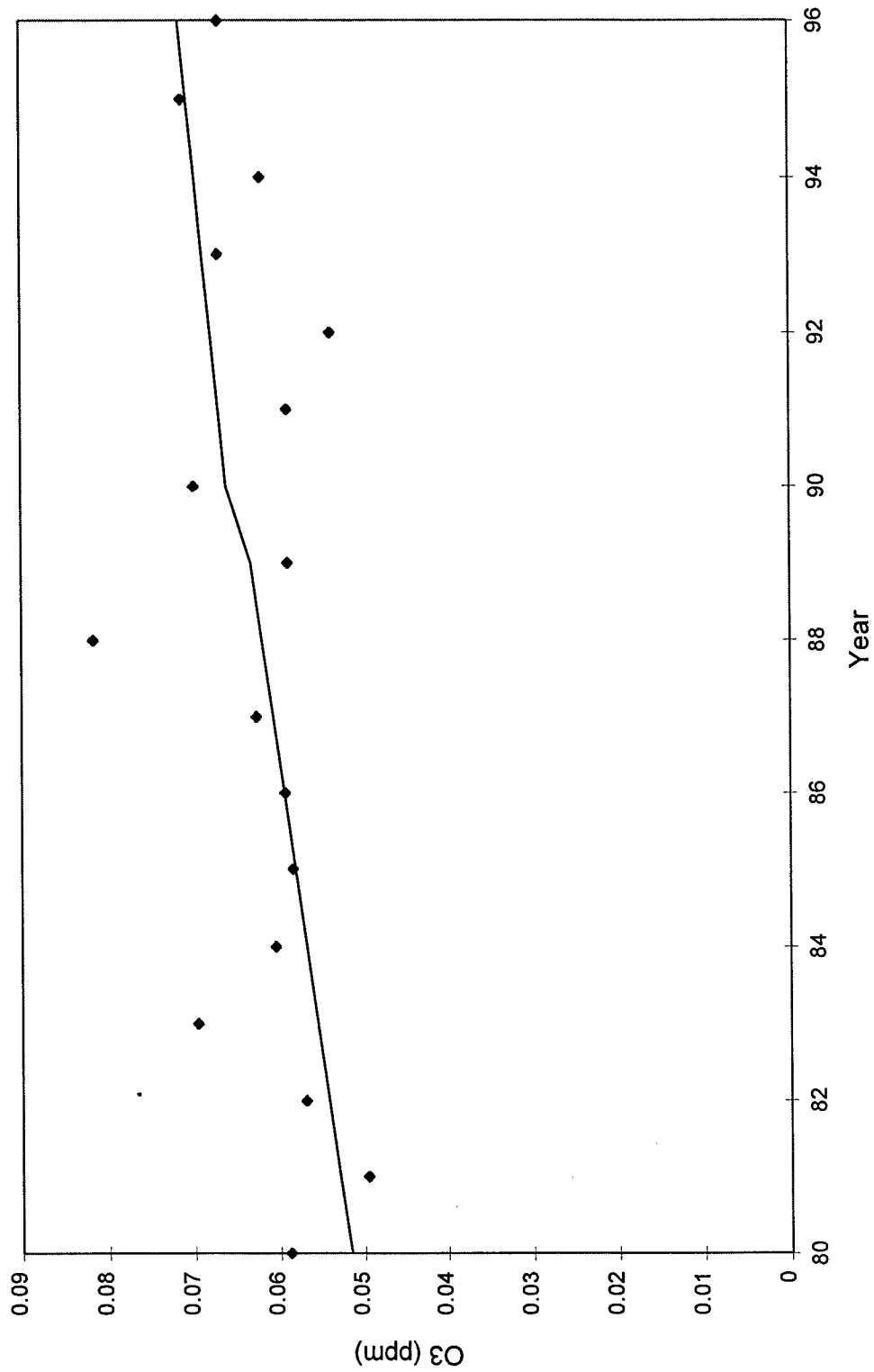
Figure 3.11. Nashville's ozone trend was positive in the 1980s, and unlike the region as a whole which leveled off during the 1990s, ozone continued to increase during the 1990s.
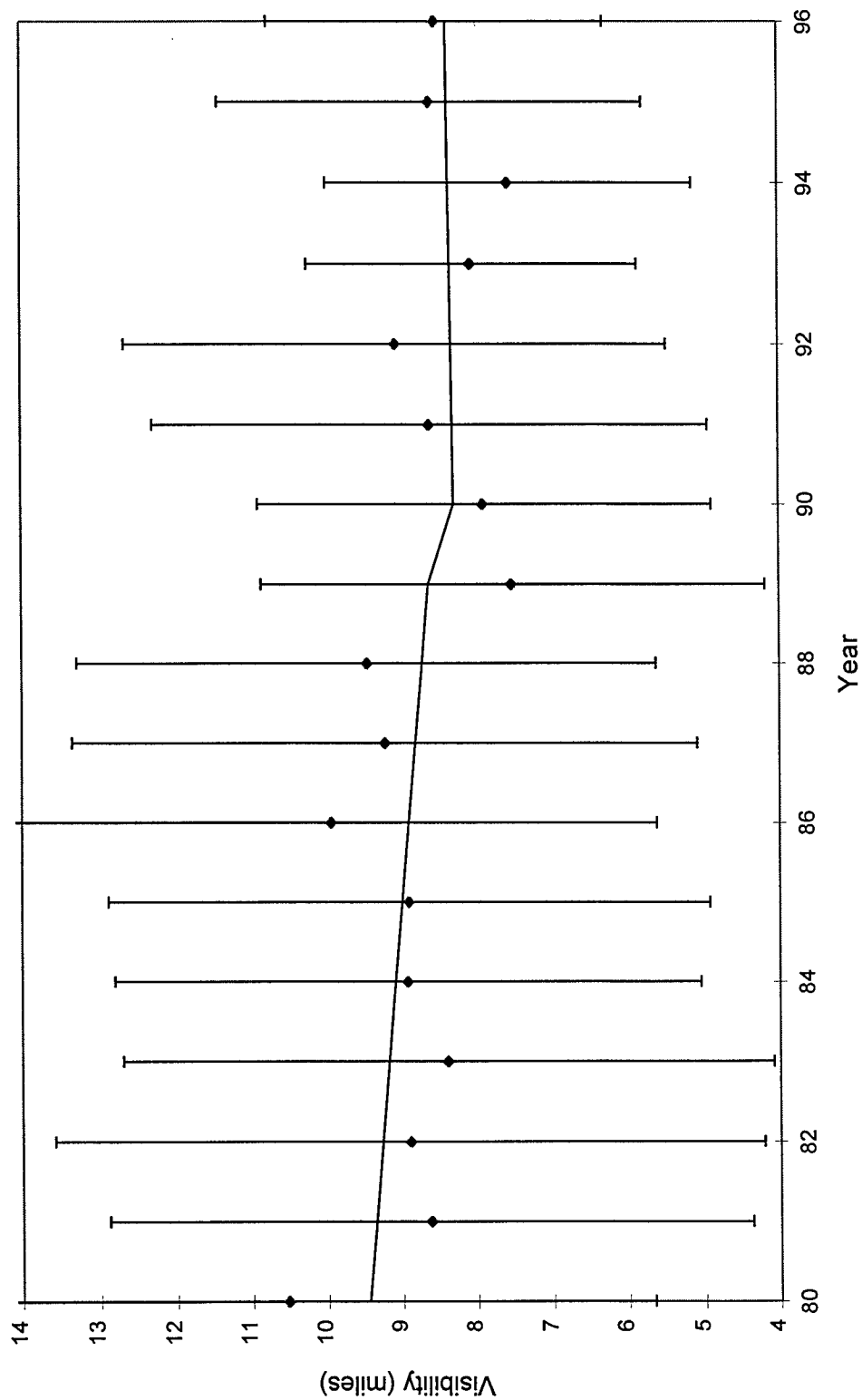
Figure 3.12. Nashville's visibility trend for the 1980s decreased consistent with the rising ozone trend during the same period; clearly showing an inverse relationship. However, the inverse relationship is not as pronounced during the 1990s.
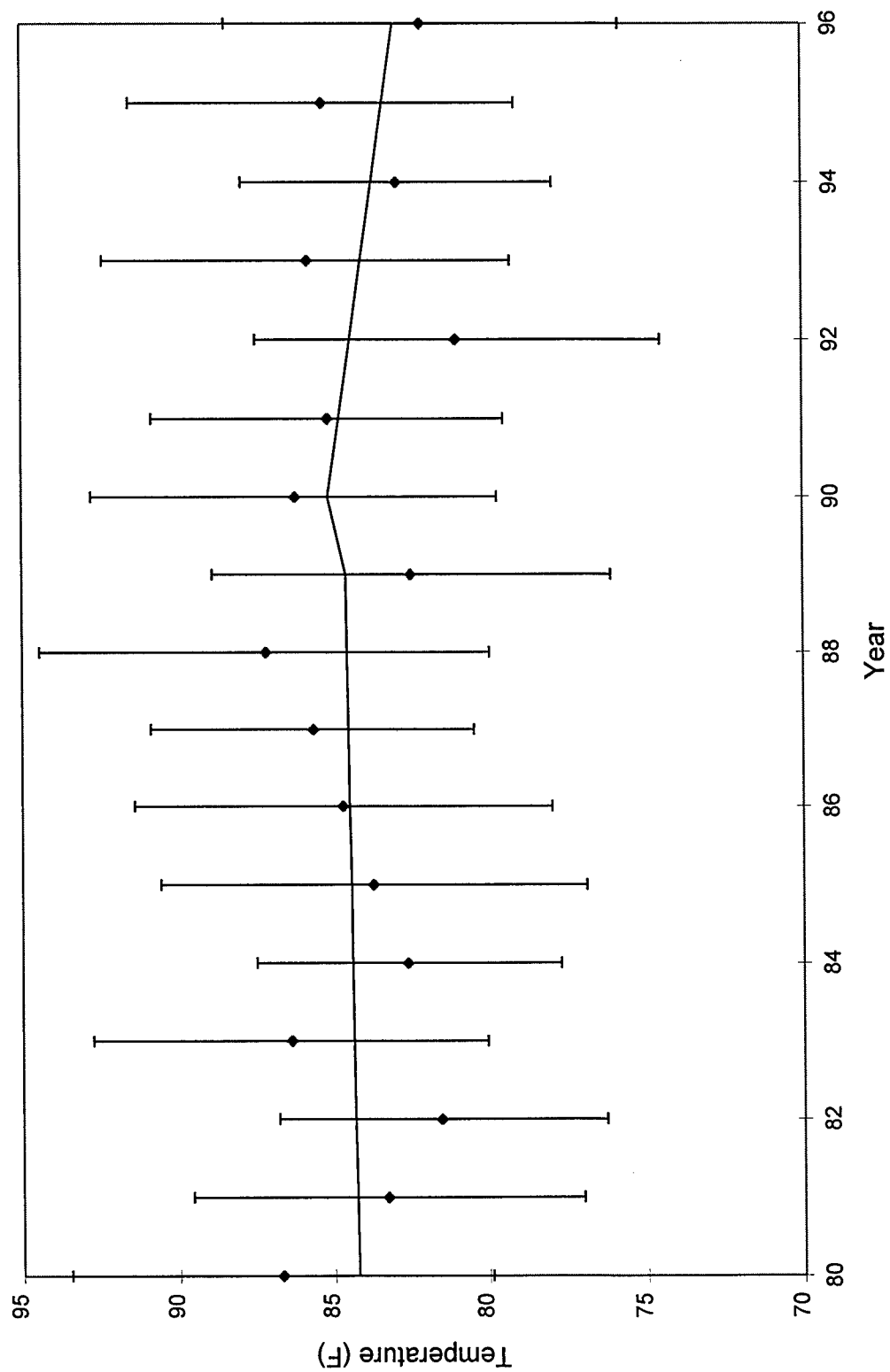
Figure 3.13. Temperature trends at Nashville were slightly positive during the 1980s and negative for the 1980s.
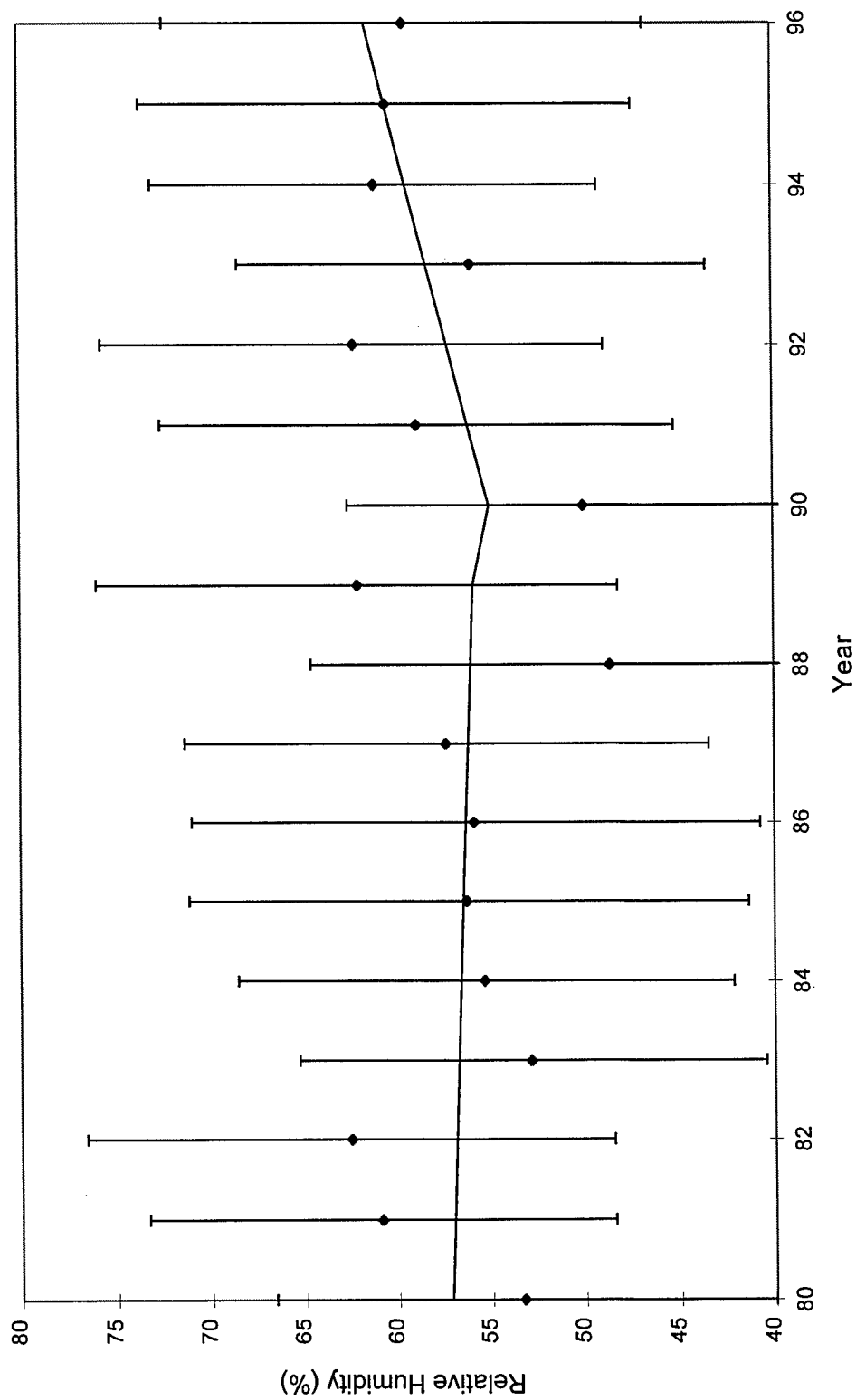
56

Figure 3.14. Relative humidity trends displayed a slightly negative slope for the 1980s and a relatively steep posative slope during the 1990s.
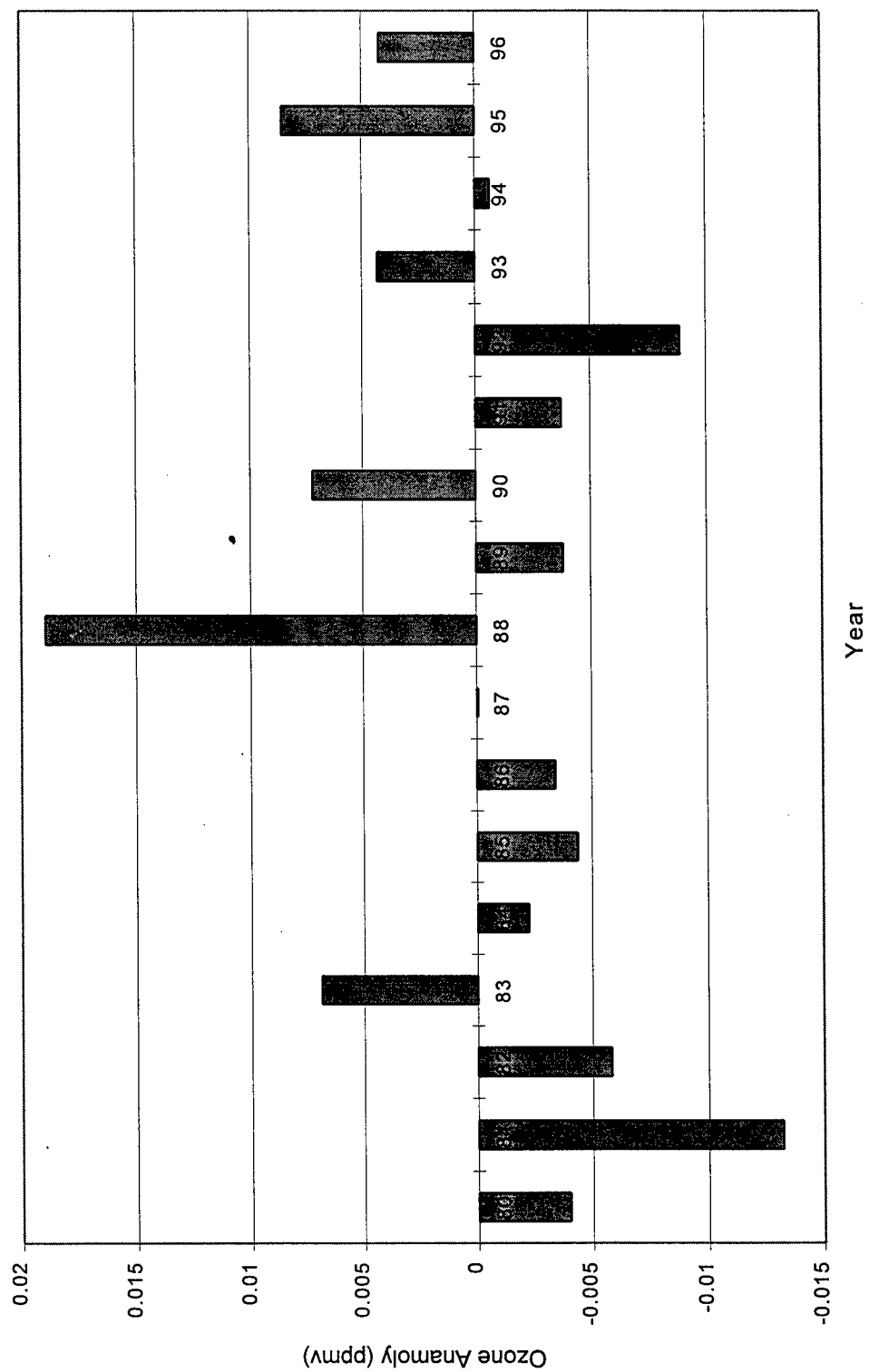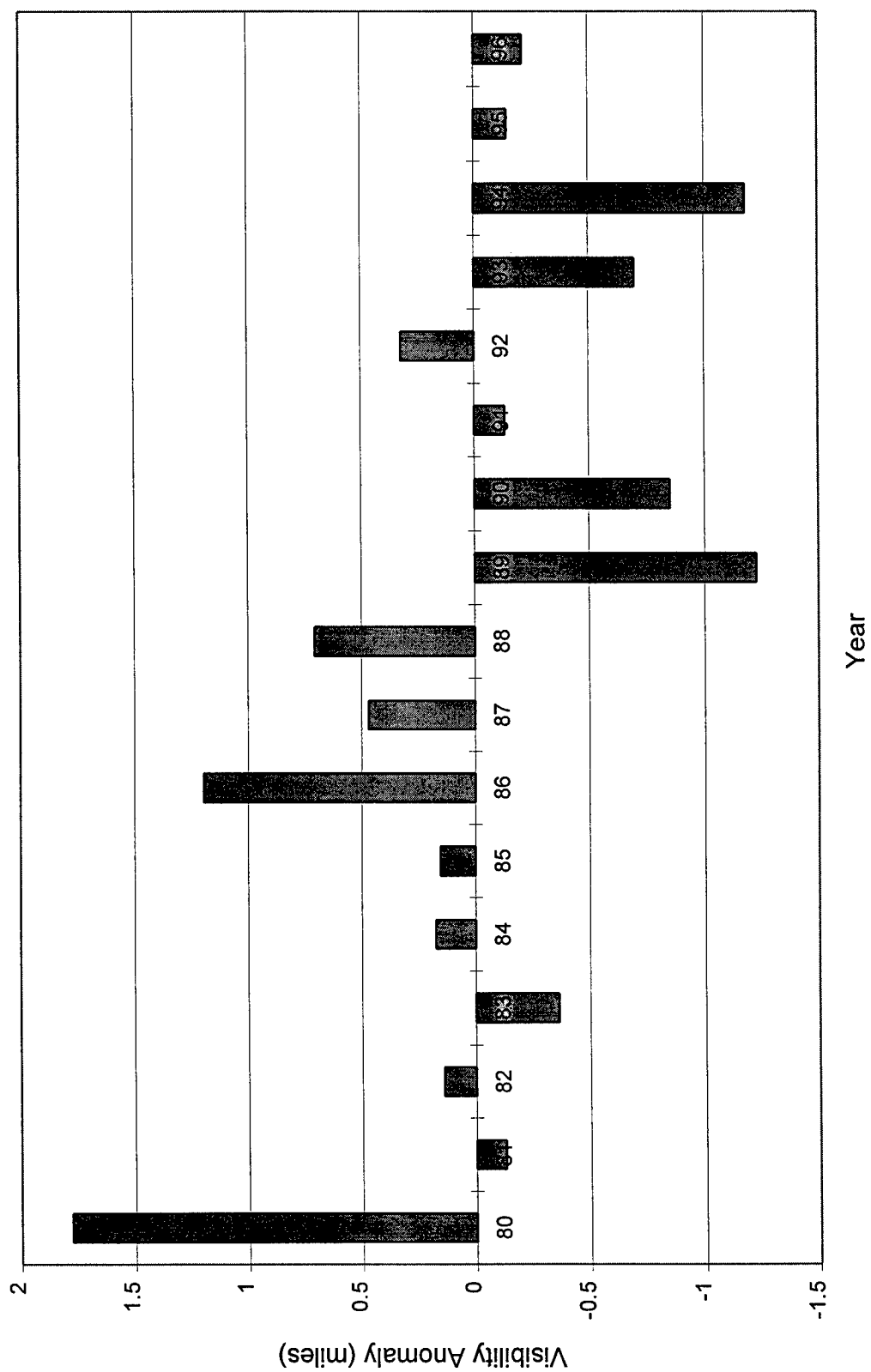
Figure 3.15. Nashville, TN ozone anamolies.

Figure 3.16. Nashville, TN visibility anamolies.
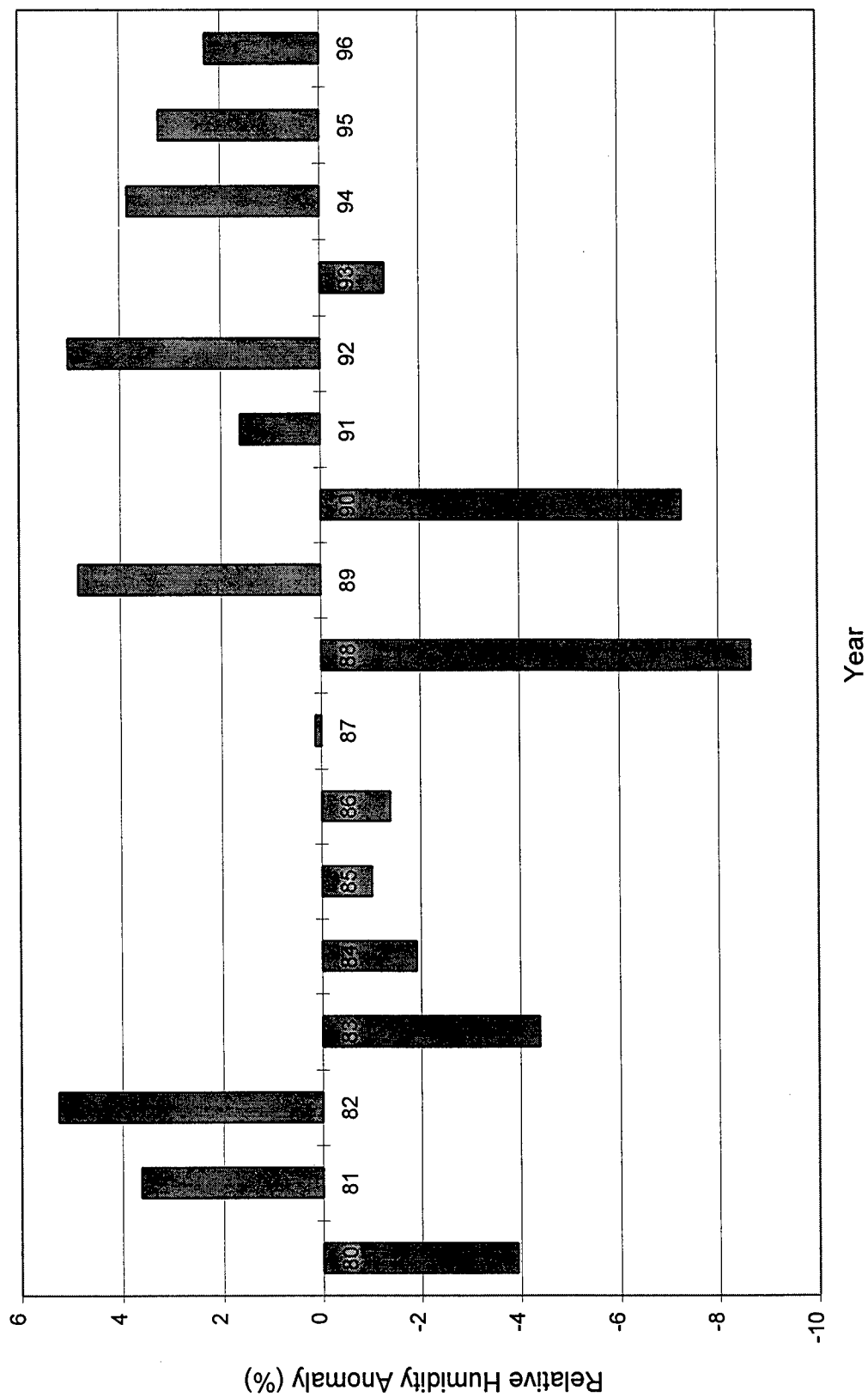
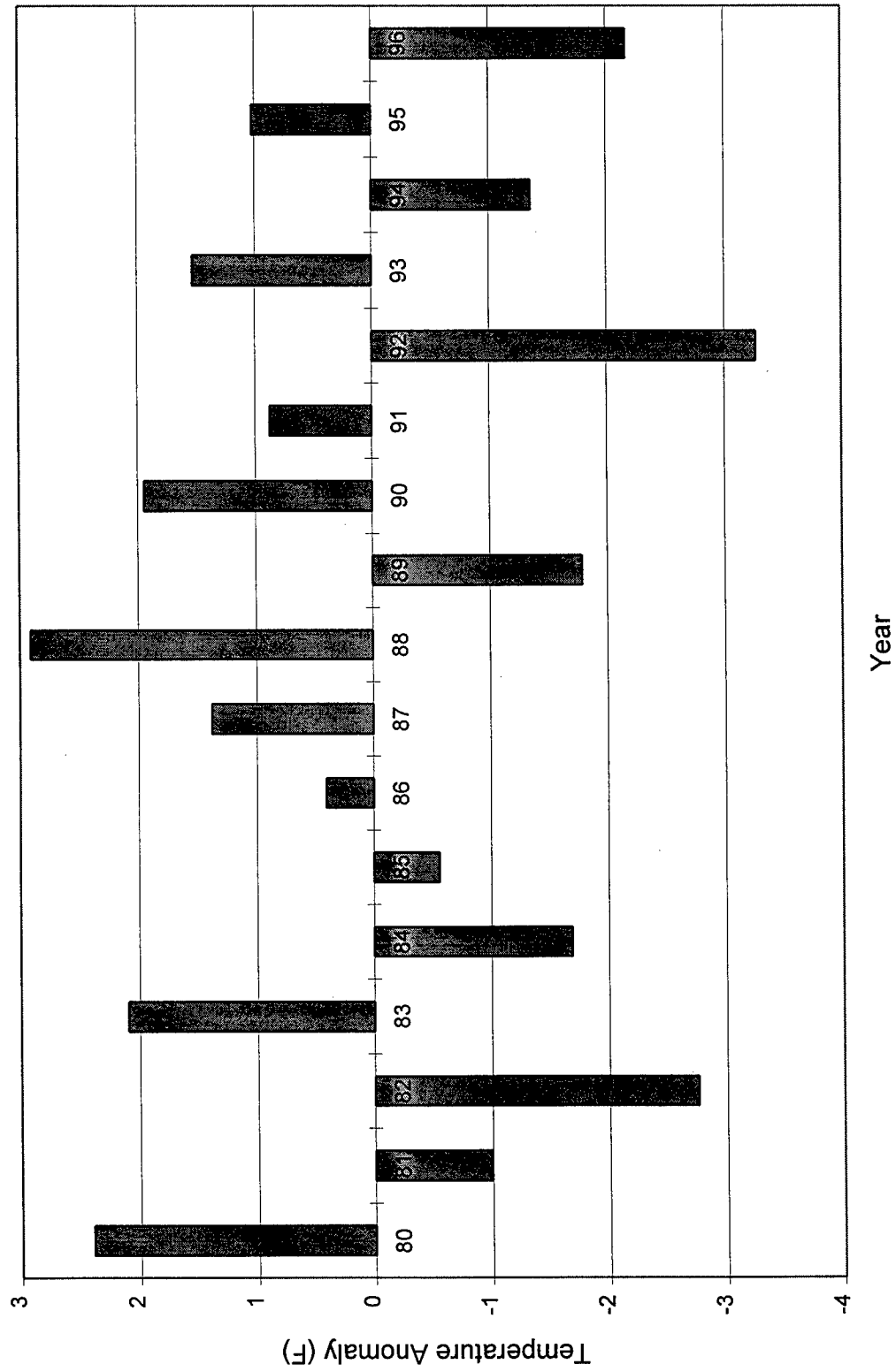Figure 3.17. Nashville, TN relative humidity anamolies.

60

Figure 3.18. Nashville, TN temperature anamolies.

61

Figure 3.19. Nashville, TN normalized daily averaged ozone and visibility (dashed line is visibility) for July 1983.

62

Figure 3.20. Nashville, TN normalized daily averaged ozone and visibility (dashed line is visibility) for June 1988.

63

Figure 3.21. Nashville, TN normalized daily averaged ozone and visibility (dashed line is visibility) for August 1990.

64
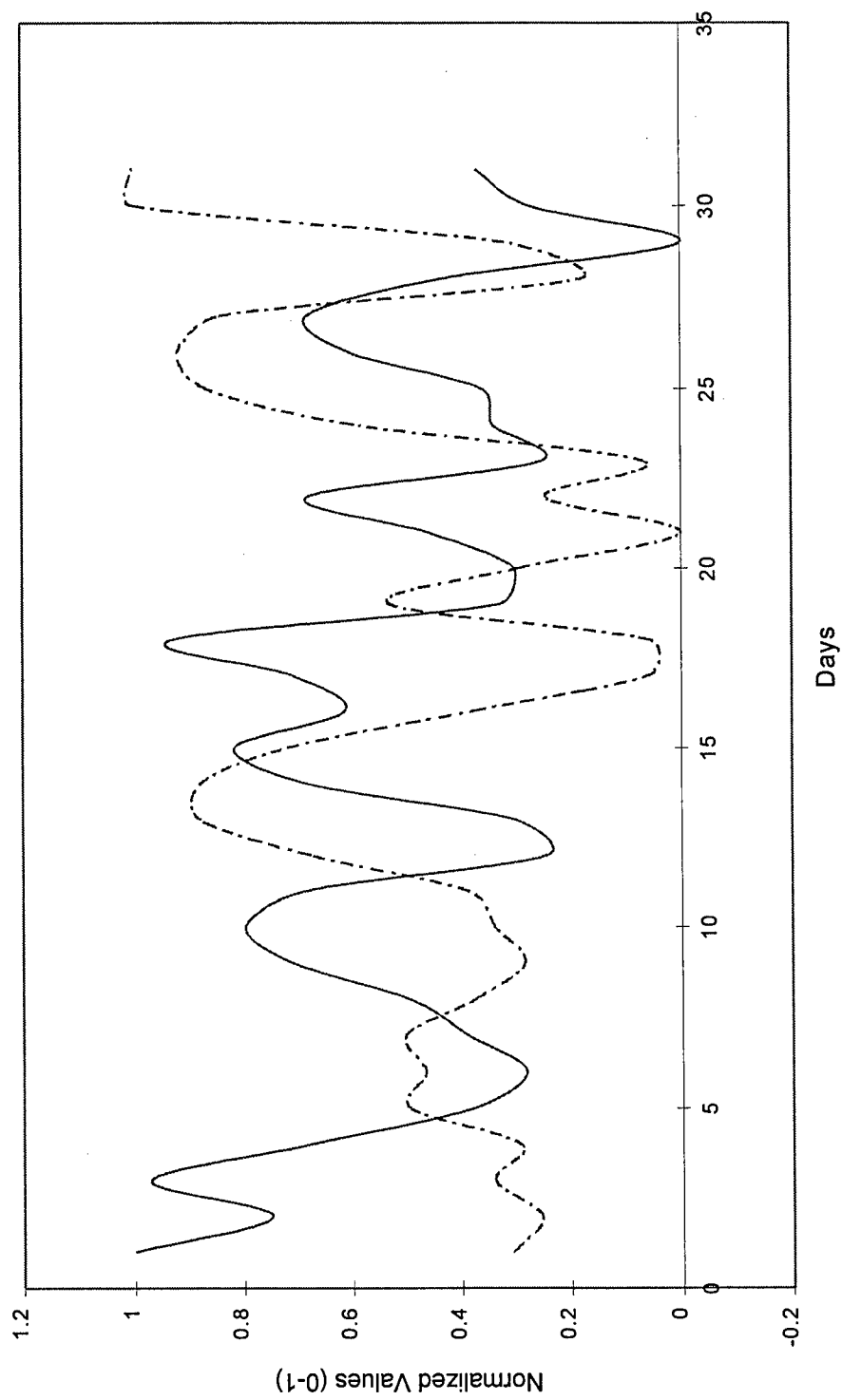
Figure 3.22. Nashville, TN normalized daily averaged ozone and visibility (dashed line is visibility) for August 1988.

The plot axes read: Normalized Values (0-1) on the vertical axis (1.2, 1, 0.8, 0.6, 0.4, 0.2, 0, -0.2) and Days on the horizontal axis (0, 5, 10, 15, 20, 25, 30, 35).
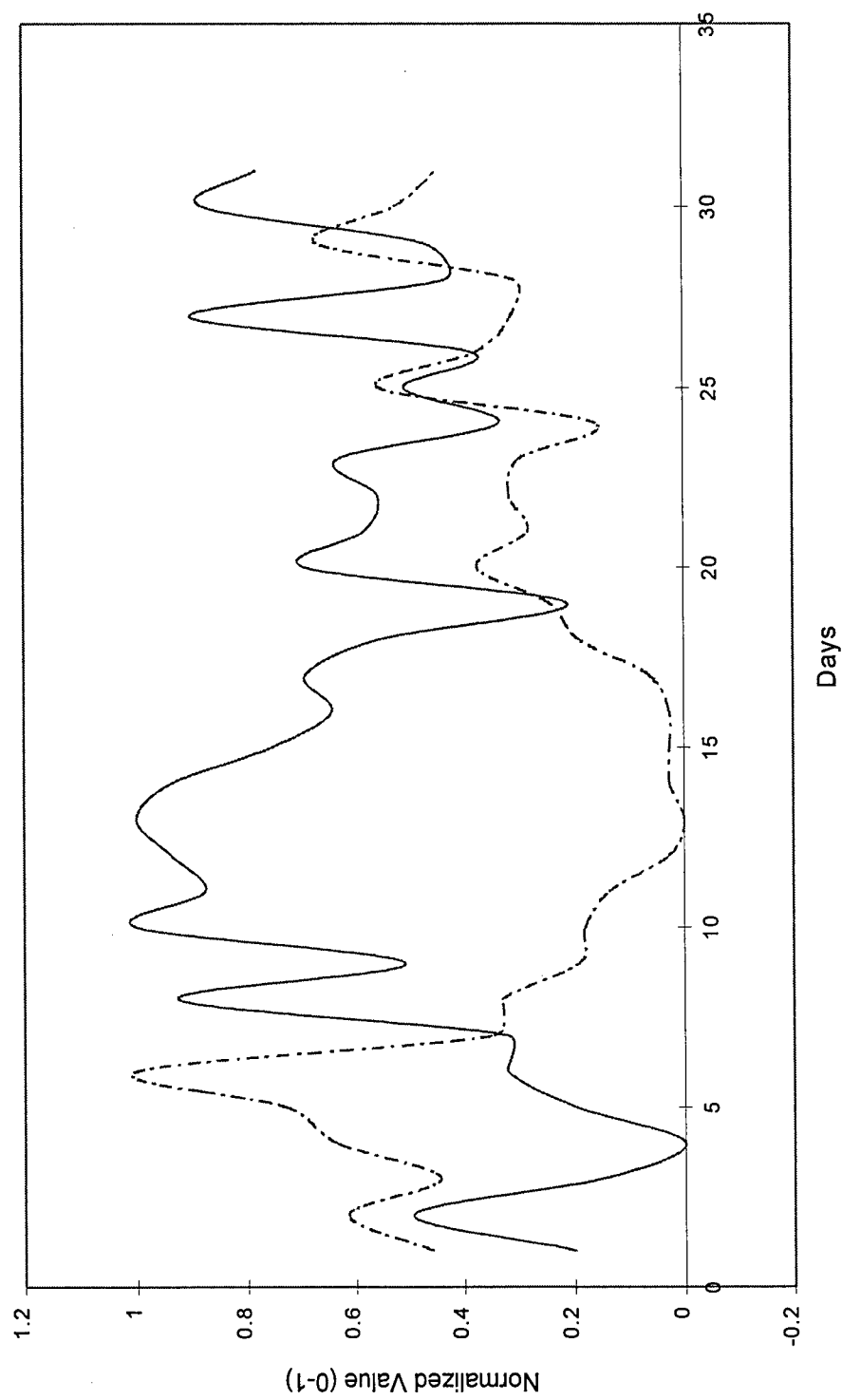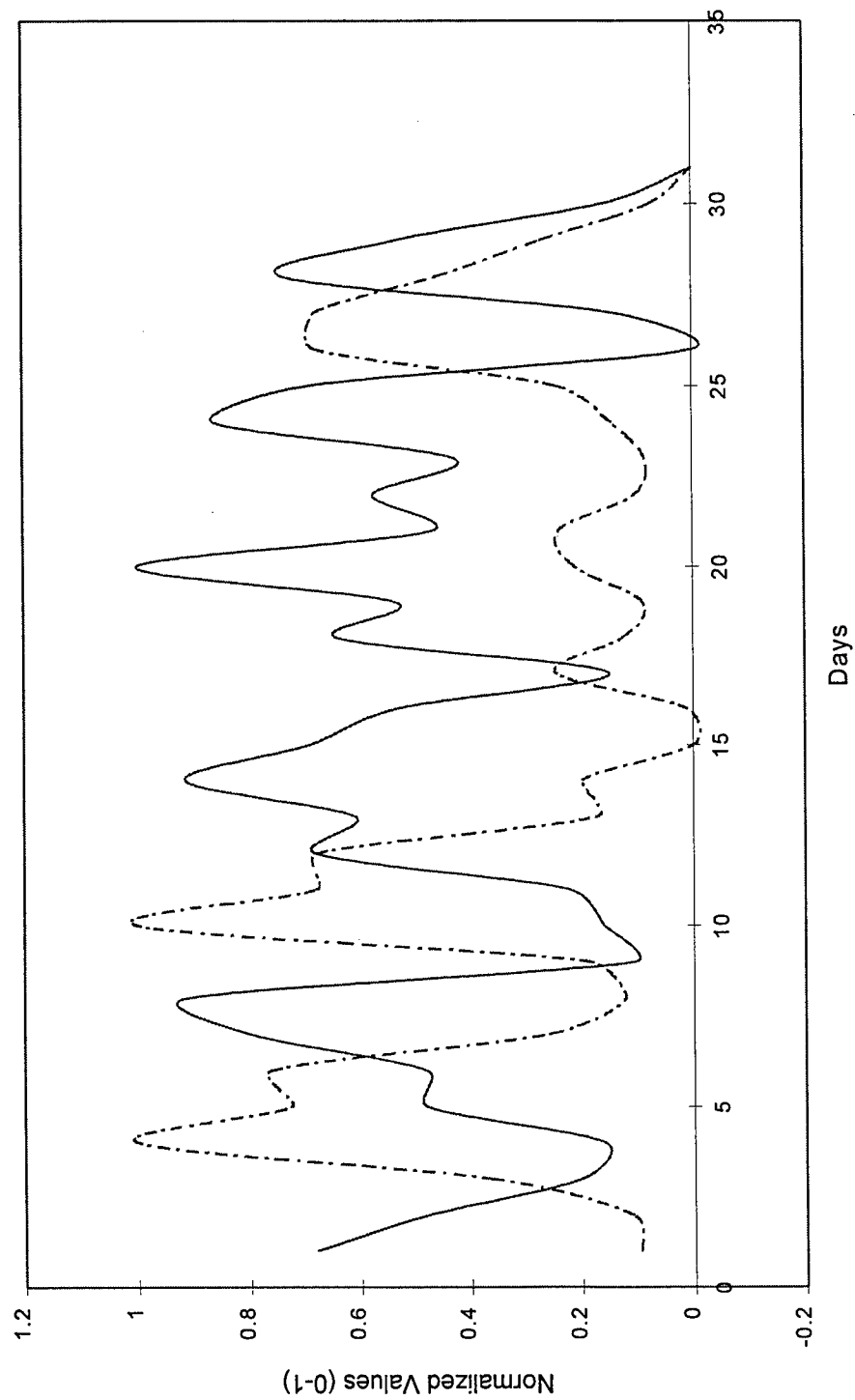
65
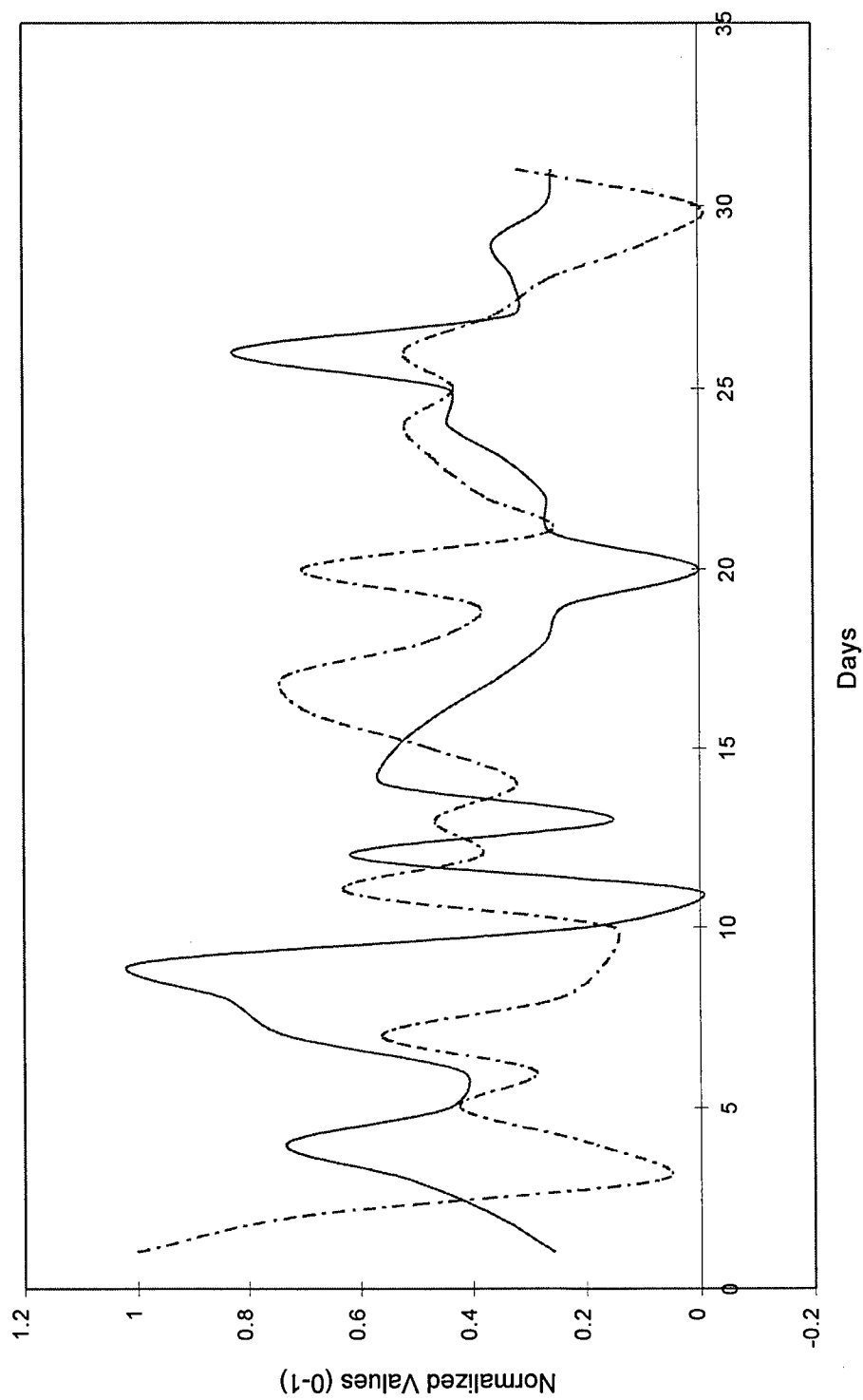
Figure 3.23. Nashville, TN normalized daily averaged ozone and visibility (dashed line is visibility) for July 1988.

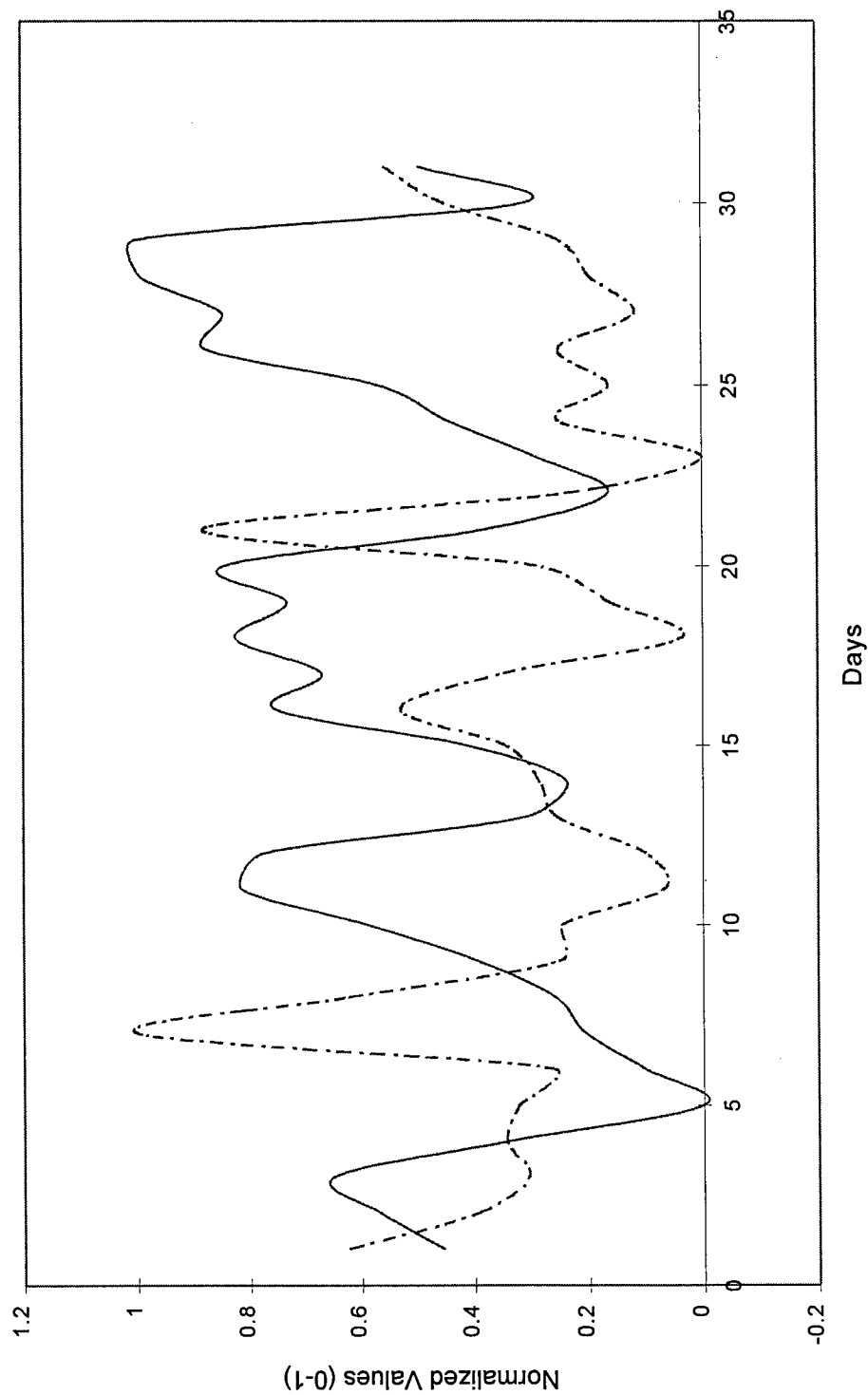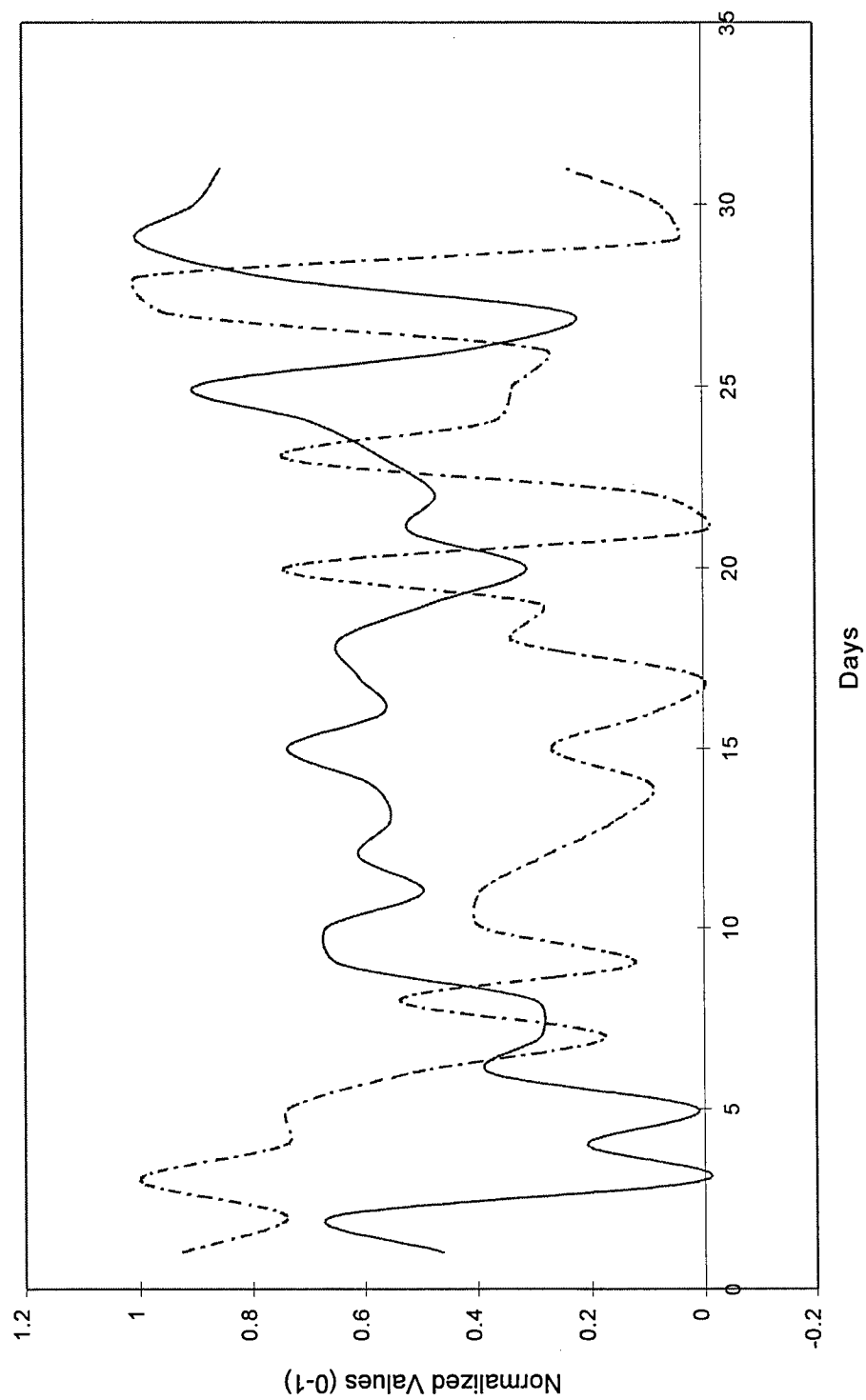Figure 3.24. Nashville, TN normalized daily averaged ozone and visibility (dashed line is visibility) for August 1995. This month was also used for the back trajectory analysis.

67
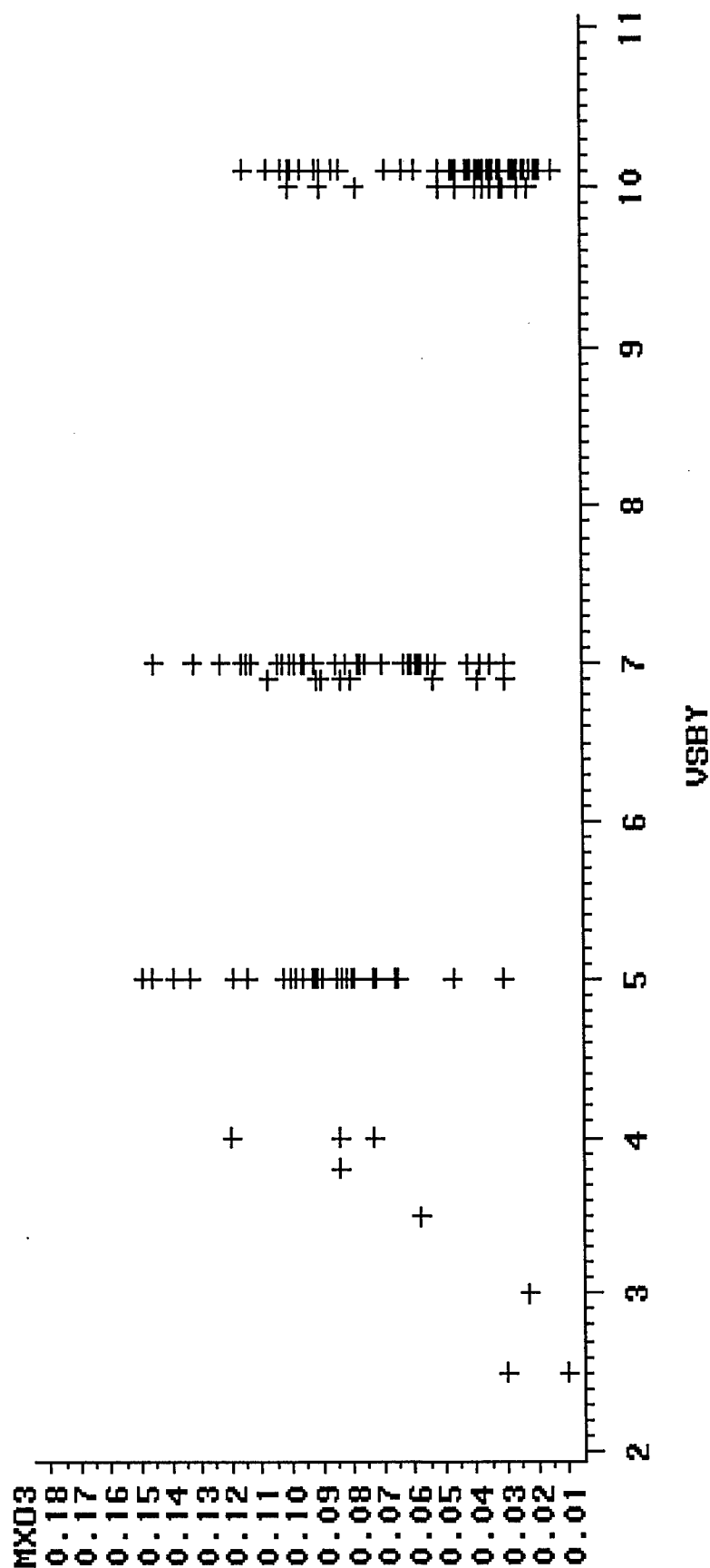
Figure 3.25. Scatter plot of visibility vs. ozone for August 1995 for Atlanta, GA.
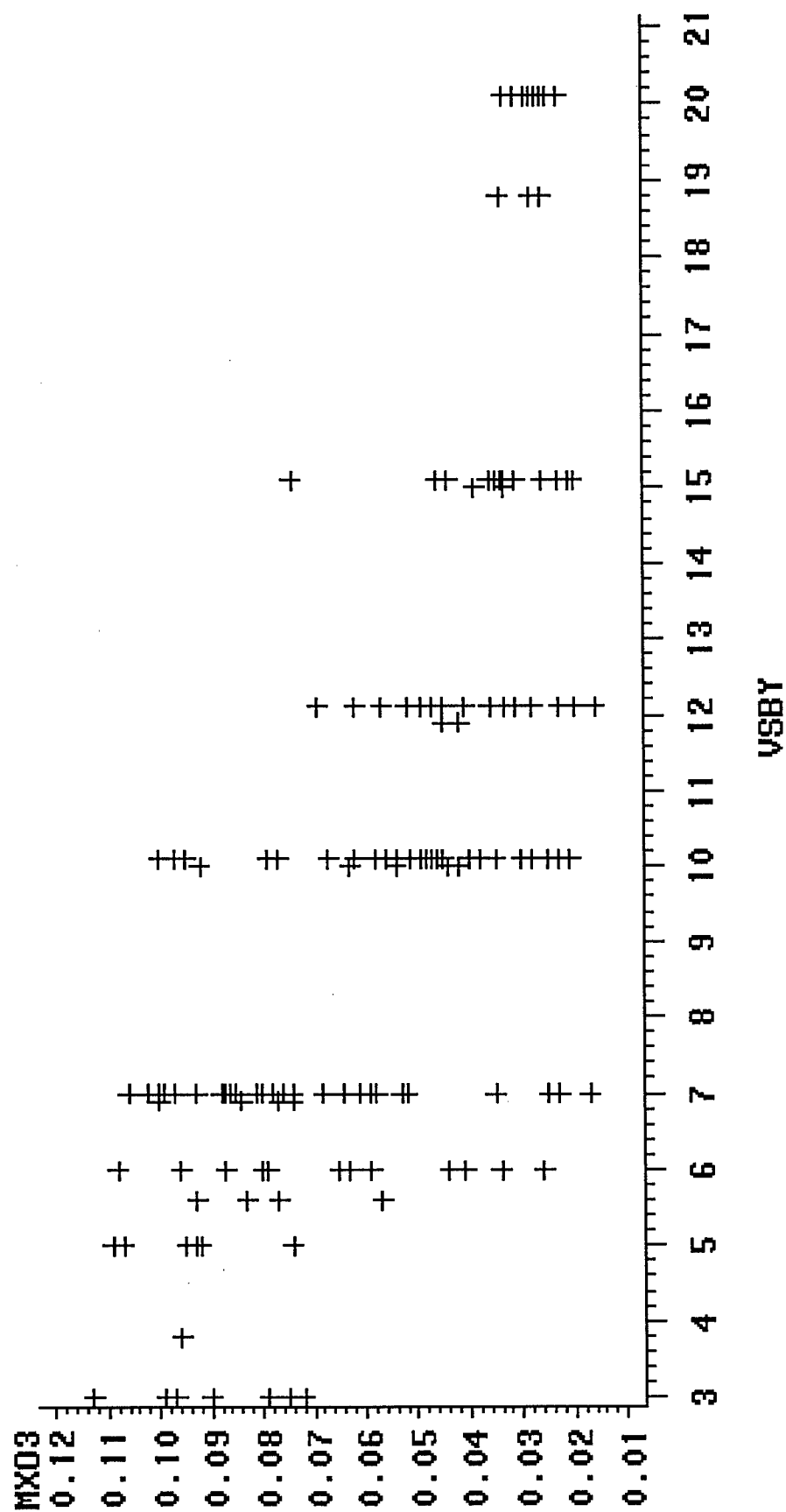
Figure 3.26. Scatter plot of visibility vs. ozone for August 1995 for Charlotte, NC.

69
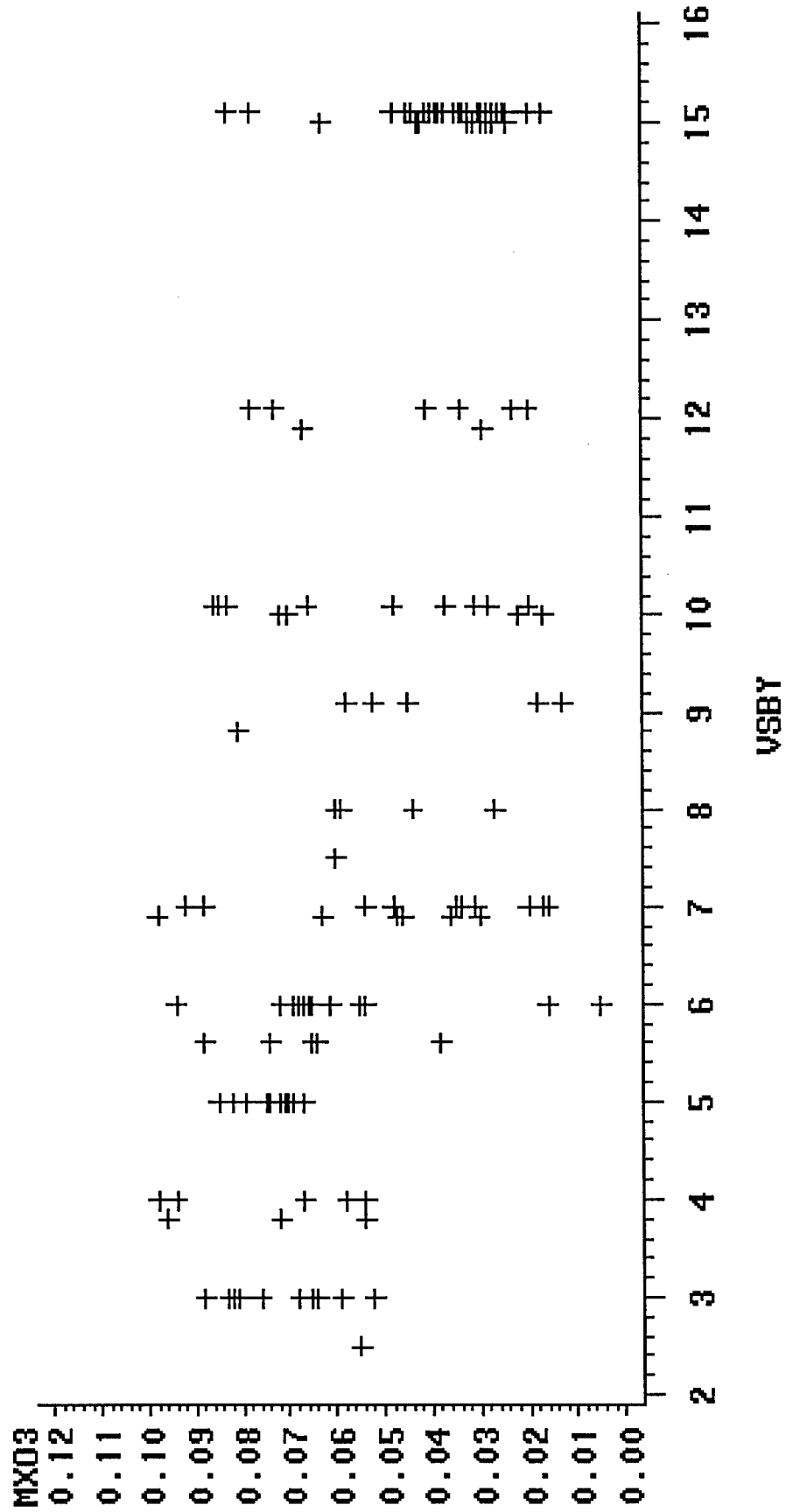
Figure 3.27. Scatter plot of visibility vs. ozone for August 1995 for Greensboro, NC.
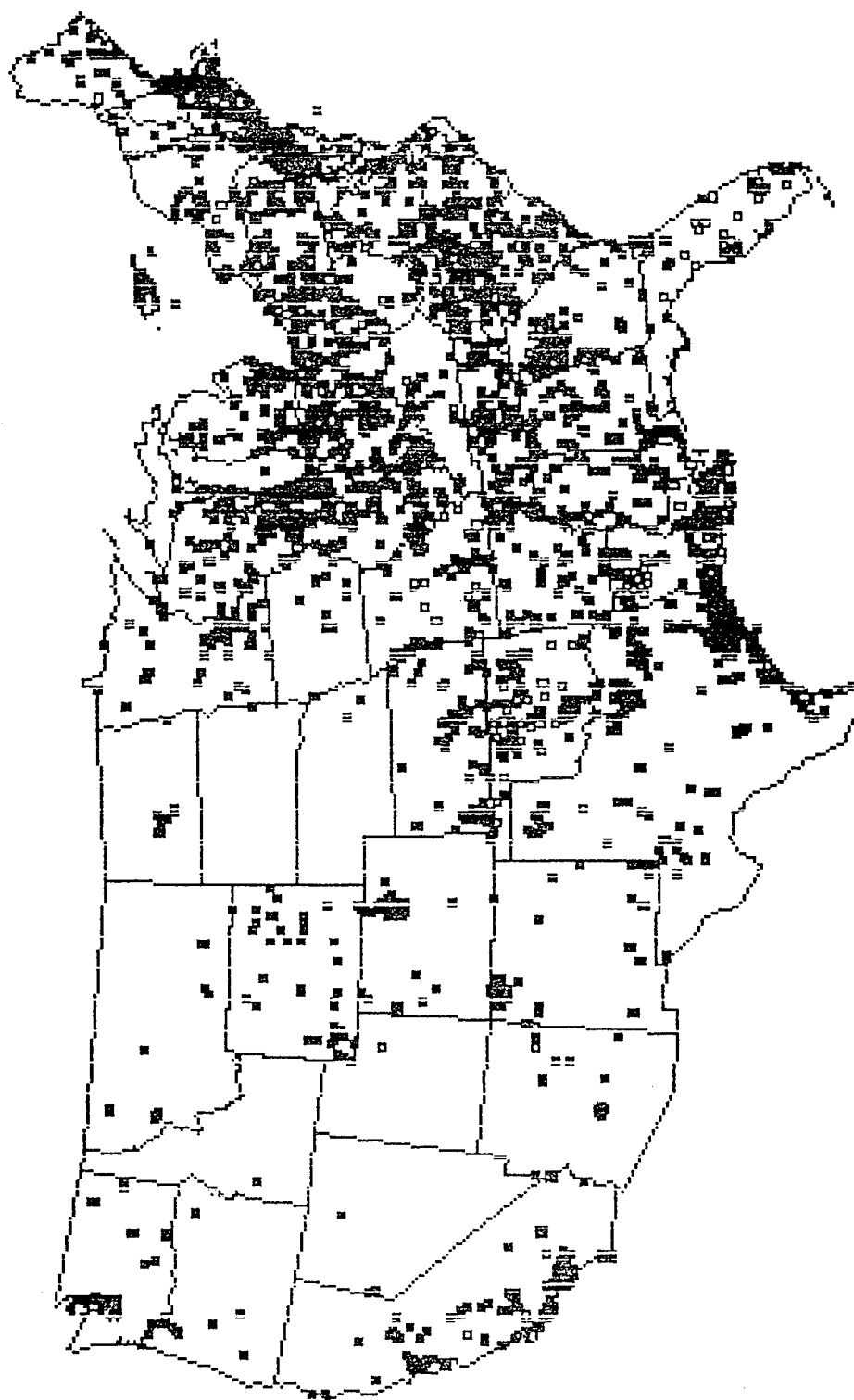
Figure 3.28. VOC Source map from US EPA Office of Air Quality Planning & Standards / Information Transfer Group.
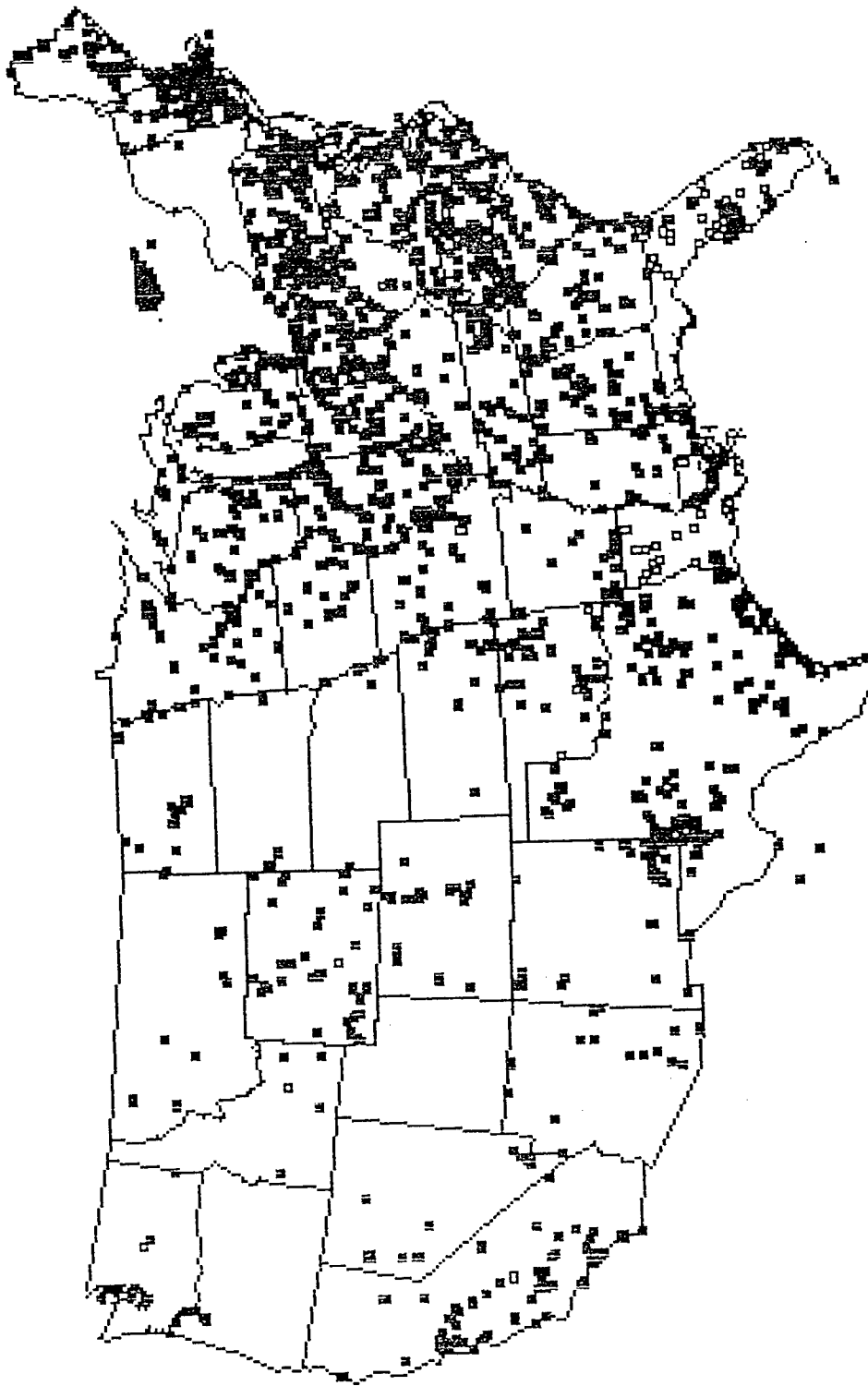
Figure 3.29. SO$_2$ Source map from US EPA Office of Air Quality Planning & Standards / Information Transfer Group.
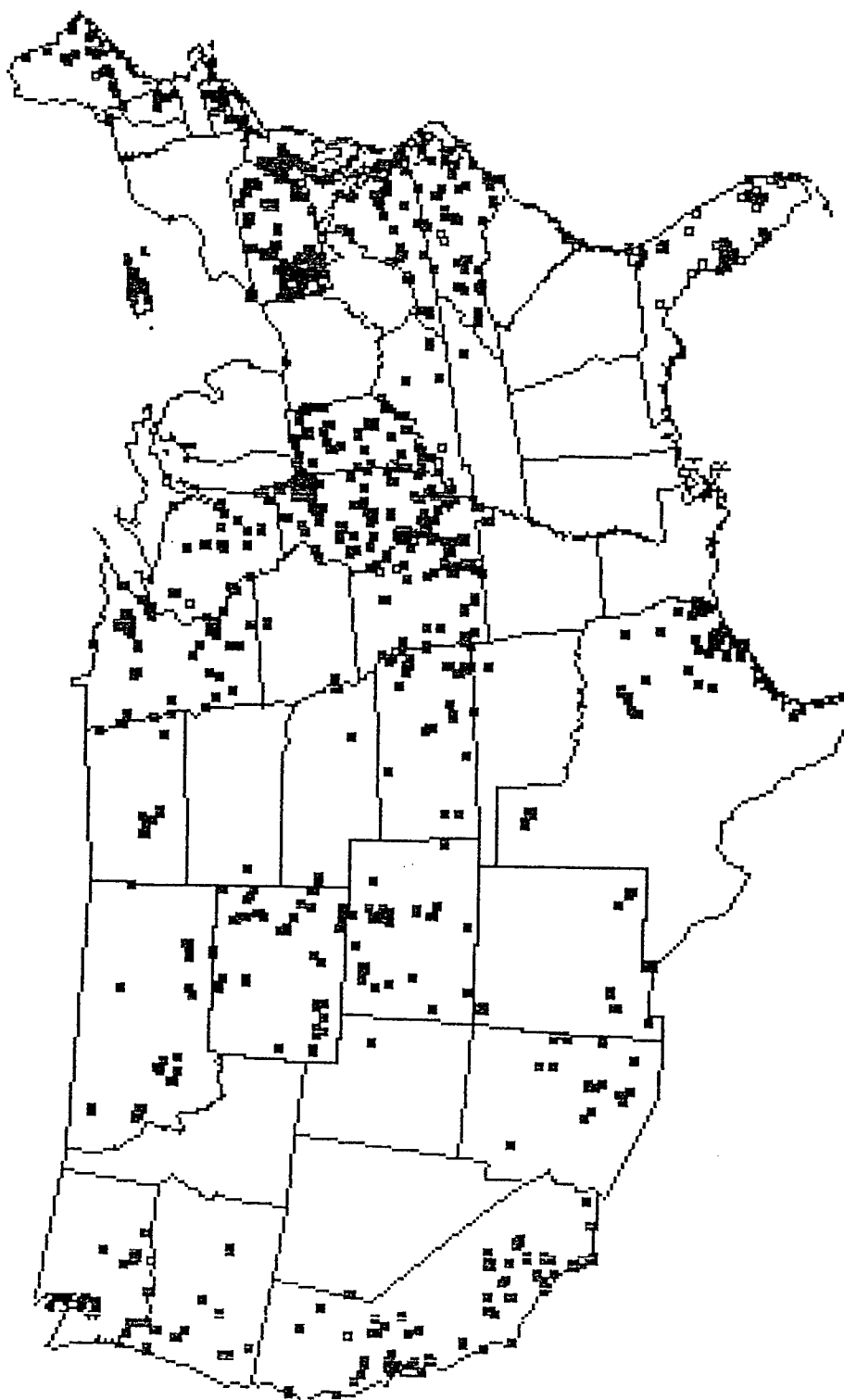
Figure 3.30. PM$_{10}$ Source map from US EPA Office of Air Quality Planning & Standards / Information Transfer Group.
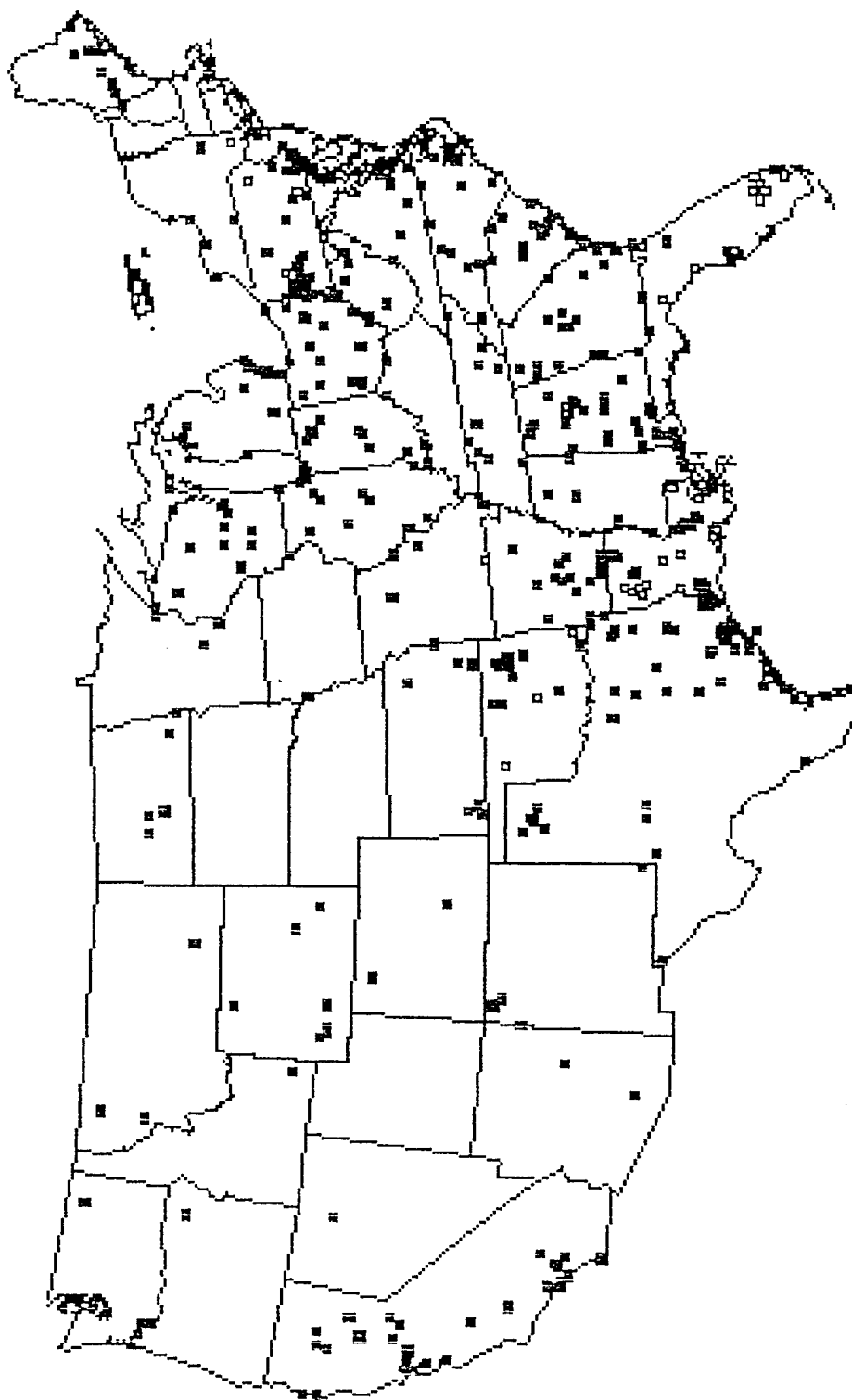
Figure 3.31. CO Source map from US EPA Office of Air Quality Planning & Standards / Information Transfer Group.
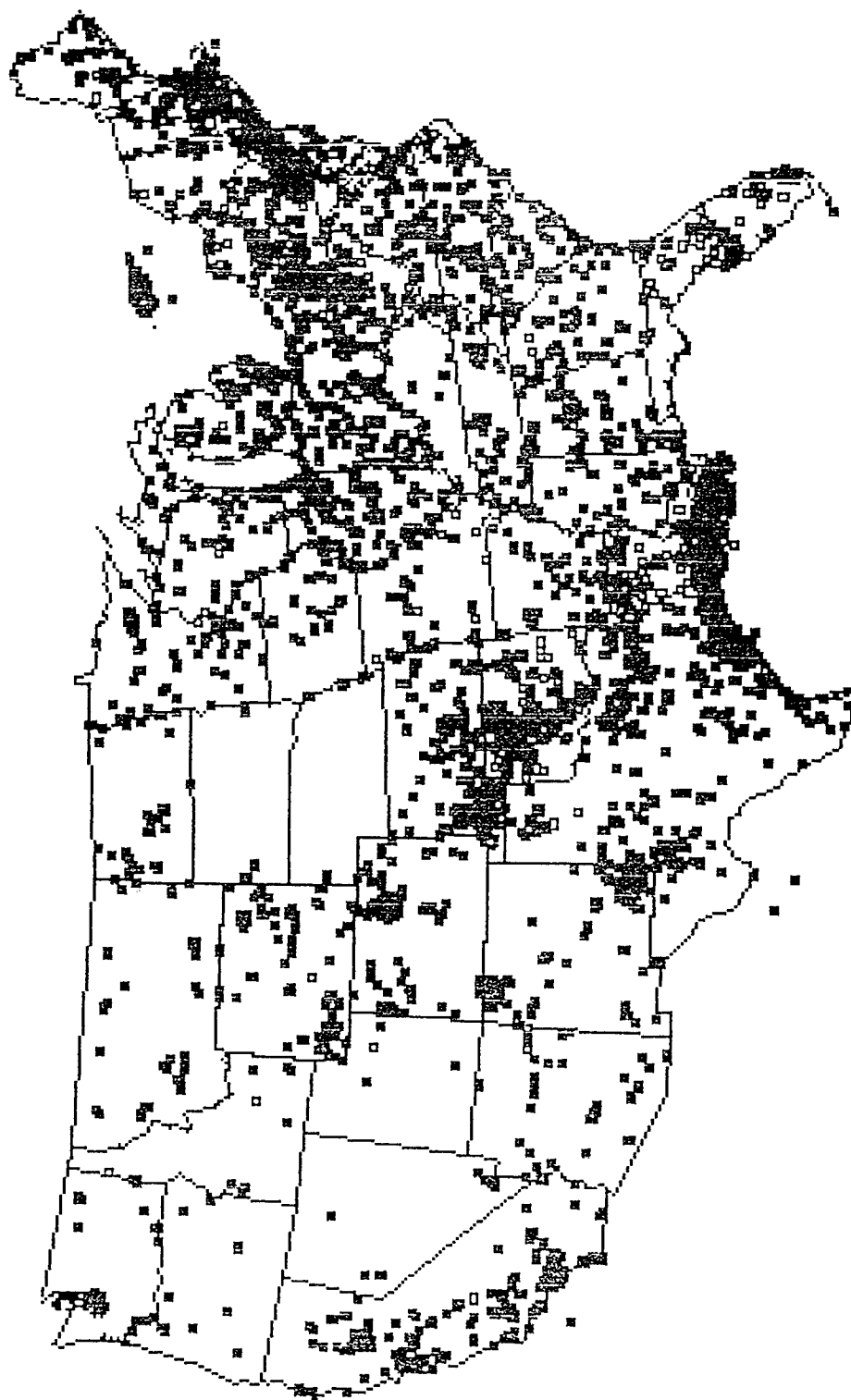
Figure 3.32. NO$_2$ Source map from US EPA Office of Air Quality Planning & Standards / Information Transfer Group.

BACKWARD TRAJECTORIES ENDING— 12UTC 02 AUG 95

Figure 3.33. Back trajectory analysis for 2 August 1995. The airmass traveled through a moderately high source region for VOCs, SO_2, and NO_2, which increased ozone. A consequence of this increased ozone was the observed reduction in visibility during this same period.

BACKWARD TRAJECTORIES ENDING— 12UTC 04 AUG 95
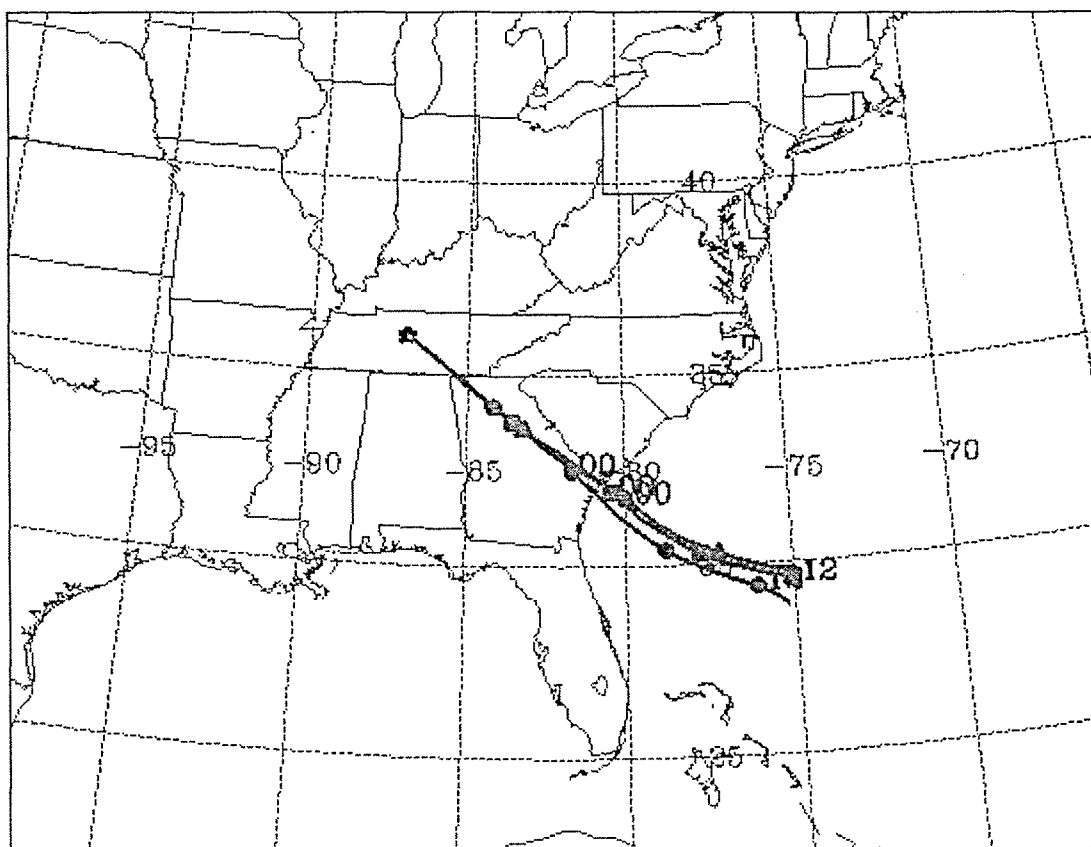
Figure 3.34. Back trajectory analysis for 4 August 1995. The model run shows that the air parcel had covered a longer path length (compared to 2 August's run) implying quick travel time, and a non-stagnating airmass. Additionally the airmass traveled over cleaner non-polluted areas; as a consequence, visibility increased and ozone decreased.

77

BACKWARD TRAJECTORIES ENDING— 12UTC 09 AUG 95
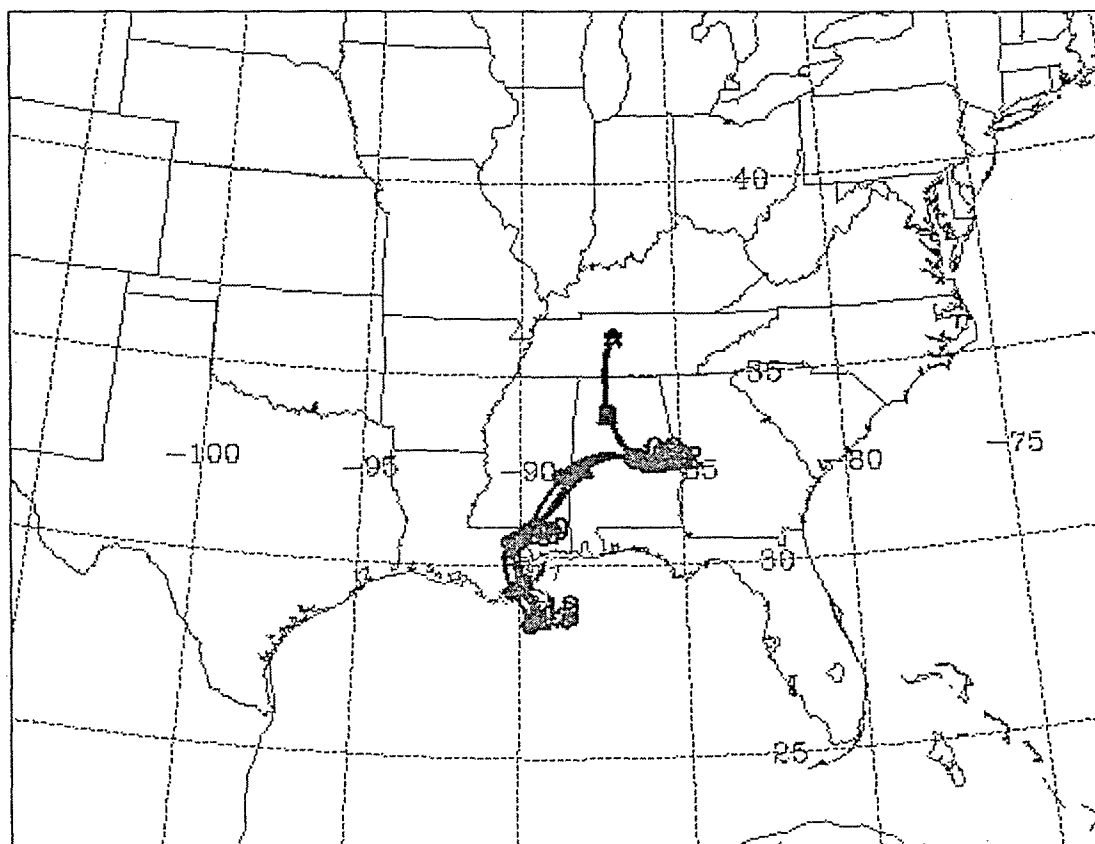
Figure 3.35. Back trajectory analysis for 9 August 1995. The run for 9 August is marked by a much shorter path legth (compared to 4 August's run) over a moderately polluted area. The path is not direct and meanders over a moderate VOC area. The result is a stagnating airmass whose ozone levels have increased and visibility decreased.

U.S. NATIONAL OCEANIC AND ATMOSPHERIC ADMINISTRATION
ARL / NCEP

BACKWARD TRAJECTORIES ENDING— 12UTC 14 AUG 95
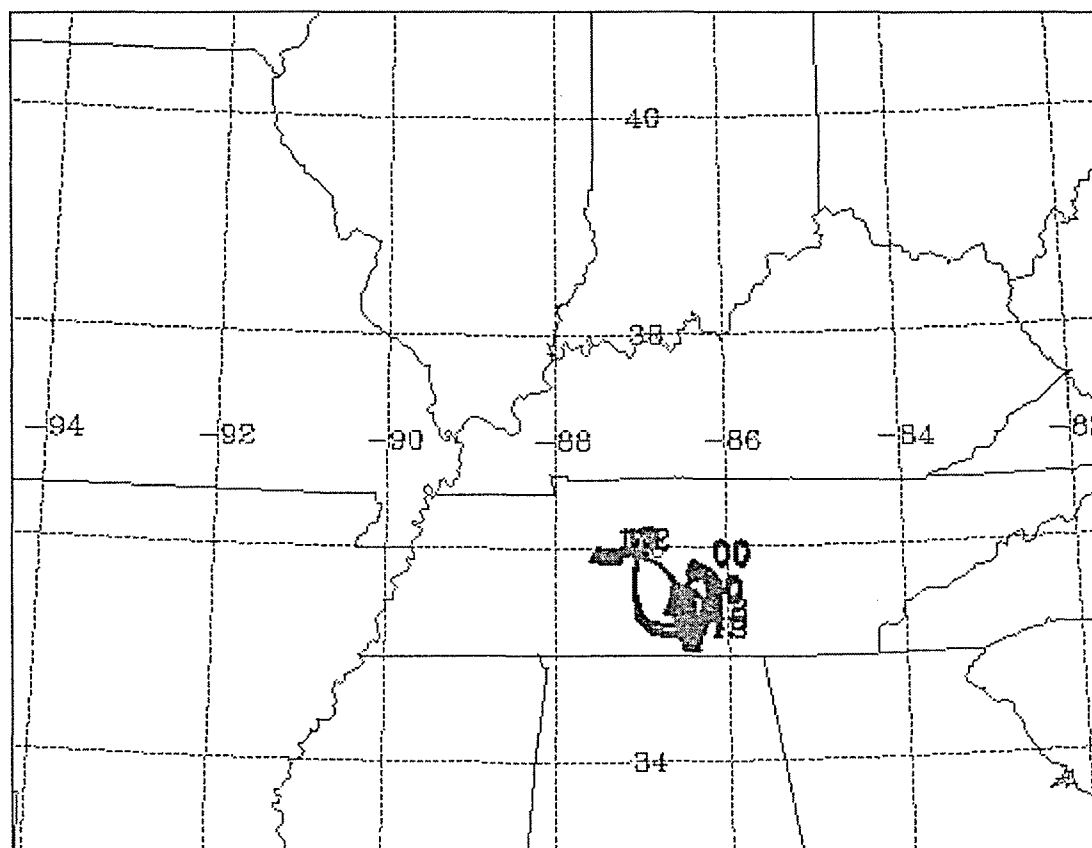
Figure 3.36. Back trajectory analysis for 14 August 1995 displays further evidence of the effects of meandering over a high VOC emission area. The result is a stagnating airmass whose ozone levels have increased and visibility decreased.

79

BACKWARD TRAJECTORIES ENDING— 12UTC 20 AUG 95

Figure 3.37. Back trajectory analysis for 20 August 1995 was marked by a decrease in ozone and an accompanying increase in visibility. The path for this air mass originally travelled through the more polluted Virginia area and then into the cleaner region of Kentucky. Distance traveled was fairly long in a short period of time implying higher speed and low stagnation.

U.S. NATIONAL OCEANIC AND ATMOSPHERIC ADMINISTRATION
ARL / NCEP

BACKWARD TRAJECTORIES ENDING— 12UTC 25 AUG 95
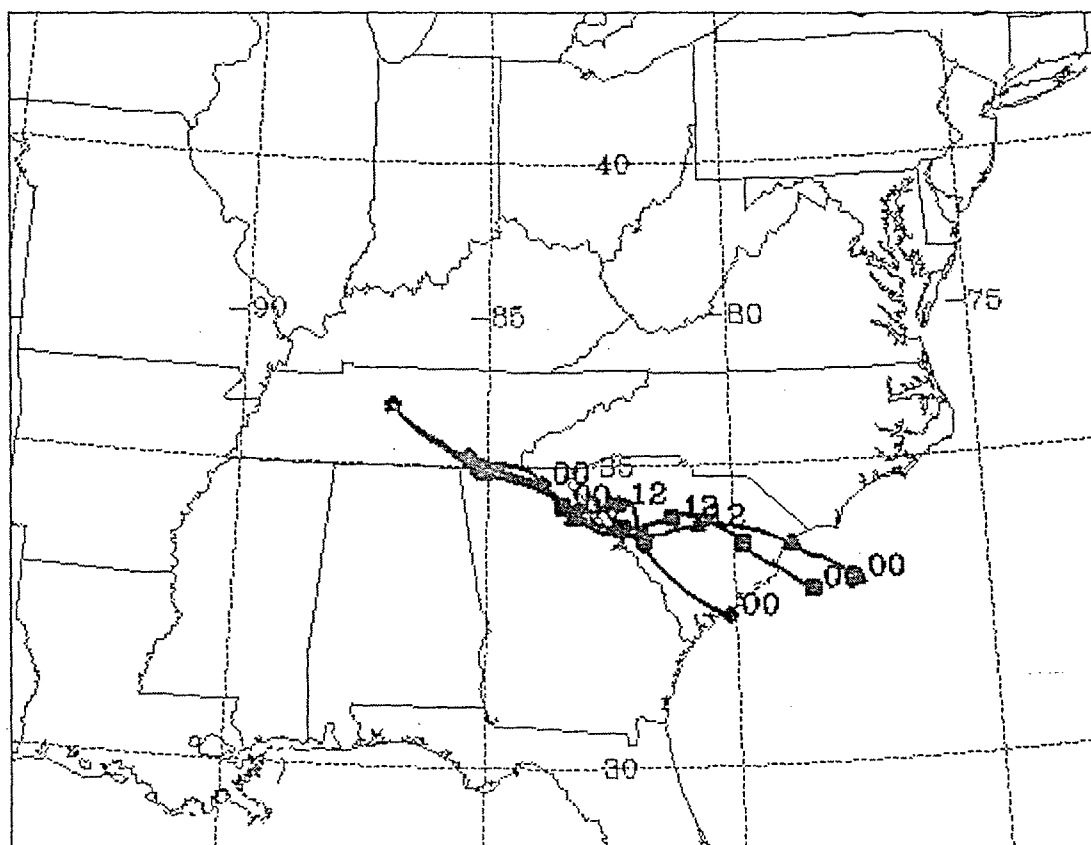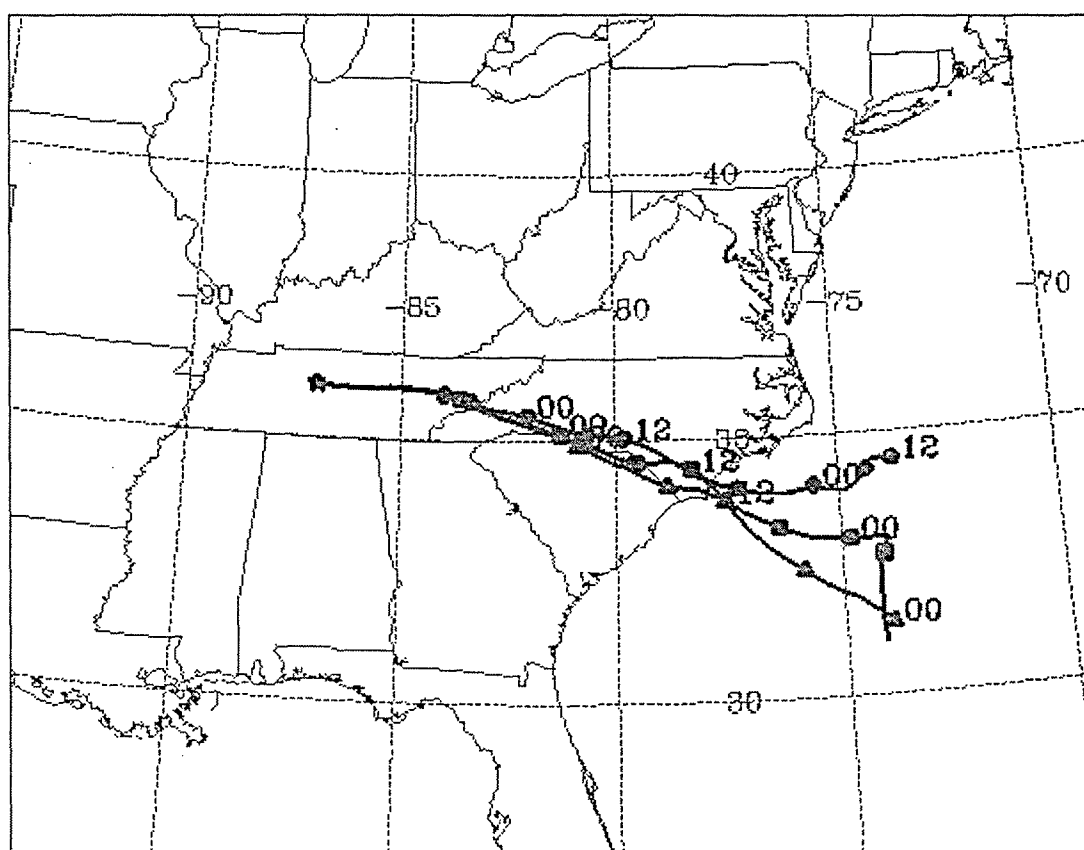

Figure 3.38. Back trajectory analysis for 25 August 1995. The airmass traveled through a high source region for VOCs, SO_2, and NO_2, which increased ozone and led to a decrease in visibility.

81

BACKWARD TRAJECTORIES ENDING— 12UTC 26 AUG 95
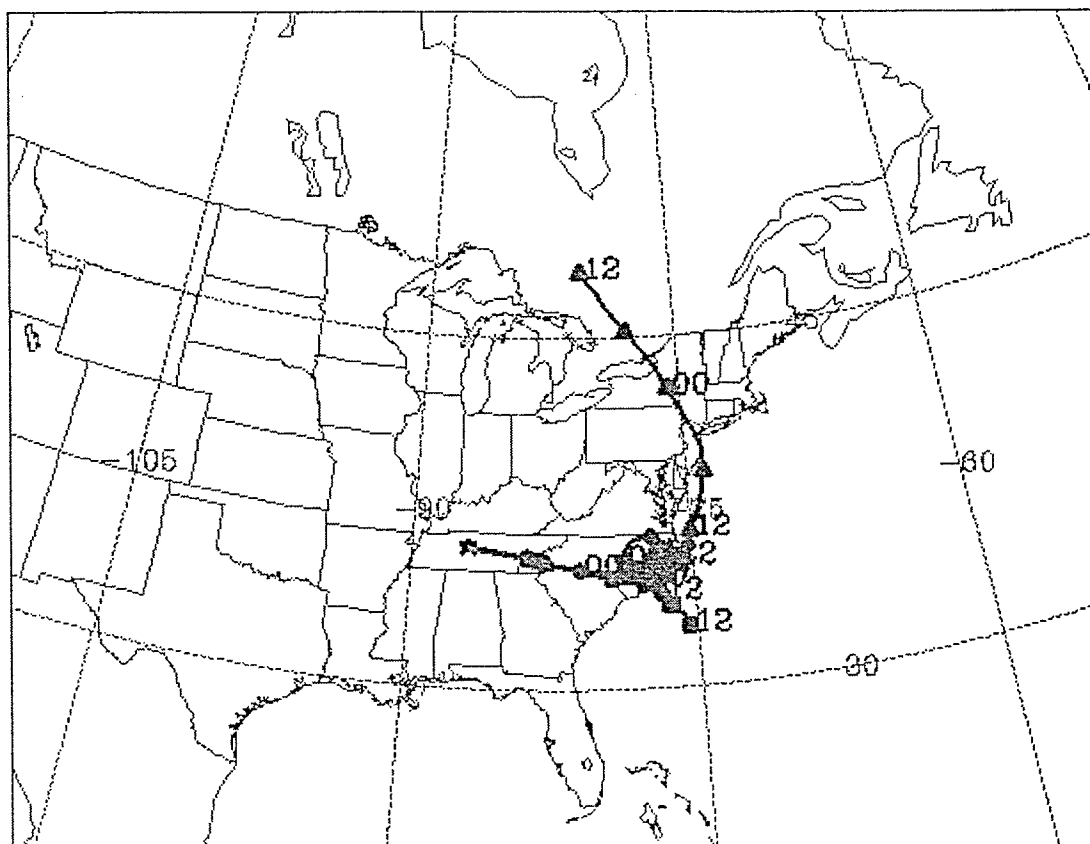
Figure 3.39. The period of 26 August is marked be a reduction in ozone and an increase in visibility, this despite a polluted source region. However, in this case the polluted airmass migrates out over the ocean where it is likey cleansed before continuing on to the Nashville.

BACKWARD TRAJECTORIES ENDING– 12UTC 30 AUG 95
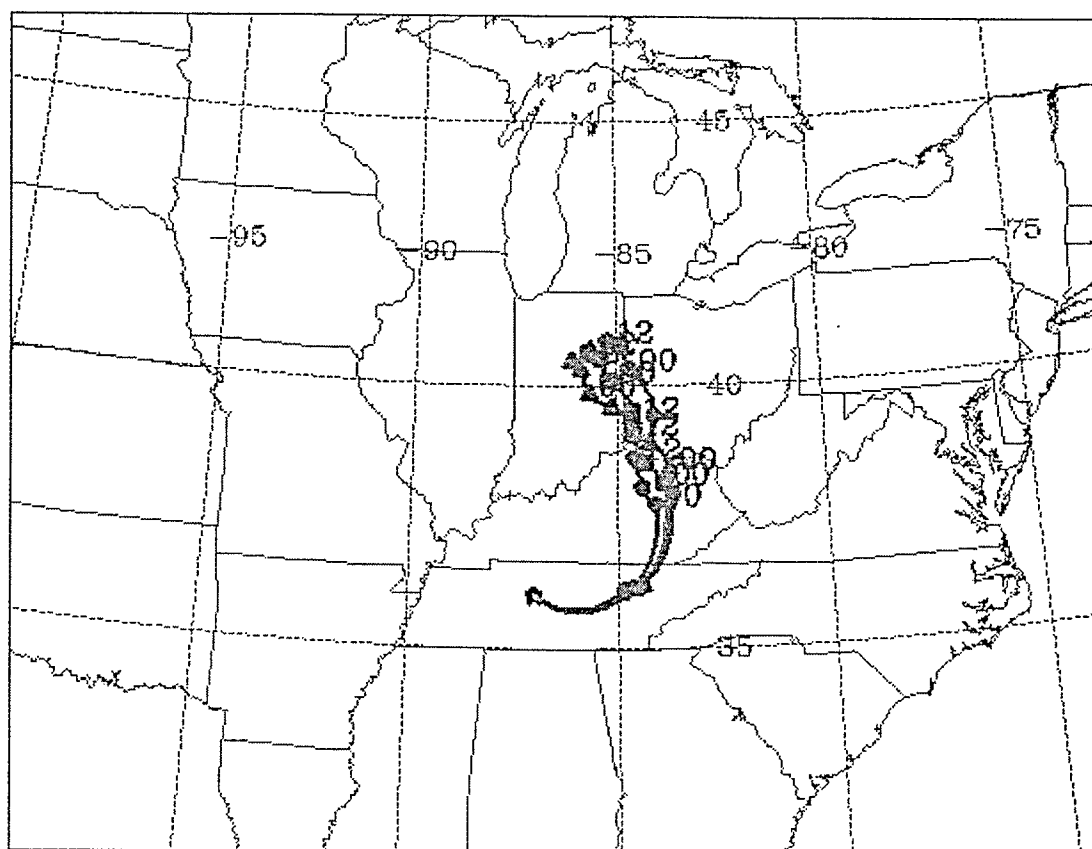
Figure 3.40. The model run for 30 August fits the classical example of: short travel path (stagnation), meandering, and polluted source region. The results are as expected with high ozone levels and reduced visibility.

Table 3.1. Daily summary regression statistics for Nashville, TN. The top section is grouped by month for the five high ozone season years. The bottom section represents daily averaged values grouped by year.

Grouping (month)	Degree of Freedom	R-squared	Prob > | T |
June 1980	29	.13	.047
July 1980	30	.001	.863
August 1980	30	.0002	.93
June 1983	29	.096	.095
July 1983	30	.135	.042
August 1983	30	.04	.28
June 1988	29	.24	.006
July 1988	30	.02	.511
August 1988	30	.03	.326
June 1990	29	.14	.05
July 1990	30	.008	.631
August 1990	30	.07	.15
June 1995	29	.001	.87
July 1995	30	.0002	.94
August 1995	30	.035	.31
Grouping (year)	**Degree of Freedom**	**R-squared**	**Prob > | T |**
1980	88	.08	.0072
1981	87	.04	.0752
1982	90	.01	.3308
1983	91	.27	.0001
1984	91	.08	.0075
1985	90	.08	.0083
1986	91	.03	.897
1987	91	.16	.0001
1988	91	.10	.0023
1989	91	.16	.0001
1990	91	.06	.0183
1991	91	.004	.5499
1992	89	.0000	.9759
1993	91	.18	.0001
1994	91	.15	.0001
1995	91	.14	.0002
1996	80	.21	.0001

Table 3.2. Summary of area specific hourly regression analysis.

Area	Grouping (month)	Degree of Freedom	R-squared	P > | T |
GSO	June 1980	29	.0341	.0138
GSO	July 1980	30	.1375	.0001
GSO	August 1980	30	.0578	.0011
GSO	June 1983	29	.0380	.0093
GSO	July 1983	30	.0418	.0066
GSO	August 1983	30	.0899	.0002
GSO	June 1988	29	.0189	.0626
GSO	July 1988	30	.1925	.0001
GSO	August 1988	30	.0499	.0017
GSO	June 1990	29	.0861	.0001
GSO	July 1990	30	.0632	.0002
GSO	August 1990	30	.0047	.3397
GSO	June 1995	29	.0352	.0146
GSO	July 1995	30	.0725	.0002
GSO	August 1995	30	.3308	.0001
RDU	June 1980	29	.0010	.0001
RDU	July 1980	30	.2045	.0001
RDU	August 1980	30	.0869	.0001
RDU	June 1983	29	.0018	.5947
RDU	July 1983	30	.0859	.0001
RDU	August 1983	30	.0614	.0004
RDU	June 1988	29	.1459	.0001
RDU	July 1988	30	.1538	.0001
RDU	August 1988	30	.0747	.0003
RDU	June 1990	29		
RDU	July 1990	30	.0956	.0001
RDU	August 1990	30	.0092	.1926
RDU	June 1995	29	N/A	N/A
RDU	July 1995	30	N/A	N/A
RDU	August 1995	30	N/A	N/A
ATL	June 1980	29	.0430	.0065
ATL	July 1980	30	.1050	.0001
ATL	August 1980	30	.0008	.7004
ATL	June 1983	29	.0298	.0194
ATL	July 1983	30	.3048	.0001
ATL	August 1983	30	.1701	.0001
ATL	June 1988	29	.0764	.0001
ATL	July 1988	30	.0757	.0001
ATL	August 1988	30	.0091	.1727
ATL	June 1990	29	.0068	.2480

Table 3.2 continued.

Area	Grouping (month)	Degree of Freedom	R-squared	P > | T |
ATL	July 1990	30	.0400	.0043
ATL	August 1990	30	.0015	.5790
ATL	June 1995	29	.001	.6681
ATL	July 1995	30	.2273	.0001
ATL	August 1995	30	.2495	.0001
CLT	June 1980	29	.0054	.3261
CLT	July 1980	30	.1356	.0001
CLT	August 1980	30	.0679	.0002
CLT	June 1983	29	.1340	.0001
CLT	July 1983	30	.1421	.0001
CLT	August 1983	30	.1191	.0001
CLT	June 1988	29	.1172	.0001
CLT	July 1988	30	.0763	.0001
CLT	August 1988	30	.0257	.0251
CLT	June 1990	29	.0375	.0060
CLT	July 1990	30	.0419	.0033
CLT	August 1990	30	.0003	.7940
CLT	June 1995	29	.0010	.6706
CLT	July 1995	30	.0166	.0712
CLT	August 1995	30	.4344	.0001

CHAPTER 5. REFERENCES

Andreae M. O., Soot carbon and excess fine potassium: Long-range transport of combustion-derived aerosols. *World Survey of Climatology, Vol. XVI Future Climate of the World.* A. Henderson-Sellers (ed.), Elsevier, Amsterdam. (In press).

Aneja V.P., S. Businger, Z. Li, C.S. Claiborn, and A. Murthy, Ozone climatology at high elevations in the Southern Appalachians. *J. Geophys. Res.,* 96, 1007-1021, 1991.

Aneja V.P. and Z. Li, Characterization of ozone at high elevation in the Eastern United States: Trends, seasonal variations, and exposure. *J. Geophys. Res.,* 97, 9873-9888, 1992.

Aneja V.P., Z. Li, and M. Das, Ozone case studies at high elevation in the Eastern United States. *Chemosphere,* 29, 1711-1733, 1994.

Aneja V. P., W. P. Robarge, L. J. Sullivan, T. C. Moore, T. E. Pierce, C. Geron, B. Gay, Seasonal variations of nitric oxide flux from agricultural soils in the Southeast United States. *Tellus,* 48B, 626-640, 1996.

ARL/NOAA: http://www.arl.noaa.gov/ready/hysplit4.html, 1997.

Chamberlain A. C., <u>Radioactive Aerosols.</u> Cambridge University Press, 1991.

Chameides W.L., R.W. Lindsay, J.L. Richardson, and C.S. Kiang, The role of biogenic hydrocarbons in urban photochemical smog: Atlanta as a case study. *Science,* 241, 1473-1475, 1988.

Chameides W.L. and E.B. Cowling, <u>The State of the Southern Oxidants Study (SOS): Policy Relevant Findings in Ozone Pollution Research 1988-1994</u>. April 1995.

Delwiche L. D. and S. J. Slaughter, <u>The Little SAS Book: A Primer.</u> Cary, NC: SAS Institute Inc., 1995.

Diederen H.S.M.A., Guicherit R., Hollander J.C.T., Visibility reductions by air pollution in the Netherlands. *Atmospheric Environment,* 19, 377-383, 1985.

Ehalts D. H., H. P. Dorn, D. Poppe, The chemistry of the hydroxyl radical in the troposphere. *Proceedings of the Royal Society of Edinburg,* 97B, 17-34, 1991.

Eldred A. E., T. A. Cahill, R. G. Flocchini, Composition of $PM_{2.5}$ and PM_{10} Aerosols in the IMPROVE Network. *J. Air & Waste Manage. Assoc.,* 47, 194-203 1997.

EPA Homepage, Homepage link to on-line publications, http://134.67.104.12/naaqspro/o3hlth.htm. World Wide Web, 1997a.

EPA Office of Air Quality Planning And Standards, Information Transfer and Program Integration Division, Information Transfer Group, RTP, NC. http://epa.gov/airs. World Wide Web, 1997b.

Farber R. J., Welsing P. R., Rozzi C., PM_{10} and ozone control stratigies to improve visibility in the Los Angeles Basin. *Atmospheric Environment,* 28, 3277-3283, 1994.

Friedlander S. K., Smoke, Dust and Haze. John Wiley, New York, 1977.

Gray H. A., D. Kleinhesselink, Evaluation of existing information on the effects of air pollutants on visibility in the Southern Appalachians. *Systems Applications International,* Final Report, 31 Oct. 1996.

Hiddleman L. M., Markowski G. R., Cass G. R., Chemical composition of emissions from urban source of fine organic aerosols. *Envir. Sci. Tech.,* 25, 744-759, 1991.

King W.J. and F.M. Vukovich, Some dynamic aspects of extended pollution episodes. *Atmospheric Environment,* 16, 1171-1181, 1982.

Korshover J., Climatology of stagnating anticyclones east of the Rocky Mountains, 1936-1975. NOAA Tech. Memo. ERL ARL-55, 26pp., 1976.

Lamb B., A. Guenther, D. Gay, and H. Westberg, A national inventory of biogenic hydrocarbon emissions. *Atmospheric Environment,* 21, 1695-1705, 1987.

Lee D. O., The influence of wind direction, circulation type and air pollution emissions on summer visibility trends in Southern England. *Atmospheric Environment,* 24A, 195-201, 1990.

Lindsay R.W., J.L. Richardson, and W.L. Chameides, Ozone trends in Atlanta, Georgia: Have emission controls been effective? *JAPCA,* 39, 40-43, 1989.

Logan J.A., M.J. Prather, S.C. Wofsy, and M.B. McElroy, Tropospheric chemistry: A global perspective. *J. Geophys. Res.,* 86, 7210-7254, 1981.

Logan J.A., Tropospheric ozone: Seasonal behavior, trends, and anthropogenic influence. *J. Geophys. Res.,* 90, 10463-10482, 1985.

Logan J.A, Ozone in rural areas of the United States. *J. Geophys. Res.,* 94, 8511-8532, 1989.

Malm W. C., J. Sisler, D. Huffman, R.A. Eldred, T.A. Cahill, Spatial and seasonal trends in particulate concentration and optical extinction in the United States. *J. Geophys. Res.,* 99, 1347-1370, 1994.

Malm W. C., J. Trijonis, J. Sisler, Pitchford M., Dennis R. L., Assesing the effect of SO_2 emission changes on visibility. *Atmospheric Environment,* 28, 1023-1034, 1994.

Mathur R., K.L. Schere, and A. Nathan, Dependancies and sensitivity of tropospheric oxidants to precursor concentrations over the Northeast United States: A model study. *J. Geophys. Res.,* 99, 10535-10552, 1994.

McNider R.T., W.B. Norris, and J.A. Song, Regional meteorological characteristics during ozone episodes in the Southeastern United States. Proceedings of the Air and Waste Management Association International Specialty Conference on Regional Photochemical Measuremnet and Modeling Studies. San Diego, CA, November 7-12, 1993.

Middleton P., T. R. Stewart, R. L. Dennis, Modeling human judgements of urban air quality. *Atmospheric Environment,* 17, 1015-1021, 1984.

Middleton P., DAQM-simulated spatial and temporal differences among visibility, PM, and other air quality concerns under realistic emission change scenarios. *J. Air & Waste Management Association.* 47, 302-316, 1997.

Moy L., R. Dickerson, W. Ryan, Relationship between back trajectories and tropospheric trace concentrations in rural Virginia. *Atmospheric Environment,* 28, 2789-2800, 1994.

NRC, Rethinking the ozone problem in urban and regional air pollution. National Academy Press, Washington, D.C., 1991.

Nilsson B. A., Model of the relation between aerosol extinction and meteorological parameters. *Atmospheric Environment,* 28, 815-825, 1994.
O'Conner J., A climatology of regional ozone: meteorological effects on ozone exceedences in the Southeast United States. Master's Thesis, North Carolina State University, Department of Marine Earth and Atmospheric Science, 1996.

Oltmans S.J., and W.D. Komhyr, Surface ozone distributions and variations from 1973-1984. Measurements at the NOAA geophysical monitoring for climatic change baseline observatories. *J. Geophys. Res.,* 91, 5229-5236, 1986.

Penkett S.A., Changing ozone: Evidence for a perturbed atmosphere. *Environ. Sci. Technol.,* 25, 631-635, 1991.

Rao S.T., I.G. Zurbenko, P.S. Porter, J.Y. Ku, and R.F. Henry, Dealing with the ozone non-attainment problem in the Eastern United States. *Environmental Manager,* 17-31, January 1996.

SAS Institute Inc., SAS Procedures Guide, Version 6, First Edition. Cary, NC: SAS Institute Inc., 1990a.

SAS Institute Inc., SAS Language Guide Version 6, First Edition. Cary, NC: SAS Institute Inc., 1990b.

Sullivan L.J., T.C. Moore, V.P. Aneja, and W.P. Robarge, Environmental variables controlling nitric oxide emissions from agricultural soils in the Southeast United States. *Atmospheric Environment,* (In press; accepted February, 1996).

Trainer M., E.J. Williams, D.D. Parrish, M.P. Buhr, E.J. Allwine, H.H. Westberg, F.C. Fehsenfeld, and S.C. Liu, Models and observations of the impact of natural hydrocarbons on rural ozone. *Nature,* 329, 705-707, 1987.

Trainer M., M.P. Buhr, C.M. Curran, F.C. Fehsenfeld, E.Y. Hsie, S.C. Liu, R.B. Norton, D.D. Parrish, E.J. Williams, B.W. Gandrud, B.A. Ridley, J.D. Shetter, E.J. Allwine, and H.H. Westberg, Observations and modeling of the reactive nitrogen photochemistry at a rural site. *J. Geophys. Res.*, 96, 3045-3063, 1991.

Vali G., Nucleation termonology. *J. Geophys. Res.*, 16, 575-576, 1985.

Vukovich F.M., Boundary layer ozone variations in the Eastern United States and their association with meteorological variations: Long term variations. *J. Geophys. Res.*, 99, 16839-16850, 1994.

Vukovich F.M., W.D. Bach, B.W. Crissman, and W.J. King, On the relationship between high ozone in the rural surface layer and high pressure systems. *Atmospheric Environment*, 11, 967-983, 1977.

Waggoner A. P., R. E. Weiss, N. C. Ahlquist, D. S. Covert, S. Will, R. J. Charlson, Optical characteristics of atmospheric aerosols. *Atmospheric Environment*, 15, 1891-1909, 1981.

Warneck P., Chemistry of the Natural Atmosphere. Academic Press, Inc. (San Diego), 1988.

Weintraub D., V. K. Saxena, Impact of nonstandard conditions on visibility measurements. Aerosols and Climate. Deepak Publishing, 1988.

APPENDIX 1. SAS® Programing Code.

The following code reads daily averaged values such as PM_{10} and TSP and was modified to run on a PC. The original code was obtained from the EPA.

```
FILENAME IN 'D:\DATA';
DATA TSP.TSP_N(KEEP=SITE YEAR MONTH DAY TSP FLAG METHOD MSA_NAME);
ARRAY VALUE (372) CONC1-CONC372 ;
ARRAY DEC (372) DP1-DP372;
ARRAY FL (372) $ FL1-FL372;
INFILE IN LRECL=4000;
INPUT SITE $ 1-9 POC 15 YEAR 20-21 METHOD 17-19
    CNTY_NAM $ 44-73 MSA_NAME $ 812-852
 @858 (CONC1-CONC31) (4. +4)  @858 (DP1-DP31) (+4 1. +3)
 @858 (FL1-FL31) (+5 $1. +2)
 @1111 (CONC32-CONC62) (4. +4)   @1111 (DP32-DP62) (+4 1. +3)
 @1111 (FL1-FL31) (+5 $1. +2)
 @1364 (CONC63-CONC93) (4. +4)   @1364 (DP63-DP93) (+4 1. +3)
 @1364 (FL1-FL31) (+5 $1. +2)
 @1617 (CONC94-CONC124) (4. +4)   @1617 (DP94-DP124) (+4 1. +3)
 @1617 (FL1-FL31) (+5 $1. +2)
 @1870 (CONC125-CONC155) (4. +4)   @1870 (DP125-DP155) (+4 1. +3)
 @1870 (FL1-FL31) (+5 $1. +2)
 @2123 (CONC156-CONC186) (4. +4)   @2123 (DP156-DP186) (+4 1. +3)
 @2123 (FL1-FL31) (+5 $1. +2)
 @2376 (CONC187-CONC217) (4. +4)   @2376 (DP187-DP217) (+4 1. +3)
 @2376 (FL1-FL31) (+5 $1. +2)
 @2629 (CONC218-CONC248) (4. +4)   @2629 (DP218-DP248) (+4 1. +3)
 @2629 (FL1-FL31) (+5 $1. +2)
 @2882 (CONC249-CONC279) (4. +4)   @2882 (DP249-DP279) (+4 1. +3)
 @2882 (FL1-FL31) (+5 $1. +2)
 @3135 (CONC280-CONC310) (4. +4)   @3135 (DP280-DP310) (+4 1. +3)
 @3135 (FL1-FL31) (+5 $1. +2)
 @3388 (CONC311-CONC341) (4. +4)   @3388 (DP311-DP341) (+4 1. +3)
 @3388 (FL1-FL31) (+5 $1. +2)
 @3641 (CONC342-CONC372) (4. +4)   @3641 (DP342-DP372) (+4 1. +3)
 @3641 (FL1-FL31) (+5 $1. +2);
I=0;
DO MONTH =1 TO 12;
 DO DAY =1 TO 31;
 I=I+1;
 TSP=VALUE(I)*(0.1)**DEC(I);FLAG = FL(I);
 IF TSP NE . THEN OUTPUT;
END;
END;
RUN;
```

APPENDIX 1b. SAS® Programing Code.

The following code reads hourly averaged values such as O_3 and was modified to run on a PC.

```
FILENAME IN 'D:\DATA\OZONE';
DATA TEMP1; INFILE IN LRECL=6066 ;
INPUT;
PUT _INFILE_;
IF _N_ IN(2,3);
DATA OZONE.OZONE; INFILE IN LRECL=6066 ;
INPUT SITE 9. @20 YEAR 2. MONTH 2. @310 UNIT 3. @;
IF MONTH IN(6,7,8);
INPUT @858 @;
DO DAY=1 TO 31;
DO HR=1 TO 24;
INPUT O3 5. DP 1. VF 1. @@;
IF 9968<=O3<=9998 THEN O3=.;
IF O3=00000 THEN O3=.;
IF DP=1 THEN O3=O3*(.1);
ELSE IF DP=2 THEN O3=O3*(.01);
ELSE IF DP=3 THEN O3=O3*(.001);
ELSE IF DP=4 THEN O3=O3*(.0001);
IF UNIT=001 THEN O3=O3*(.00051);
ELSE IF UNIT=007 THEN O3=O3*(1);
ELSE IF UNIT=008 THEN O3=O3*(.001);
OUTPUT;
 END;
 END;
 RUN;
```